



FACULTY OF ENGINEERING AND TECHNOLOGY

JMEE MASTER PROGRAM IN ELECTRICAL ENGINEERING

MODELLING, CONTROL AND SIMULATION OF FLYWHEEL ENERGY
STORAGE IN MICROGRIDS

نَمْدَجُهُ وَمُحَاكَاةُ أَنْظِمَةِ تَخْرِينِ الطَّاقَةِ بِاسْتِخْدَامِ الْحَدَّافَةِ فِي الشَّبَكَاتِ الْكَهْرَبَائِيَّةِ الصُّغْرَى

Author:

Aws Saleh

Supervisors:

Dr. Abdalkarim Awad

Dr. Wasel Ghanem

August 6th, 2019

This Master Thesis is submitted to the Master Program in Electrical Engineering in partial fulfilment of the requirements for the master's degree in electrical engineering.



Faculty of Engineering and Technology
Master in Electrical Engineering

**Modelling, Control and Simulation of Flywheel Energy Storage in
Microgrids**

نُمدِجَةُ ومُحاكاةُ أنظِمةِ تَحْزِينِ الطَّاقَةِ بِاسْتِخْدامِ الحَدَافَةِ في الشَّبَكَاتِ الكِهْرَبائِيَّةِ الصُّغْرَى

By

Aws Saleh

Supervisors:

Dr. Abdalkarim Awad

Dr. Wasel Ghanem

Committee Signature

Dr. Abdalkarim Awad

Dr. Wasel Ghanem

Dr. Mahran Quran

Dr. Hakam Shehadeh

August 6th, 2019

إهداء

إلى نبض الحياة ودفء الخنان.... إلى أملي وقرّة عيني... إلى سبب سعادتي وتوفيقي... إلى من مهّدوا لي الطريق...
حصّدوا الأشواك وزرّعوا لي الورود وحفّوها بالحبّ والحنان... إلى والديّ الحبيبين... فمهما صغّت من الحروف وخطّطت من
الكلمات قلن أوفيكما حقّكما.

إلى أساتذتي المجلّين الأكارم وأخصّ بالذكر مشرفي الدكتور عبد الكريم عواد والدكتور واصل غانم الذين بحثوا لي عن
مفاتيح النجاح ولم يخلوا عليّ في إسداء النصّح وتقديم العون.

إلى العزيز على قلبي المهندس جهاد دريدي فأنت النّيراس الذي أرشدني وأضاء لي الطريق الحافل بالمصاعب وشدّ على
يديّ عند كلّ محطة من محطاته.

إلى زوجتي الغالية... التي تطلّ لي نعم السند والمعين.

إلى زهرتي وطفّلتى المدلّلة (دانية) التي أسنّسرت لها مستقبلًا حميداً مشرقاً.

إلى أخوتي الذين أسنّسعروا معهم دفة الحياة.

إلى كلّ الذين تمنّوا لي هذا النجاح ودعّوا الله لي في ظهّر الغيب أن يوفّقني ويرعاني.

أهدي إليكم هذا العمل الذي أسأل الله أن يتفّعنا به في الدنيا والآخرة.

قوله تعالى
وَالَّذِينَ آمَنُوا وَعَمِلُوا الصَّالِحَاتِ
لَنَجْزِيَنَّهُمْ أَجْرًا كَبِيرًا

Contents:

إهداء iii

Contents:	iv
List of Figures:	vi
List of Tables:	ix
List of abbreviation	x
ملخص	xi
Abstract	xii
Chapter 1. Introduction	1
1.1 Problem statement	3
1.2 Thesis Contribution	3
1.3 Thesis Organization	5
Chapter 2. : Energy Storage Systems (ESS) And Microgrids	6
2.1 Batteries	6
2.1.1 Battery For grid-scale energy	6
2.1.2 Wide range application batteries	7
2.2 Electromechanical Capacitors	7
2.3 Pumped Hydros	7
2.4 Compressed Air Energy Storage (CAES)	8
2.5 Flywheel Energy Storage System (FESS)	10
2.5.1 NASA FESS Model Specifications:	11
2.5.2 Electrical model of permanent magnet synchronous machine(PMSM) :	12
2.5.3 Machine Drive Design:	17
2.6 Microgrids	24

2.6.1	Definition	24
2.6.2	Power quality in Microgrids	24
Chapter 3.	Related Work	27
3.1	Flywheel Energy Storage System (FESS) in power system.	27
3.2	Common DC bus topology with FESS	31
Chapter 4.	System Modelling	34
4.1	Characteristics of PV panels	36
4.2	DC to DC converter	37
4.3	On-grid inverter	38
4.4	Control System of FESS	43
Chapter 5.	Simulation & Results	47
5.1	Fluctuating Solar Irradiation	47
5.2	Constant power flow with fluctuating solar irradiation and variable inductance load with power factor correction mode.	54
5.3	Charging FESS from the Utility Grid and PVs.	63
5.4	The PV and FESS cover the load (100% penetration level of PVs continuously)	69
5.5	UPS Mode with variable load.	75
5.6	Efficiency Calculation and Measurement:	83
	Conclusion & Future work	87
	References	88
	Appendix:	94

List of Figures:

Figure 1-1 New system topology. _____	4
Figure 2-1 Compressed Air Energy Storage components [11]. _____	9
Figure 2-2 NASA FESS. _____	12
Figure 2-3 Flywheel design by Xiaojun Li [10]. _____	15
Figure 2-4 Topology of the five-phase BFSPM machine [16] _____	15
Figure 2-5 The angle between the rotor flux and the per unit current EMF in the stator. _____	18
Figure 2-6 The d-q axis of SM rotor [19]. _____	19
Figure 2-7 Sensing Current of Three Phase Machine. _____	20
Figure 2-8 phaser diagram of net current of three phase machine _____	20
Figure 2-9 Phaser diagram of measuring command vector current. _____	21
Figure 2-10 Convert 3-phase to 2-phase by Clarke transformation. _____	22
Figure 2-11 Transform d-q coordinate system to rotating d-q coordinate system by Park transformation. _____	23
Figure 2-12 The block diagram of permanent magnet synchronous flywheel. _____	24
Figure 3-1 The system which studied in [27]. _____	27
Figure 3-2 The structure of optimization system to manage the power by using FESS [28]. _____	28
Figure 3-3 MATLAB-Simulink schematic of the IWPS with FESS [29]. _____	29
Figure 3-4 Flywheel control diagram. _____	30
Figure 3-5 UPS system using flywheel to supply a critical load [30]. _____	31
Figure 3-6 A common DC bus topology proposed by TOODEJI [31]. _____	32
Figure 3-7 Control diagram of FESS with common DC bus [31]. _____	32
Figure 3-8 Hybrid Energy Storage System (HESS) Coupled to a Photovoltaic (PV) Plant [32]. _____	33
Figure 4-1 System topology of LV microgrid. _____	35
Figure 4-2 Microgrid components. _____	36
Figure 4-3 PV panel design and characteristic. _____	37
Figure 4-4 DC to DC maximum power point converter _____	38
Figure 4-5 V_d & V_q references. _____	39
Figure 4-6 Reference value of the real power and reactive power extracted from the	

inverter. _____	40
Figure 4-7 d-q reference currents for on grid mode. _____	41
Figure 4-8 d-q vectors generated from the controller for UPS mode _____	42
Figure 4-9 Control diagram of the inverter. _____	42
Figure 4-10 Converter Control Model of PMSM _____	45
Figure 4-11 Flywheel and its driver. _____	45
Figure 4-12 Flywheel units connected in parallel. _____	46
Figure 5-1 Power Flow in the system at variable radiation with compensate the power factor. _____	48
Figure 5-2 Power Flow in the system at variable radiation without compensate the power factor. _____	49
Figure 5-3 Constant DC voltage even when there is fluctuation irradiance. _____	50
Figure 5-4 Load voltage and current. _____	51
Figure 5-5 Grid Frequency on the Load Bus. _____	52
Figure 5-6 Flywheel speed (rpm), currents (Amps) and torque (N.m) at constant power flow to the network. _____	53
Figure 5-7 Direct and quadrature currents of flywheel and its referace value. _____	54
Figure 5-8 Power flow through all components at variable load and constant power flow from the inverter with power factor correction mode. _____	56
Figure 5-9 Voltage and Currents When Load And Radiation Is Variable. _____	57
Figure 5-10 Grid Frequency with fluctuating solar irradiation and variable load. _____	58
Figure 5-11 Status of system elements with fluctuating solar irradiation and variable load. _____	59
Figure 5-12 Flywheel speed (rpm), currents (Amp) and torque (N.m) at variable load and variable radiation. _____	60
Figure 5-13 Zoom in at secound 1 of Flywheel speed (rpm), currents (Amp) and torque (N.m) at variable load and variable radiation. _____	61
Figure 5-14 Direct and quadrature currents of flywheel with fluctuating solar irradiation and variable load. _____	62
Figure 5-15 Power flow at variable load and radiation when charging from the utility grid with compensating the power factor. _____	63
Figure 5-16 The DC bus voltage, irradiance and Flywheel speed when the system imports	

the power from the utility grid at variable radiation and variable Load. _____	64
Figure 5-17 The Grid frequency when the system extracts the power from the grid at variable radiation and variable load. _____	65
Figure 5-18 The current and voltage when The system extracts the power from the grid at variable radiation and variable load. _____	66
Figure 5-19 Speed, currents and torque of FESS when The system imports the power from the grid at variable radiation and variable load. _____	67
Figure 5-20 Id, Iq and referace value of Iq when the FESS charges from the grid. _____	68
Figure 5-21 Power flow in the system when variable radiation and variable resistive load, inverter produce power equals to demands. _____	69
Figure 5-22 Voltage, Current from the utility grid and currents to the load when the inverter covers the total load demand. _____	70
Figure 5-23 The status of DC voltage, radiation and the FESS speed, when the inverter covers the load. _____	71
Figure 5-24 Electrical frequency on the grid. _____	72
Figure 5-25 Actual speed, reference speed, current and Torque of FESS. _____	73
Figure 5-26 Iq , Iq and the referance Iq when the PV and the FESS cover the load. _____	74
Figure 5-27 system behavior through UPS mode with variable load and variable radiation. _____	76
Figure 5-28 Status of FESS element at UPS mode. _____	77
Figure 5-29 Frequency of the system at UPS mode. _____	79
Figure 5-30 Voltage and current profile of the system at UPS mode. _____	80
Figure 5-31 FESS speed, current and torque at UPS mode. _____	81
Figure 5-32 Flywheel Id, Iq and Iq referance at UPS mode. _____	82
Figure 5-33 System topology of FESS without PVs. _____	83
Figure 5-34 Flywheel speed through charging and discharging period. _____	85
Figure 5-35 Energy meter through charging and discharging period. _____	86

List of Tables:

Table 2-1 FESS specification [13]. _____	13
Table 2-2 Flywheel Specification by Xiaojun Li [10]. _____	14
Table 2-3 The PQ problems classified regarding their time range, IEEE Std-1159-2009. _____	25
Table 4-1 DC to DC boost converter specification. _____	38
Table 4-2 The specification of the three level inverter from ABB library. _____	43
Table 4-3 The specification of the FESS _____	46
Table 5-1 Energy flow and efficiency table. _____	85

List of abbreviation

AC: alternating current.....	17
BFSPM: bearing-less flux-switching permanent magnet.....	15
DC: direct current.....	17
DG: Distributed Generator	27
DOE: Department of Energy	25
EMF: electromagnetic field.....	18
ESS: Energy storage systems	6
HESS:hybrid energy storage system	33
Id: direct current	42
Iq: quadrature current	42
MG: Mirco-grid.....	2
PM: permanent magnet	19
PMSM: Permanent magnet synchronous machine.....	15
UPS: uninterruptible power supply	2
VSC: Voltage Source Converter	32

ملخص

يتميز التخزين بالحدافة بعمر افتراضي أطول من البطارية العادية، ويمكن أن توفر قدرة كهربائية عالية لفترة قصيرة. إن أنظمة تخزين الطاقة بالحدافة تمتلك العديد من الخصائص التي تجعلها عنصرًا مهمًا في شبكات الطاقة المستقبلية، وخصوصًا في الشبكات المحلية التي تحتوي على مصادر طاقة متجددة بشكل تكاملي. وفي هذه الأطروحة، سوف نقدم نموذج محاكاة مفصل للشبكة المحلية مع التخزين بالحدافة. بما يتيح لنا محاكاة مختلف المشكلات ضمن ظروف معينة. يتضمن هذا السيناريو الحالات المتصلة والمعزولة للشبكات المحلية، ومستويات عالية من مشاركة أنظمة الطاقة الشمسية. بحيث تضمن الحدافة استمرارية الطاقة الكهربائية في كل هذه الظروف، خاصةً أثناء الفصل عن الشبكة الخارجية عند حدوث انقطاع في المصدر الرئيسي.

في النماذج التقليدية للحدافة، يكون لكل حدافة في الشبكة عاكس متصل بالشبكة، وبالتالي فإن نماذج الحدافات ونظام الطاقة الشمسية مستقلان. تعد إضافة عاكس الحدافة على نفس خط التيار المستمر لمحطة الطاقة الكهروضوئية مساهمة علمية مهمة لهذه الدراسة في مجال تنظيم الطاقة، وذلك باستخدام عاكس ربط واحد مع الشبكة مما يؤدي إلى وجود نظام رخيص وفعال. بحيث يتم تشغيل إدارة تدفق الطاقة في هذا النظام من خلال خط التيار المستمر فقط. ويحدث هذا عن طريق توصيل أطراف التيار المستمر لعاكس الحدافة مع أطراف التيار المستمر لمحول استخراج الطاقة القسوى من الخلايا الضوئية.

Abstract

The fluctuating nature of many renewable energy sources introduces new challenges in power systems. As flywheel Energy Storage Systems (FESS) have many applications in these systems, since they have longer life span than a normal battery, and they can provide high power for short time, this will make them an important element for future power microgrids with integrated renewable energy sources. In this thesis, it will provide a detailed simulation model of microgrids with FESS in different scenarios including connected and isolated status of microgrids and high levels of PV penetration. Adding the FEES to the dc-bus of the PV inverter is the most significant contribution of this study; using one inverter leads to have a cheap and an efficient Flywheel.

In the traditional models of FESS every flywheel in the network has an on-grid inverter, so the flywheels units and the PV system are independent. But in this proposing model managing the power flow in this system will run into the DC bus only by connecting the FESS in the same DC bus of the inverters PV. FESS will ensure the continuity of electric power at all situations, especially during islanded mode when an interruption of the main source occurred.

Chapter 1. Introduction

Contents

1.1 Problem statement	3
1.2 Thesis Contribution	3
1.3 Thesis Organization	5

Energy is a very critical element for every country and can be used as an indicator on its development. Fossil-fuel energy sources have negative impact on the environment, while the renewable energy sources present an attractive alternative to cover the demand. Yet, there are challenges accompany the integration of renewable energy sources in the power grid. For instance, the intermittent nature of renewable energy sources (RES) represents one of the big challenges of these energy sources. This stimulates the researchers to find optimal approaches to utilize RES and increase its share in the power supply [1].

Solar energy is the cleanest source of energy. In addition to be the most economically viable energy source, the technology of power electronics has facilitated the process of controlling renewable energy. The progress in this area has achieved useful and excellent results in the case of on-grid connected inverter with low penetration levels [2].

Despite of all advantages of solar power plants, they still have some critical issues that reduce their usage as an alternative source of generation for electricity. The first one is the lack of continuity of the solar radiation. The second challenge is the instability of the intensity of solar radiation at a constant rate. In order to maintain the stability of production, it is important to use innovative approaches to store energy at high supply periods, and then to re-use later to maintain the stability.

However, the use of solar energy as the only source of electricity in an isolated area suffers from the low efficiency and economic feasibility. This is mainly due to the inefficiency of existing systems to extract and regulate the use of energy efficiently, e.g. to store surplus and then provide it when there is low supply. The use of batteries is infeasible in many scenarios as the frequent charge and discharge of the batteries reduces

significantly the lifespan of the battery.

Microgrid (MG) is intended to operate in the two different operating conditions; the first one is normal interconnected mode where the MG is connected to a main network, either being supplied by it or injecting some amount of power into the main system. The second one is an emergency mode where the MG operates autonomously, in a similar way to physical islands, when the disconnection from the upstream MV network occurs [3].

FESS is an electric machine operates at charging mode as a motor, in this mode; it converts the electrical power into mechanical power. While in the discharging mode it operates as a generator and converts the stored mechanical power into electrical power. FESS operates at low and high frequencies, a back to back converter converts variable frequency to custom frequency and vice versa, this converter runs through two steps: the first step is to convert AC current to DC current and vice versa, then the second step is to invert DC current to AC current. The second step uses the same topology of PV panel converter [4].

This FESS operates on-grid with PV panels in the same DC bus. At the sunny hours, the inverter supplies the load and charges the Flywheel, then it works as UPS system at sunset or in long cloudy hours. FESS is a popular ESS in the short and medium term (from seconds to minutes), that can be used in isolated wind plants and PVs [5]. This isolated grid has three scenarios to work; the first one is when the PV panels produce the power and is regulated by FESS. The Second scenario is when the main supply is disconnected, and FESS works as UPS until diesel generator is ready to cover the load. The third scenario is when the PV panels work in high penetration level in the Microgrid. So, FESS regulates the voltage profile and frequency. In this case, changing in solar radiation or changing the load or both won't affect the system. The design should be able to manage these three scenarios.

This thesis aims to investigate the performance of the FESS in a microgrid. The performance will be evaluated regarding efficiency which in section 5.6, reliability by working as UPS system which in section 5.5, and the stability of the grid (e.g., voltage profile, frequency) which in Chapter 5. Different scenarios will be explored, e.g. the effect

of changing of solar radiation and/ or load on the performance of the grid will be studied.

This study will highlight the significance of using FESS in different scenarios, where we are going to present several metrics such as voltage profile and supply continuity.

To reduce the system cost, it is proposed to use the same DC bus of PV panels, the same on-grid inverter of PV system, so the common back-to-back converter with the standard decoupled d-q controller is used. The energy is stored by the inverter based on a flywheel for improving power quality and reliability of a power distribution system.

1.1 Problem statement

In traditional FESS there are two bidirectional inverters that convert from AC to DC and vice versa. One of them is connected between the grid and the DC bus. The other is connected between the flywheel machine and the DC bus. This is like PVs panel which has an on-grid inverter between the MPPT DC converter and the grid.

In the conventional system, in case of charging the FESS by extra power produced from the PVs, the system needs to save it in a storage system. The sequence of saving this power will be shown in the following steps:

PV on-grid inverter converts the power from the DC bus of PV panels to AC synchronized with the utility grid.

FESS on-grid inverter converts the AC power from the grid to DC again when it is charging.

The flywheel driving circuit converts the DC power from the Flywheel DC bus in its inverter to AC for the flywheel.

FESS on-grid inverter converts the DC power from flywheel DC bus to AC synchronized with the utility grid, when it is discharging.

1.2 Thesis Contribution

In the proposed new system, these steps above were reduced to increase the system efficiency. The current flow path will be changed from the MPPT converter of PVs to the flywheel drive inverter directly.

In the new proposed topology, the on-grid inverter for PVs and FESS will be the same as shown in Figure 1-1, so the sequence of power flow will be as follows:

The flywheel driving circuit converts the DC power from the PV DC bus in its inverter to AC for the flywheel.

PV on-grid inverter converts the power from the DC bus of PV panels and flywheels to AC synchronized with the utility grid, when it is discharging.

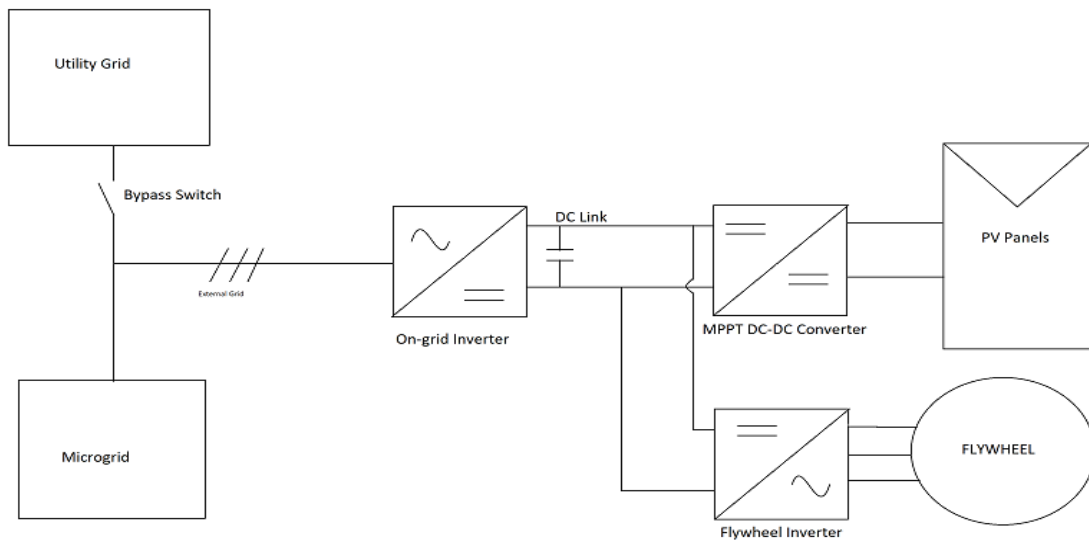


Figure 1-1 New system topology.

It is clear that, the proposed system skips over two of the steps of power conversion. Therefore, the efficiency should be improved when the flywheel is used to regulate the PV power.

The FESS characteristics represent an appropriate method for regulating the microgrid power quality, especially when it works in UPS scenario [1]. Detailed MATLAB Simulink will be presented, which contains load, supply, PV and FESS. The FESS will secure the continuity of power to the load during different scenarios. The following scenarios will be studied:

- Fluctuating PV supply.
- Step changing in the load.
- 100% of PVs penetration level.
- Power factor correction in the utility grid.
- Interruption from the main grid and operating as UPS.

1.3 Thesis Organization

The rest of this thesis is organized as follows. Chapter 2 discusses the differences between the energy storage systems. Chapter 3 presents designs of the FESS and its applications. Chapter 4 discuss all FESS types and presents related work. Chapter 5 defines the microgrids and the power quality issues that effected by adding FESS. Chapter 6 shows how to create a system modeling in using MATLAB/SIMULINK. Chapter 7 concludes the studied scenarios and its results. At last, chapter 8 discusses the conclusion.

Chapter 2. Energy Storage Systems (ESS) And Microgrids

Contents

2.1 Batteries	6
2.2 Electromechanical Capacitors	7
2.3 Pumped Hydros	7
2.4 Compressed Air Energy Storage (CAES)	8
2.5 Flywheel Energy Storage System (FESS)	10
2.6 Microgrids	24

Energy can be stored in a mechanical, electrical, thermal or electrochemical way. The electrochemical methods, in particular batteries, have drawn considerable attention in the last decades due to the high cycle efficiency of these devices. In this chapter, the types of energy storage systems (ESS) and its characteristics discussed to make it comparable with FESS.

2.1 Batteries

Batteries are currently the most popular devices to save energy, which is generated by renewable sources. These battery systems are known as stationary energy storage devices. In addition, batteries are also using for providing mobile devices with energy. However, the increase of batteries sales is hard to be predicted due to factors such as cost, technology, infrastructure, consumer acceptance and governmental regulations [5].

2.1.1 Battery For grid-scale energy

Dehghani-Sanij *et al* [6] reviewed a battery system for grid-scale energy, grid scale battery able to have a large power to reach to the peak load and fast response. There are two types suitable for micro-grids, which are flow batteries and Sodium-Sulphur batteries.

Flow batteries (redox flow batteries RFBs): They have electro-active materials, which are dissolved into a liquid electrolyte, electric current passes through the reduction

and oxidation reactions occurring in separate half-cells. It is easy to control the power by the cell stack, no self-discharging, easy monitoring and flexible design capability. Although it is quite expensive storage system.

Sodium-Sulphur (Na-S) batteries: They are high temperature batteries using liquid sodium and Sulphur. In general, they are low cost, high energy density, flexible operation, and have high life cycle. However, the main drawback is the high temperature.

2.1.2 Wide range application batteries

1) *Zinc-carbon (Zn-C) batteries*

In 2004, the ratio of zinc-carbon batteries in the European market was around 39% [7]. They are low cost and have variety of design for different applications. The main disadvantages of these batteries are their low energy density, high drop voltage, poor leakage resistance, and proper landfill disposal [6].

2) *Alkaline batteries*

Their design is like the Zn-C batteries, but their performance is factor of two to ten than the Zn-batteries. They have low temperature and high performance, long life and low cost [8].

3) *Lithium Cells*

Lithium cells have dominated high-performance with high voltage, long life, flat discharge and good power density [9].

2.2 Electromechanical Capacitors

These are special type of capacitors, which are also known as super capacitors. They have high power in very short bursts. Therefore, they save low amount of energy.

The advantages of electrochemical capacitors are very high life cycle, high efficiency and high power. But the disadvantages are short discharge time, fast decreasing voltage due to low specific energy.

2.3 Pumped Hydros

Pumped hydros storage system is used for large-scale grid in power systems. Such system works in two modes, which are “pumping mode” and “generating mode”. The

storage system works in “pumping mode” when production from the renewable energy sources is increased or the load is decreased. The pumps pump the water from the lower reservoir to the upper reservoir to store the energy as kinetic energy. Therefore, during the peak hours of the electric load the system works in “generating mode” by releasing the water [10].

2.4 Compressed Air Energy Storage (CAES)

At charging process during the periods of low power demand the surplus electricity drives a reversible motor-generator unit to run chain of compressors for injecting air into a storage vessel. For large-scale systems, a high-capacity underground salt cavern is used, where the energy is stored in the form of high-pressure air. The pressure typically 40 to 80 bar for small systems. An over ground air tank can be used for the compression process and it is normally used in two coolers. Coolers are used to reduce the working temperature of the injected air. Thus, improving the compression efficiency in minimizing thermal stress on the system component, since the pressure of compressed air on the walls in over ground tank is up to 300 bar.

At the discharging process when the power generation cannot meet the load demand, the stored compressed air releases heat and heating by a heat source which can be the heat generated from the combustion of fossil fuel or the heat recovered from the compression process.

The turbine captures the compressed air energy. A recuperator unit can also recycle the waste heat from the system exhaust. The same process takes place in the case of over ground air tank. The system discharges the high price electricity generated, which can be sold to the grid [11] as shown in Fig. 2.2 below.

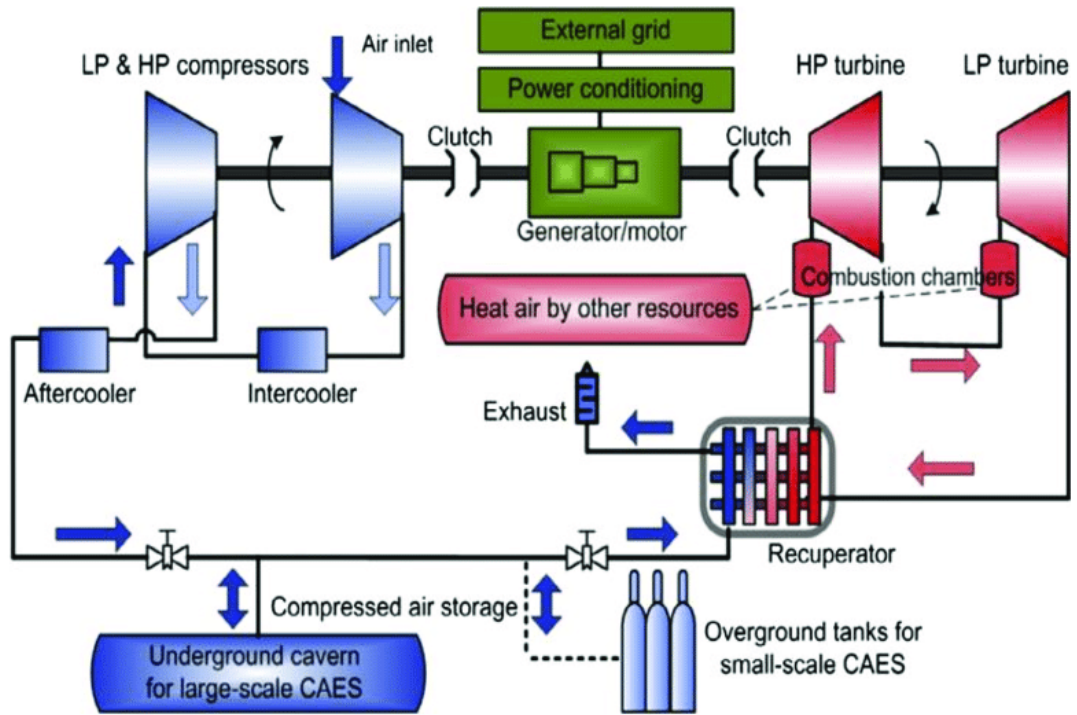


Figure 2-1 Compressed Air Energy Storage components [11].

2.5 Flywheel Energy Storage System (FESS)

Flywheel energy storage system (FESS) converts electric energy to mechanical rotational energy. Flywheels classified mainly into two types: it could be low speed with a high mass or high speed with a low mass which is the better due to high density of energy. Flywheels in general manage the energy flow rapidly with low limitations. They convert the electric energy into kinetic energy with a very high- response speed. There is a big difference between the limitations on FESS and Battery Storage Systems (BSS), as in FESS the limitation is in the power ratings and audible noise while in batteries the limitation is the chemical reaction rate.

Flywheel converts the electrical energy to rotational mechanical energy, the amount of this energy is the speed of rotational inertia as given in equation (2-1), the power is the rate of changing in this speed, so the power flow in the flywheel is due to the change in speed.

The energy equation is written by:

$$E = \frac{1}{2} m \cdot v^2 \quad (2-1)$$

Where; E : kinetic energy m : mass.
 v : rotational velocity.

The instantaneous power of an angularly accelerating body is:

$$P = T * \omega \quad (2-2)$$

$$\text{In addition, } v \text{ can be expressed as: } v = r \omega. \quad (2-3)$$

Where:

r : radius of the wheel w : angular speed.

So, the equation and be rewrite in this form

$$E = \frac{1}{2} m \cdot (r \cdot \omega)^2 ; \quad (2-4)$$

The flywheel mass is equal to the density multiplied by the volume.

$$m = \rho \cdot \text{volume}; m = \rho \cdot \pi \cdot l \cdot r^2; \quad (2-5)$$

Where

ρ : density of the wheel; l : length of wheel (height of the wheel);

r : radius of the wheel.

But the polar moment of inertia can be written as

$$J = \int r^2 \cdot dm = m \cdot r^2. \quad (2-6)$$

Where J : wheel inertia. m : mass of the wheel.

So, Equation (3) Becomes

$$E = \frac{1}{2} J \cdot \omega^2 \quad (2-7)$$

2.5.1 NASA FESS Model Specifications:

NASA Glenn Research Center [12] designed a flywheel storage system for laboratory environment. This flywheel is 1 kW, 60000 rpm and 525 W-h has 90% efficiency with 90 minutes of charge/s. They developed this device for an aerospace energy storage and international power and attitude control (IPACS) applications. This module includes magnetic bearing, touchdown bearing, high density titanium rim of the rotor which are two poles and mounted on the hub of the rotor, generator/motor and vacuum house as shown in the Figure 2-2 below.

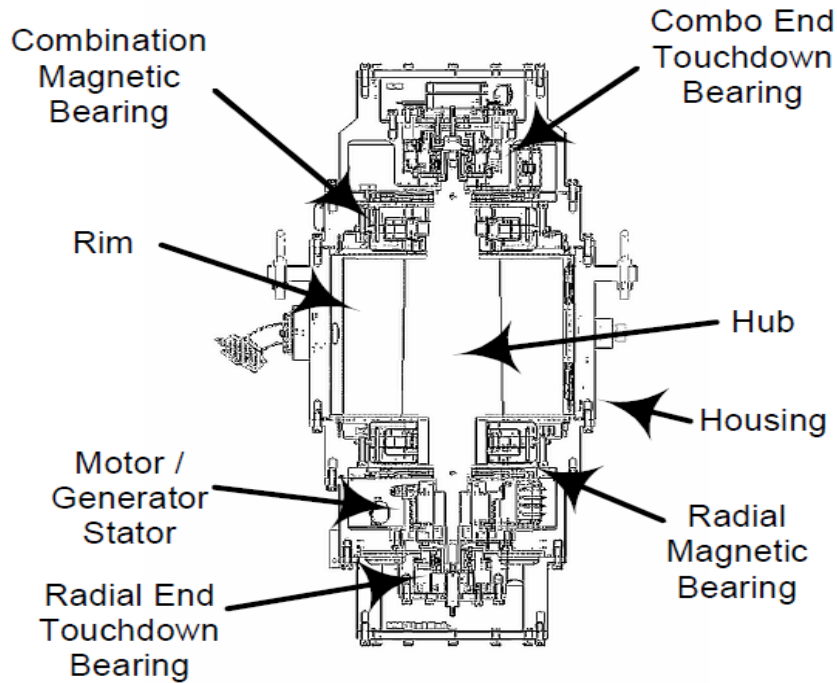


Figure 2-2 NASA FESS.

2.5.2 Electrical model of permanent magnet synchronous machine (PMS) :

Carrillo *et al.* [13] managed to design a coreless permanent magnet flywheel machine. The system is developed practically, and they took efficiency measurement and obtained 98%. The design has the following mechanical and electrical specifications in the table below:

Table 2-1 FESS specification [13].

Motor/Generator Mechanical Specifications			Motor/Generator Electrical Specifications		
Parameter	Quantity	Unit			
Outer rotor diameter	2133.6	mm	Winding type	concentric	-
Air-gap/groove stack height	50	mm	Number of phases	3	-
Motor/generator stack length	50	mm	DC bus voltage	600	V
Magnet height	25	mm	Maximum allowed current density	<5	A/mm ²
Air-gap/groove outer diameter	1904.4	mm	<i>Number of poles - Number of slots</i>		<i>Average Torque (N.m)</i>
Air-gap/groove inner diameter	1842.5	mm	24 poles-36 slot		158
Winding height	50	mm	48 poles-72 slot		167
Magnet thickness	15.54	mm	50 poles-75 slot		168
Number of turns for each coil	40	-	60 poles-90 slot		176
Magnet type	NdFeB48	-	64 poles-96 slot		195
Magnet embrace	0.72	-	<i>Speed (rpm)</i>	<i>Current (A)</i>	<i>Current density (A/mm²)</i>
Cooling system	Air cooler	-	5000 (rated)	210 (rated)	3
			4000	220	3.3

The machine supplies 100 kW over an hour with decreasing in the rotor speed from 5000 rpm to 1928 rpm.

Arghandeh *et al.* [14] designed a MATLAB SIMULINK for UPS flywheel application, they built model by comparing simulation results with manufacturer supplied data. They used the FESS for a critical load, the microgrid in this study contains a diesel generator, Flywheel provides a security for a critical load.

Xiaojun Li *et al.* [15] developed a low-cost design of flywheel, they introduce their design as a commercially viable flywheel energy storage technology. The model is 100 kW power with 100 kWh capacity and 5443 kg weight. More specification details in the Table 2-2 below.

Table 2-2 Flywheel Specification by Xiaojun Li [10].

Parameter Name	Quantity	Unit/standard
Outer diameter/ Height	2133/203	[mm]
Mass	5443	[kg]
Moment of inertia	3087	[kg·m ²]
Rotational speed	5000	[rpm]
Tip speed	558	[m/s]
Energy/Power capacity	100/100	[kWh/kW]
Materials	4340	AISI
Material tensile strength	1500	[Mpa]
Linear relative permeability	200	-

The special in this design is a shaft with a hole through its center, its shaft-less, hub-less and high strength flywheel. On the top of the flywheel there is a combination active magnetic bearing which is suspense the rotor. These components work in a vacuum chamber. The electrical driver of this flywheel is a six-step current-regulated voltage source current as shown in Figure 2-3 below.

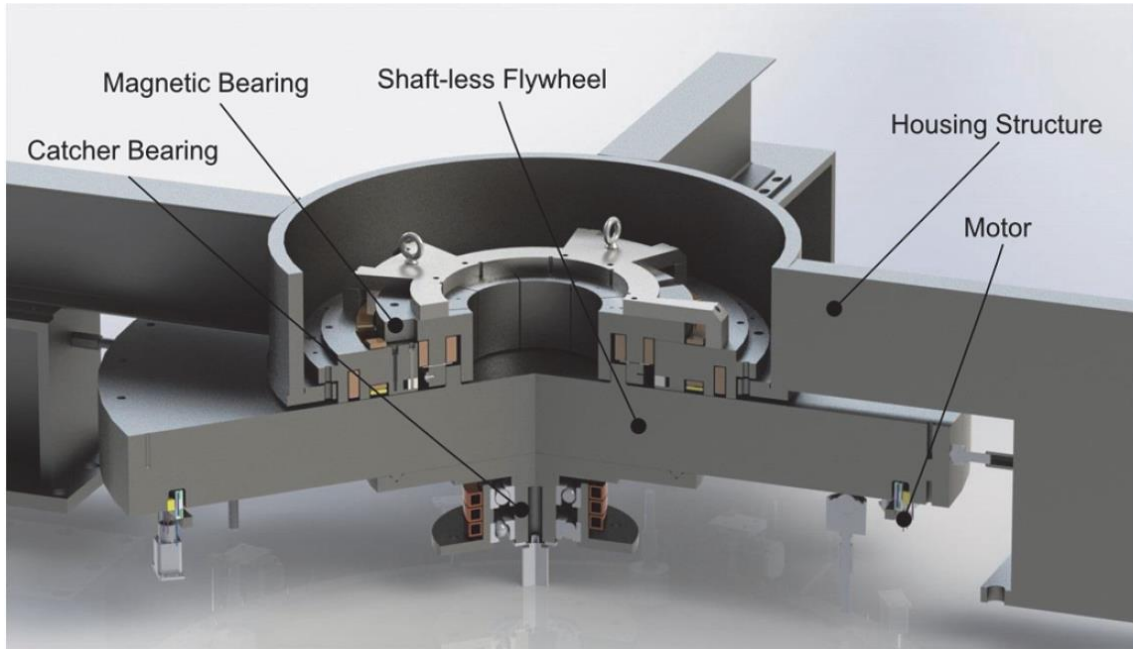


Figure 2-3 Flywheel design by Xiaojun Li [10].

Sun *et al* [16] improve the electromagnetic performance of the FESS, they design a five-phase bearing-less flux-switching permanent magnet (BFSPM) machine with E-core stator as shown in the Figure 2-4 below. So, they improve of the torque and suspension force with increased amplitude and smaller fluctuation.

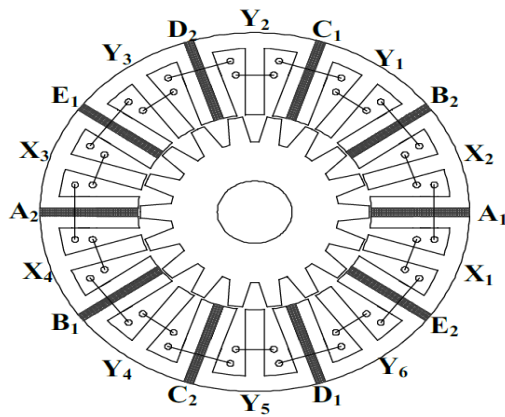


Figure 2-4 Topology of the five-phase BFSPM machine [16]

The equation of PMSM with Park transformation can be represented as [17]:

$$v_q = R_s i_q + \frac{d}{dt} \lambda_q - \omega_r \lambda_d \quad (2-8)$$

$$v_d = R_s i_d + \frac{d}{dt} \lambda_d - \omega_r \lambda_q \quad (2-9)$$

$$\lambda_q = L_q i_q \quad (2-10)$$

$$\lambda_d = L_d i_d + \lambda_f \quad (2-11)$$

Substituting equations (2-10) in (2-8), and (2-11) in (2-9)

$$v_q = R_s i_q + L_q i_q - \omega_r L_q i_q \quad (2-12)$$

$$v_d = R_s i_d + (L_d i_d + \lambda_f) - \omega_r L_d i_d \quad (2-13)$$

The developed torque is given by

$$T_e = \frac{3}{2} p (\lambda_d i_q - \lambda_q i_d) \quad (2-14)$$

$$T_e = \frac{3}{2} p (\lambda_f i_q - (L_d - L_q) i_q i_d) \quad (2-15)$$

$$T_e = B_v \omega_m + T_l + J \frac{d\omega_m}{dt} ; \quad (2-16)$$

But in the flywheel $B_v \cong 0$; and $T_l \cong 0$; so

$$\text{So, } T_e = J \frac{d\omega_m}{dt} ; \quad (2-17)$$

$$\omega_m = \omega_r \frac{2}{p} \quad (2-18)$$

v_q : is the q component of the voltage. v_d : is the d component of the voltage.

λ_f : is the PM flux linkage.

R_s : stator resistance. i_q : q axis current. i_d : d axis current.

ω_r : Angular velocity of electrical magnet field in the rotor.

ω_m : the rotor mechanical speed (synchronous speed).

J : the inertia of flywheel.

λ_q, λ_d : the q and d component amplitude of the flux induced by the permanent magnets of the rotor in the stator phases.

p : number of electrical poles. J : flywheel inertia.

T_e : electromagnetic torque. B_v : viscous damping.

T_l : Input Torque (mechanical coupling torque which is zero in the flywheel).

2.5.3 Machine Drive Design:

1) *Machine drive methods:*

Machine drive methods have been improving continuously side by side with power electronic renaissance, at the beginning of last century. Machine drive was limited to DC machine drive, due to its linearization characteristic between speed and voltage, but the weight and the maintenance cost of DC machine have promoted the designer to improve AC machine drives. AC machines are cheaper, less maintenance, less weight, and less size than DC machine [18].

Due to the advancement of power electronics, most systems nowadays use AC machines. Now, the well-known types of AC machines are synchronous and induction machines. Although it has great torque-speed characteristic, synchronous machine is used in few applications due to high requirements of the transient period at starting. Induction machine is used in large applications due to its simple starting and controlling with slip control or scalar control V/F. But this has not precise results because the speed changes with slip.

Four steps illustrate the simple process of current mode control. These steps constitute the process of performing current mode control. In the controller processor each step can be done thousands or even ten thousand times every second.

These steps are the process of a simple PI current controller:

Measure and take the sample reading of the current which already flowing in the machine.

Compare between the measured current and the desired current and generating the error signal.

Simplify the signal to generate a correction voltage.

Control the current by using voltage. If the current is low, the voltage must increase and vice versa.

These currents in space vector diagram create a current vector with a certain magnitude and a certain angle. So, by controlling these 3-phase currents to be the right values. Controller can create a current vector to be in any angle and any magnitude that it wants. So, the question is 'What angle and magnitude should the controller look for to

drive the machine?

The torque produced by PMSM in Equation (2-19) is a function of the angel between the rotor flux and the current EMF in the stator as shown Figure 2-5. It has zero torque at zero degree. When the current vector is on top of the flux vector, either at +90 degree or -90 degrees it can be observed, at that point, the maximum amount of torque can be obtained for given moment current. So, we should try to orient our stator current EMF vector to be 90 degrees with respect to the rotor flux if this is achievable.

$$T_{en} = \frac{3 V_{\phi} E_A}{X_s \omega_s} \sin \delta \quad (2-19)$$

Where T_{en} : is torque produced by PMSM, V_{ϕ} :is the terminal voltage,

E_A : EMF voltage

ω_s : angular speed of the rotor.

δ : the angel between the rotor flux and the current EMF in the stator.

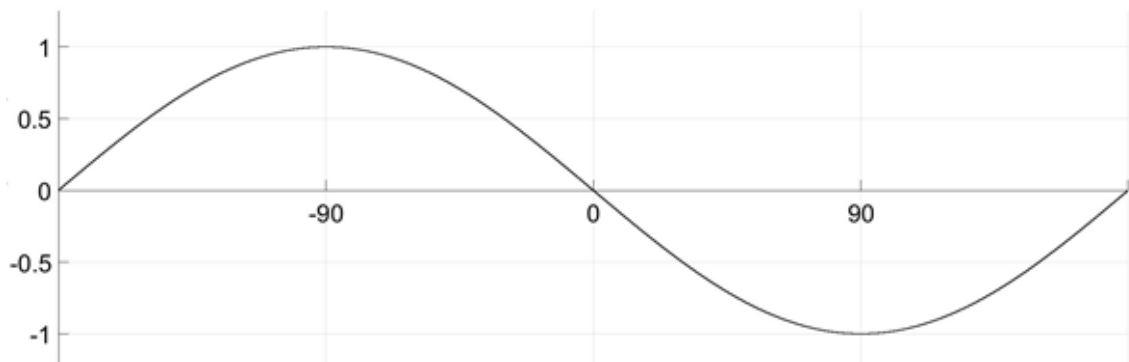
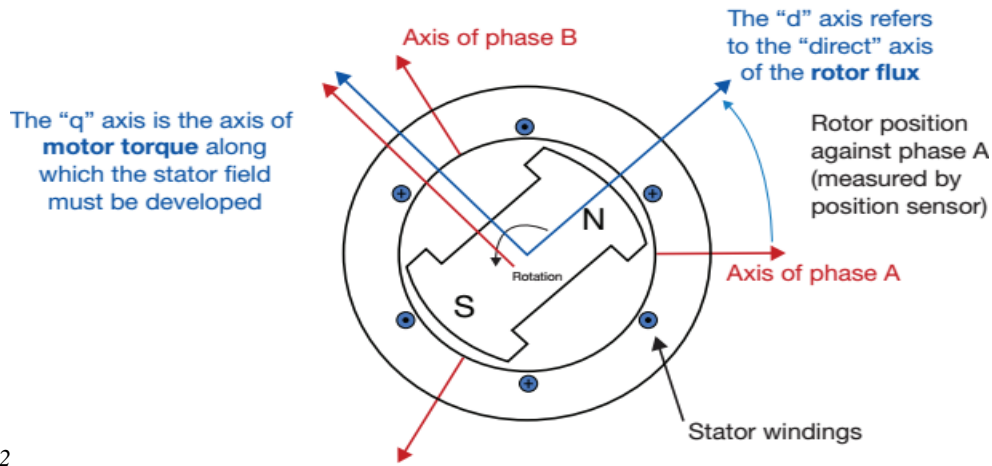


Figure 2-5 The angel between the rotor flux and the per unit current EMF in the stator.



2

Figure 2-6 The d-q axis of SM rotor [19].

The torque equation (2-20) is the applied torque of 3-phase PM machine, which is proportional to the product of the rotor flux times the component of the stator current factor, which is 90 degree with respect the rotor flux to control the torque of the machine. The controller shouldn't change the angle of the stator current factor with respect to the rotor flux. It always leaves that at 90 degrees because this gives maximum torque for Amp. Instead the amplitude of stator current factor is regulated.

$$Torque = \frac{3P}{2} \frac{1}{2} [\lambda_{dr} I_{qs}] \quad (2-20)$$

λ_{dr} : direct component of rotor flux; I_{qs} : quadrature component of stator current factor.

So, to do this on a digital process, it can give something like subroutines to measure rotor flux angle, then calculate the current of Phase A, Phase B and Phase C to create a vector to be 90 degrees with measured rotor flux angle. a interrupt is called. By this time the rotor has moved to a different angle. So, the processor needs to read the new angle then recalculate the current values again over and over. This is the brief process of field-oriented control.

2) The Process of field-oriented control of PMSM:

Controllers do not need to measure all three phase currents as show in Figure 2-7. If the scalar value of the current is measured in any two phases the current of the third

phase can be calculated.

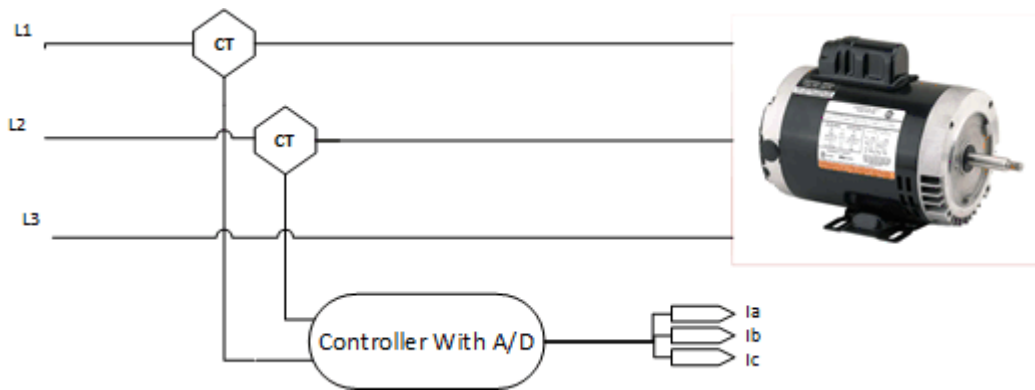


Figure 2-7 Sensing Current of Three Phase Machine.

The scalar values of these currents can be reflected along the magnetic axes for each one of the phases as shown in the Figure 2-8.

So, take the scalar reading for phase A that goes along the A axis, the same thing in phase B and take both amplitudes and negate them then reflect them in C axis. Now three current vectors can be calculated. you can create a net current vector which is represents the quadrature current in the stator, and the controller needs this vector to be oriented by 90 degrees with respect to rotor flux.

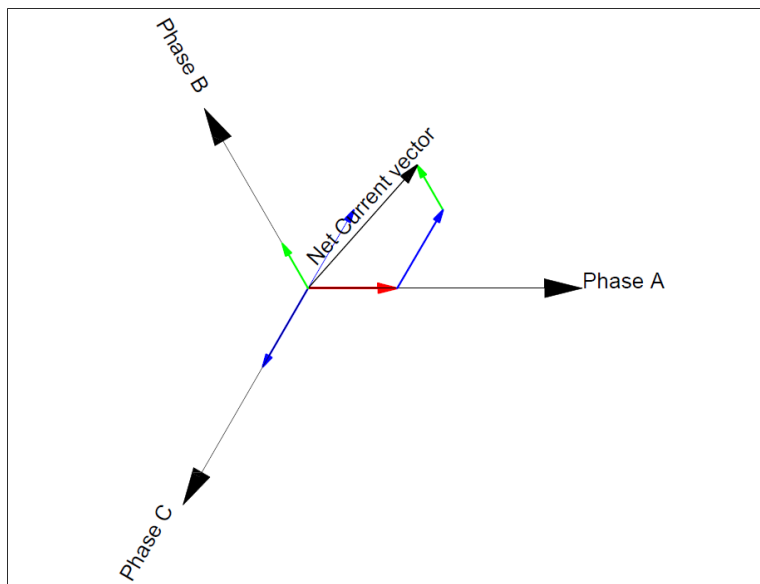


Figure 2-8 phaser diagram of net current of three phase machine

3) Compare the measured Current (vector) with the desired current (Vector) and

generate error signal.

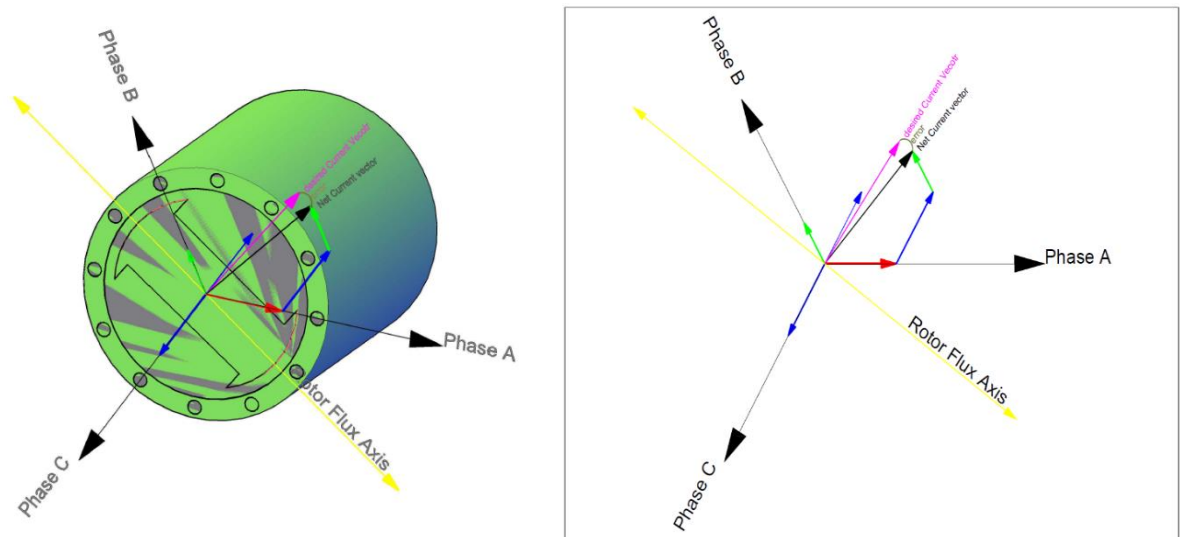


Figure 2-9 Phaser diagram of measuring command vector current.

The flux angle is the rotor angle which captured from a sensor (encoder in the rotor). This is the reason to call this machine a “synchronous Machine”, because the angle of rotor flux never changing with respect to angle of the rotor. The desired current vector must be perpendicular to the flux axis, which is called “direct” or “d” axis.

If it has a calculated current vector from the current sensors, we also need to know the desired current vector from the encoder, the error is the deference angle between them as shown in Figure 2-9 . so the processor correct this by regulating the input current i_a , i_b and i_c to the right value, so that it moves stator currents vector to be on the same axis with commanded current vector.

In order to specify the rotor, angle system needs a coordinate system with two axes not three. In reality we have with a 3-phase machine, but it has a redundant phase, it can simplify the calculation by converting 3-phase machine into a 2-phase machine, so you can actually think of the machine as a 2-phase machine, where the coil was reminding 90 degree with respect to each other, so it has a sine coil and cosine coil, now obviously it is not changing the machine which changes how it look, so it is going to create 2-axis: the first one is alfa α , and the second one is beta β -axis by equation (2-21). Then it take 3-phase currents and translate those into the equivalent α , β coordinates, which is called

Clark transformation and the equation is to do this is very simple as shown in Figure 2-10.

$$i_\alpha = \sqrt{\frac{3}{2}} i_a; \quad i_\beta = \frac{\sqrt{2}}{2} i_a - \frac{\sqrt{2}}{2} i_c; \quad (2-21)$$

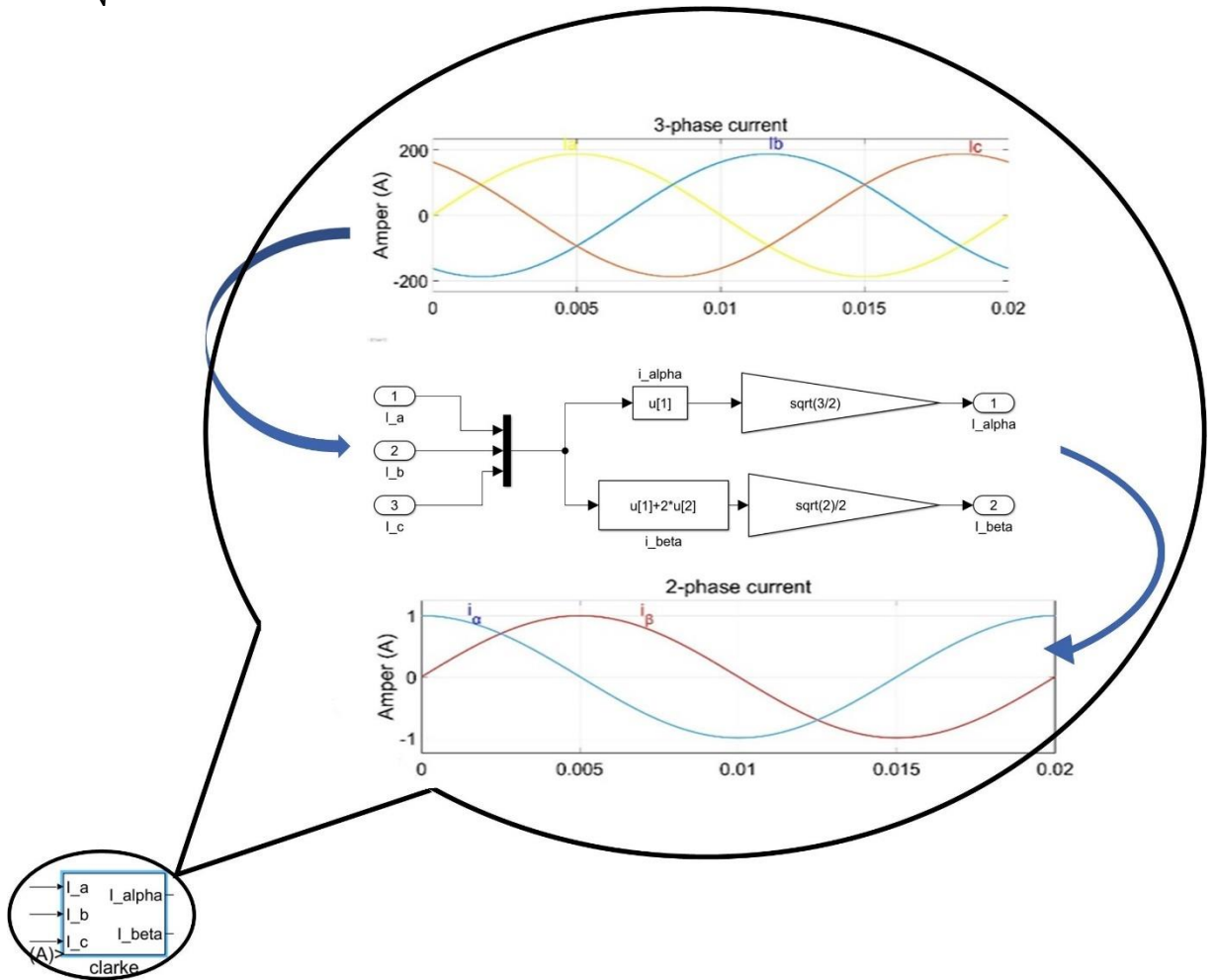


Figure 2-10 Convert 3-phase to 2-phase by Clarke transformation.

Let's take alfa and beta currents and represent them in another coordinate system that is actually rotating synchronously with the rotor flux, the most common orientation of this rotating reference frame one where one of these axis is line up directly with rotor flux angle that's why that particular axis is called d-axis and the quadrature axis with respect to that is called q-axis, the process of doing this is referred to the forward park transformation, and the equation (2-22) represents this transformation.

$$i_d = i_\alpha \cos \theta_d + i_\beta \sin \theta_d; \quad i_q = -i_\alpha \sin \theta_d + i_\beta \cos \theta_d; \quad (2-22)$$

Now, the system needs to take the angle of the rotor flux with respect to ‘A’ magnetic axis and we have to do some gematric calculation with that, in most cases we just simply use a lot of table in memory to drive this angle, but still does require a little bit math more than the forward Clark transformation.

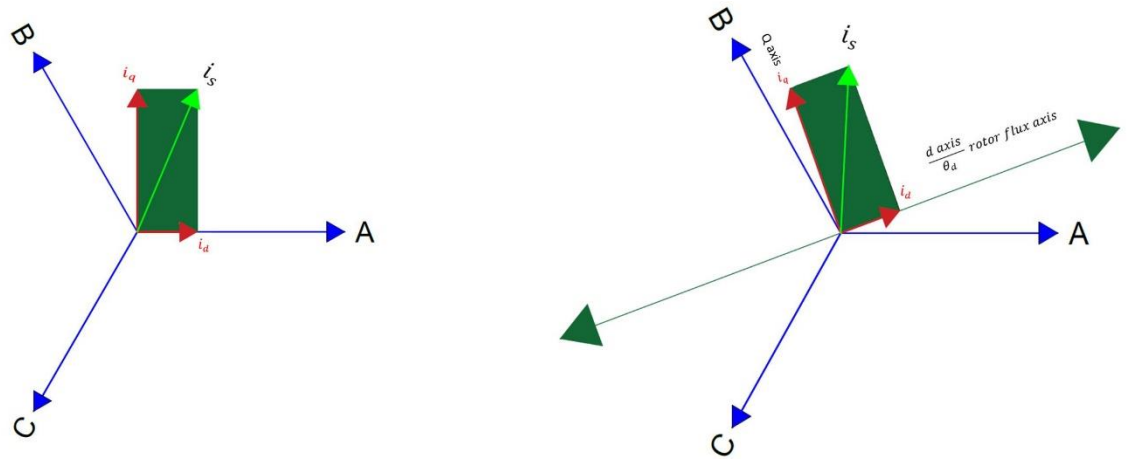


Figure 2-11 Transform d-q coordinate system to rotating d-q coordinate system by Park transformation.

So you can see in Figure 2-11 how to use Clarke transformation to simplify the current regulation process, once again the phase currents are measured, the forward Clarke transformation turn those currents into two equivalent currents, which exist on alfa and beta references and the system do the regulation in the reference form to compare these current to desired current to generate correction voltages in the V_α and V_β .

The reverse Clarke transformation uses to turn V_α and V_β voltages in the 3-phase voltages, then the system can drive the 3-phase machine. So, you can see the driver has reduced the currents regulated from three to one [20]. The control diagram of vector control for PMSM as shown in Figure 2-12.

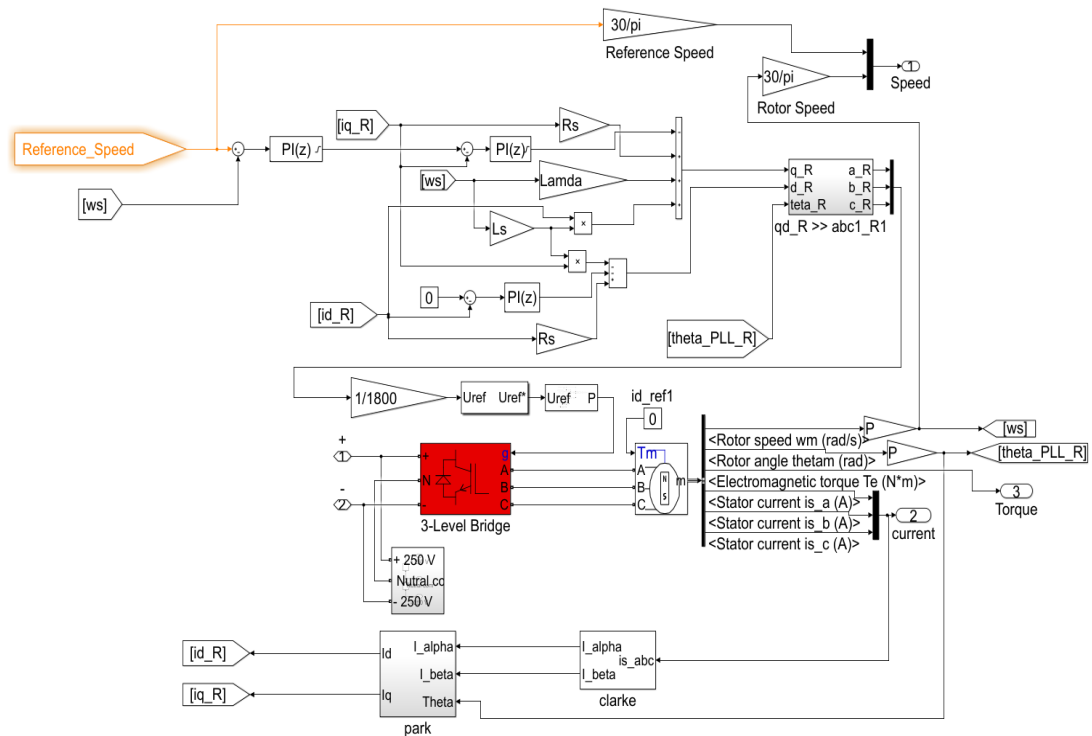


Figure 2-12 The block diagram of permanent magnet synchronous flywheel.

2.6 Microgrids

2.6.1 Definition

There are several definitions of Microgrids. One of the most well-known of them is according to United States Department of Energy (DOE), which is “A microgrid is a group of interconnected loads and distributed energy resources within clearly defined electrical boundaries that acts as a single controllable entity with respect to the grid. A microgrid can connect and disconnect from the grid to enable it to operate in both grid-connected or island-mode” [21].

Other researchers construe it into more than one sides like Lasseter [22]. He explicates Micro-Grids:

Critical Components of Micro-grids:

2.6.2 Power quality in Microgrids

Table 2-3 summarizes voltage related power quality issues.

1) Voltage Sag

The voltage drops below the accepted range for very short time period is called voltage sag. According the IEEE standard, the voltage sag occurs if the voltage drops between 10 and 90% for less than one minute [23].

Voltage Sag is one of the main reasons for malfunctions of low-voltage electrical devices. In major systems, usually uninterruptible power supply (UPS) or power conditioners are used to prevent voltage sags [23].

The reasons lead to voltage sags:

2) *Voltage Swell*

The increase of the voltage beyond 110% of the nominal voltage for less than one minute is called voltage swell. It is one of the main reasons for malfunctions of low-voltage electrical devices. In major systems, they use uninterruptible power supply (UPS) or power conditioners to limit the effect of voltage swell [24].

The reasons lead to voltage swell:

3) *Overvoltage*

The increase of voltage beyond 110% of the nominal voltages and continued for more than one minute. It can cause damage for of low-voltage electrical devices [25].

There are three types of overvoltage:

4) *Voltage Interruption.*

Voltage interruption occurs if the voltage drops below 10% of nominal voltage and lasts less than one minute.

The reasons lead to voltage swell:

Table 2-3 The PQ problems classified regarding their time range, IEEE Std-1159-2009.

<i>Voltage Event</i>	<i>Magnitude</i>	<i>Duration</i>
<i>Sag</i>	<i>90 % -10 %</i>	<i>≤ 1.0 min</i>
<i>Undervoltage</i>	<i>90 % -10 %</i>	<i>> 1.0 min</i>
<i>Interruption</i>	<i>< 10 %</i>	<i>≤ 1.0 min</i>
<i>Sustained Interruption</i>	<i>< 10 %</i>	<i>> 1.0 min</i>
<i>Swell</i>	<i>> 110 %</i>	<i>≤ 1.0 min</i>
<i>Overvoltage</i>	<i>> 110 %</i>	<i>> 1.0 min</i>

5) *Power Factor*

Power Factor is the efficiency of incoming power which is used in your electrical system. Or, is defined as the ratio of real power to apparent power. In major system a power factor correction controller is used to improve the power factor. This power factor correction may be capacitor banks or permanent magnet synchronous machine, STATCOM, or on-grid inverter of Distributed Generator (DGs) [26].

Chapter 3. Related Work

Contents

3.1 Flywheel Energy Storage System (FESS) in power system.	27
3.2 Common DC bus topology with FESS	31

3.1 Flywheel Energy Storage System (FESS) in power system.

Hamsic *et al* [27] used the FESS to increase the penetration level of renewable energy. They used it in isolated grid, which has diesel generator and wind turbine as shown in Figure 3-1 below. They measured the effects of adding the FESS for a one year, and it noticed that FESS decreases the limitation of penetration in the system. They showed clearly that the fuel usage is decreased, the system stability is increased, and the power quality is improved. But this is high cost and its not coupled with RES.

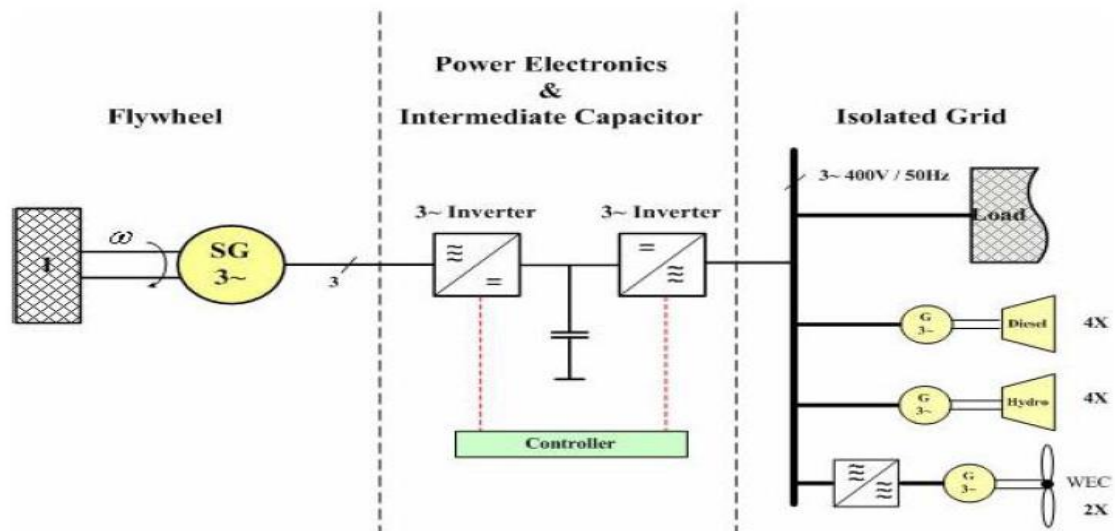


Figure 3-1 The system which studied in [27].

Awad *et al* [28] explored the optimization methods to manage the energy in the power grid by using FESS. It is clear that next generation of power systems will have high penetration levels of renewable sources. They suggested a smart system consists of linear programming based of moving average by FESS to solve the fluctuating nature in

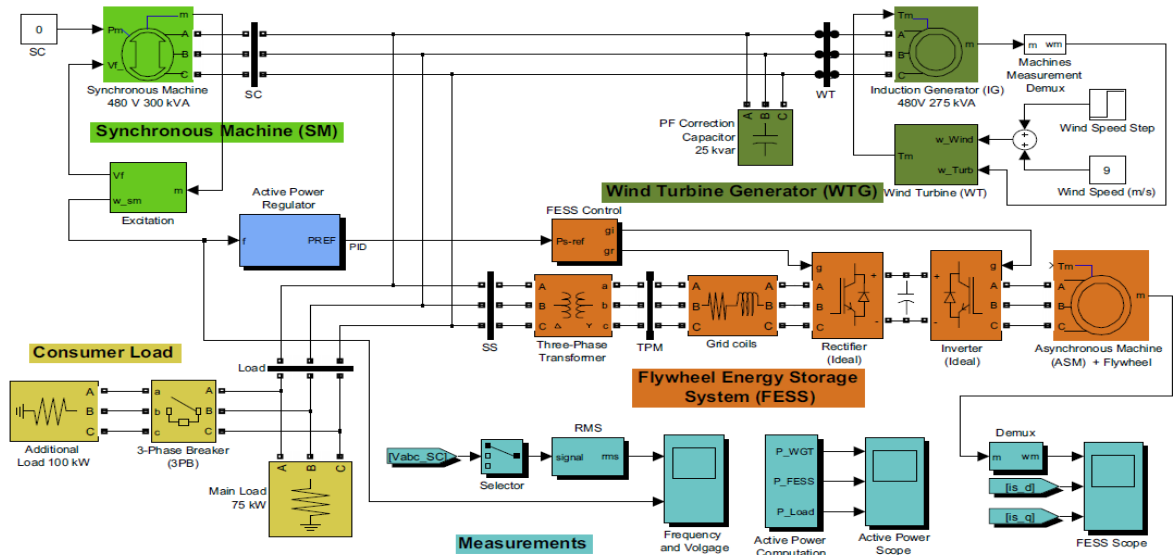


Figure 3-3 MATLAB-Simulink schematic of the IWPS with FESS [29].

In [13], the medium- and short-term FESS energy storage system used a simple flywheel coupled to asynchronous generator and spanned at low speed. They obtained a constant speed with only 5% variation, where a clutch is used as the connector between the diesel generator and the flywheel.

For maximum energy capture from PV panels, in [27] and [30] they used flywheel in case of stand-alone systems. In [27], they studied the case with FESS and BESS, where the system is an isolated hybrid system with high penetration level of PV panels. The results of simulation over one-year period proved the positive effects of adding FESS and any other storage systems. It is clearly appeared in the power system stability, the diesel fuel consumed, the PV panel penetration level, and the power quality.

Zhou et al [23] [24] developed a model control of FESS as shown in Figure 4 4, This FESS spins from 1000 rpm up to 4000 rpm. The FESS has a power electronic circuit control, bi-directional inverter managing the power flow. The result is a FESS regulating the DC bus voltage continuously. The voltage sag will appear less than three cycles until the flywheel starts to discharge the energy. This fast response proves that the FESS is suitable for UPS applications and voltage profile correction. But due to low-speed of the FESS the energy density and efficiency will be low.

A MATLAB Simulink is used to build the controlling model of Interior Permanent

Magnet Synchronous Motor (IPMSM). They used a low-speed flywheel, which consists of high tensile steel and mechanical bearings, which has a low cost and low complexity. Their contribution was to create a low-cost long-life UPS by using FESS, and a method to regulate the power quality parameters by using FESS.

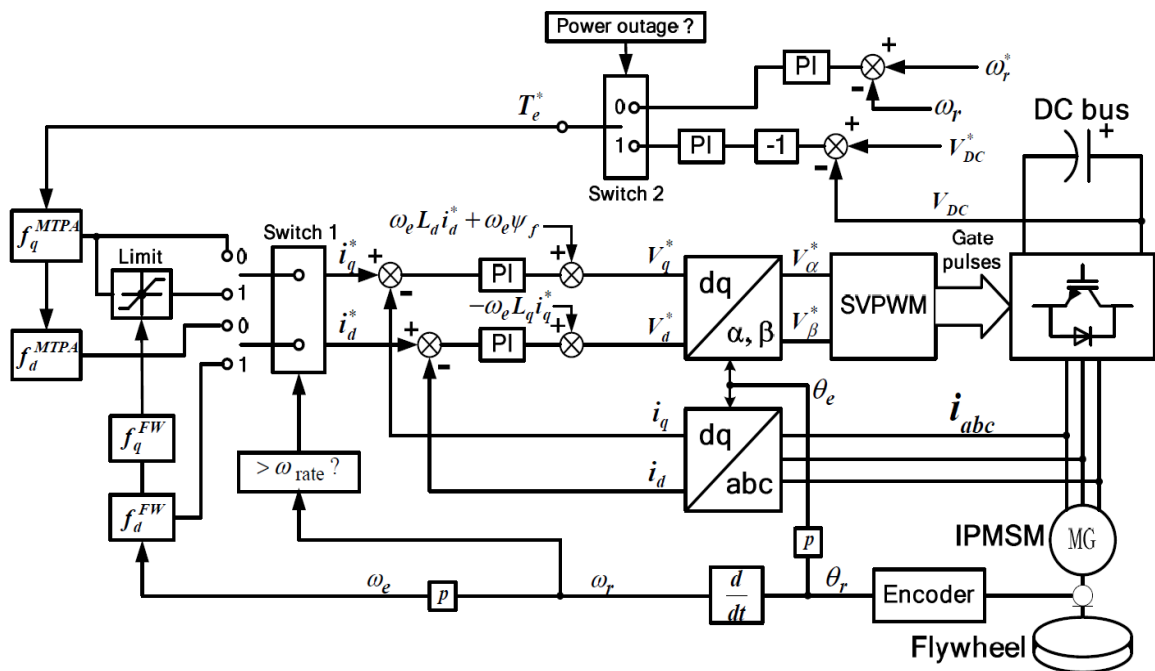


Figure 3-4 Flywheel control diagram.

Ghanaatian and Lotfifard [30] discussed the FESS and they suggested using it in various structures and applications in power systems. One of these is a UPS system using flywheels to supply a critical load as shown in Figure 3-5.

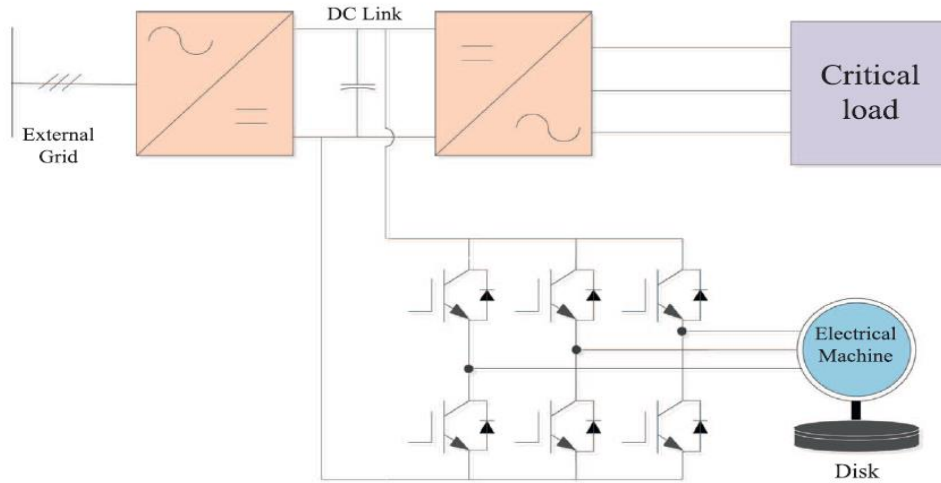


Figure 3-5 UPS system using flywheel to supply a critical load [30].

3.2 Common DC bus topology with FESS

TOODEJI [31] proposed a novel design to combine between FESS and super capacitors, which are located inside the rotating disk. Such topology should improve the dynamic performance of the FESS with minimal effects of its size and weight. The configuration of the proposed design is shown in Figure 3-6 below. A common DC bus is utilized for the flywheel, super capacitor, and PV energy source. The DC bus is connected through a Voltage Source Converter (VSC) and contactless power transfer system.

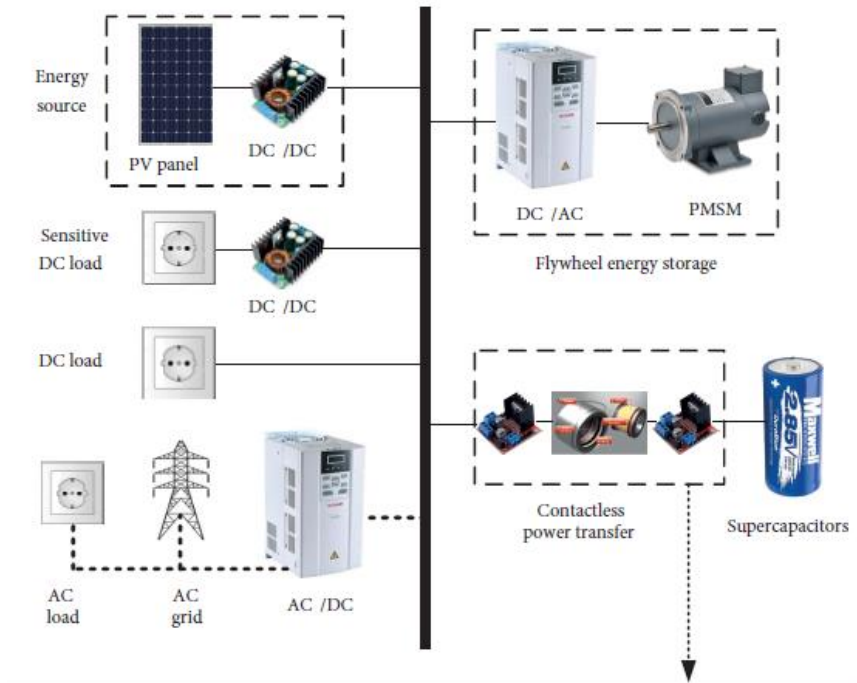


Figure 3-6 A common DC bus topology proposed by TOODEJI [31].

TOODEJI [31] used a field oriented control for the PM, the angular reference speed changes with the changes in the error value in the DC bus as shown in the below Figure 3-7. However, the priority of energy exchange is given to the super capacitors.

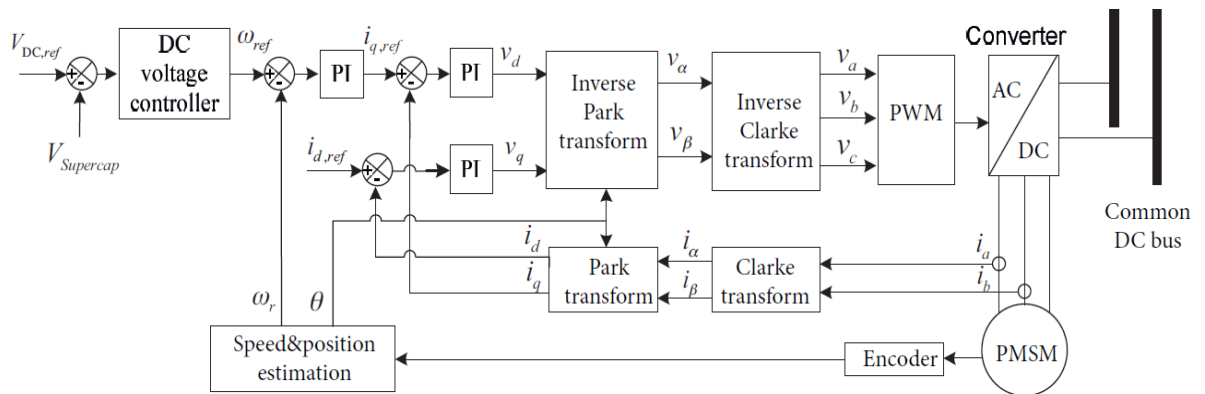


Figure 3-7 Control diagram of FESS with common DC bus [31].

Barelli *et al* [32] investigated the advantages of integrating the hybrid-energy storage system (HESS) in a residential micro-grid, coupled to a PV plant as shown in Figure 3-8 below where the battery hybridization with mechanical flywheel is integrated. The effects

of flywheel on the battery life was estimated, resulting in a significant improvement with respect to non-hybrid configurations.

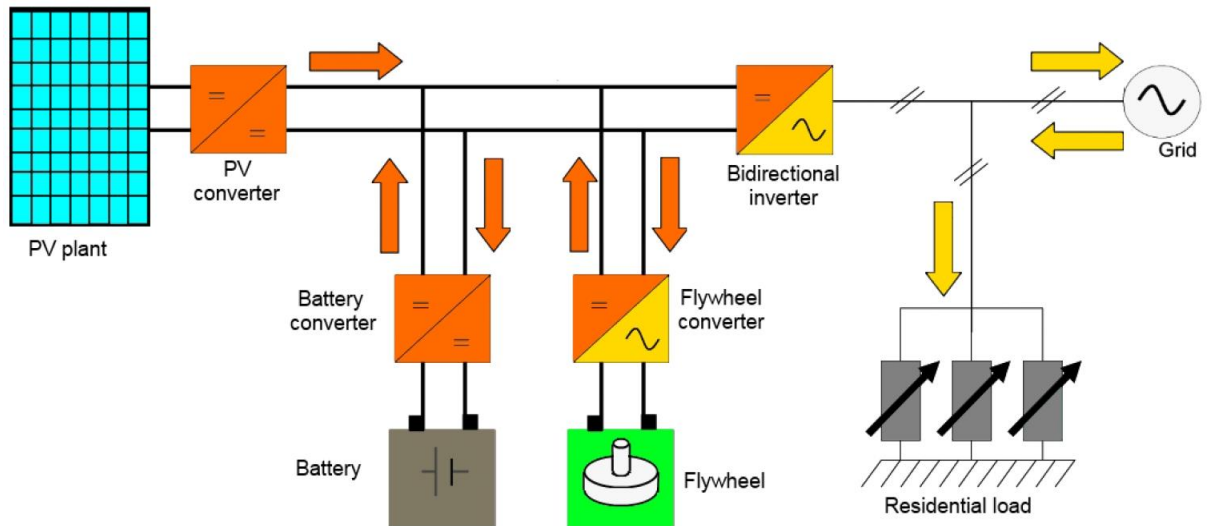


Figure 3-8 Hybrid Energy Storage System (HESS) Coupled to a Photovoltaic (PV) Plant [32].

From the energy point of view, they proved that the hybrid- energy storage system has allowed a relevant increase in the self-consumption with respect to the PV production with a contextual decrease in the total amount of purchased electricity. Moreover, they showed that the flywheel introduction largely contributed to the improvement of battery duration. Preliminary estimations showed that, the HESS battery duration almost tripled for lead-gel packs and even more for ion-lithium ones. Although of the increasing battery life, the storage system still depends on the batteries [32].

In this thesis, it will improve the feasibility of the model shown in Figure 1-1 by adding PV panels in the DC bus of the FESS inverter. In such topology, the system will be able to increase the penetration levels by saving the overflow energy to the FESS while decreasing the consumed power. On the side, the cost of using FESS will be decreased. Due to decreasing the inverter components.

Chapter 4. System Modelling

Contents

4.1	Characteristics of PV panels	36
4.2	DC to DC converter	37
4.3	On-grid inverter	38

In this chapter, a simulation model is presented to explore different scenarios. The simulation model can translate the high-level energy management commands into power electronic level.

The system contains a microgrid with hybrid system of FESS with PVs, this microgrid has load which consists of active and reactive loads in addition to transmission lines. it can control the value of the load during the simulation by connecting/disconnecting parts of the load by using signal builder to control the circuit breaker for each part of the load as shown in Figure 4-2.

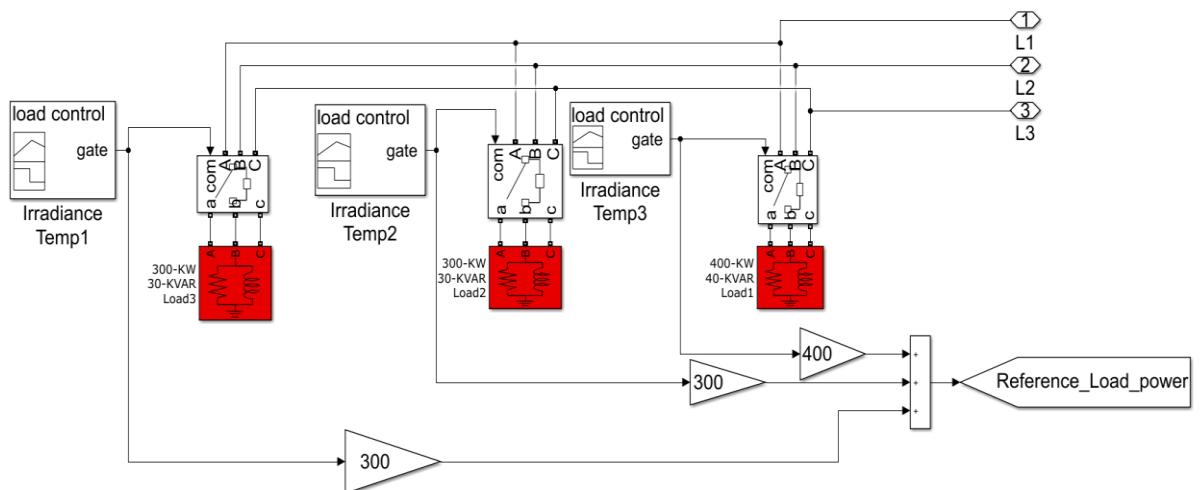


Figure 4-2 Microgrid components.

Also, it has a connection to the main utility grid which is large source power with 33KV and has a very large load. There is an interface between the utility grid and the micro-grid which is a bypass or fast switch (TRAIC). This switch is used to connect or disconnect from the main grid. Yet, the switch can be used to disconnect from the main grid when a problem occurs, e.g., when sag or swell occurs beyond the accepted limits or when interruption happened [33].

the following main components of hybrid FESS which are explained in the next sections:

4.1 Characteristics of PV panels

MATLAB-based model of a PV module can be used to simulate PV systems such

that it can be study the effect of temperature, radiation, and load variation on the available power [34].

PVs panel consists of 80 parallel strings, each string contains 40 modules, the characteristic of each module is 320W max Power. The voltage at maximum power point is 36.7 V, it has 45.6V open circuit voltage, 8.72A currents at maximum power point, 9.08A short circuit current. Figure 4-3 illustrates these parameters in MATLAB.

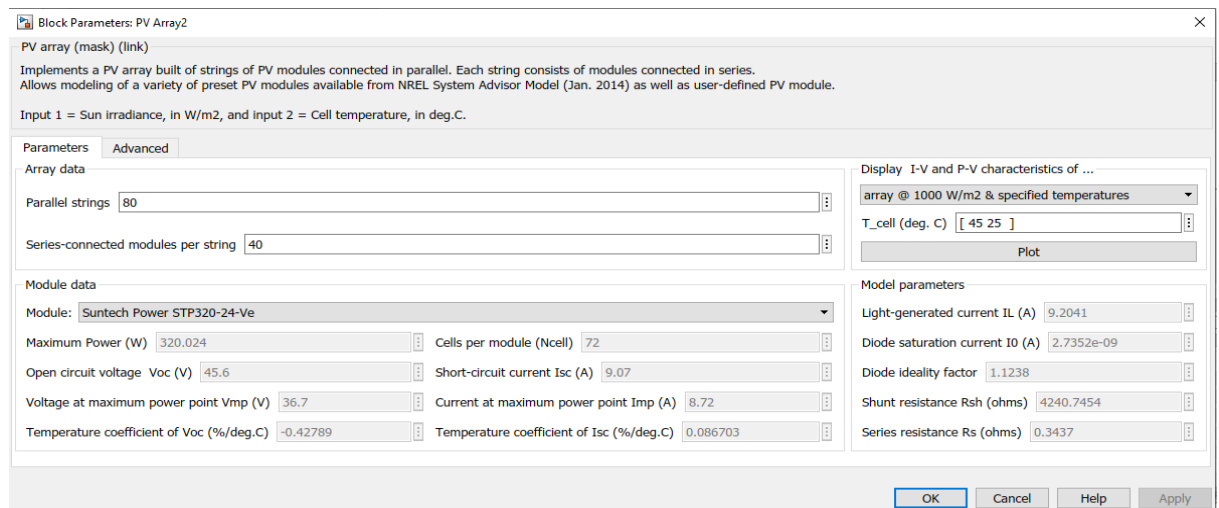


Figure 4-3 PV panel design and characteristic.

The terminal Voltage and current of the string, at maximum power point, are 1468 V, 8.72 A, respectively. The total current of PV panel will be 688 A and hence the power around 1MW. The input radiation in this simulation can be changed by the signal builder block.

4.2 DC to DC converter

The interface device between the PV panel and the DC bus is "DC to DC" boost converter. It extracts the maximum power points of PV panel [35]. PV panel is a current source, the variation in radiation will lead to variation on current with a small variation in voltage. By using MATLAB function based on the Perturb & Observe algorithm, the system can evaluate if it's on the maximum power or not. The function code of the MPPT controller is in the appendix.

This converter has a close loop control on the input voltage and current to keep the PV at the maximum power point by changing the duty cycle as shown in Figure 4-4.

Table 4-1 DC to DC boost converter specification.

The components	The specification
Coil inductance	1 mH
Coil resistive	0.5 m Ω
Capacitor	16 mF
IGBT resistance	1 m Ω
Snubber resistance	0.1 M Ω
Diode resistance	0.1 m Ω

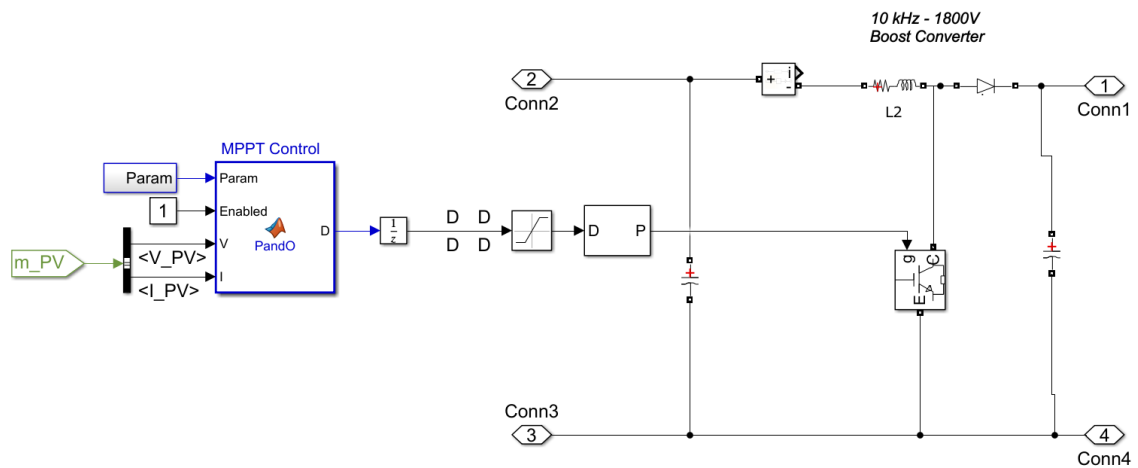


Figure 4-4 DC to DC maximum power point converter

4.3 On-grid inverter

On-grid inverter produces a synchronized voltage with the network like synchronous generator [36]. It injects controlled amounts of real power and reactive power to the network. The System contains a controller with several internal loops. In this thesis, a new method of controlling the real and reactive power is proposed which exploits the existence of Flywheel energy system. This approach enables us to manage bidirectional flow of active and reactive power. i.e. from the grid to FESS and the other way around. The FESS is coupled with PV system. Moreover, this inverter provides the power continuously even if an interruption in the utility grid happened. This is done by disconnecting the bypass switch and changing the mode to UPS mode for the same inverter with considering power quality issues using closed loop control.

The reference voltage of the inverter must be synchronized with the measured

voltage in the grid at normal mode but in the UPS mode, the inverter controls the voltage and frequency. The controller transfers the voltage from three phase system to d-q system.

The PLL instrument measure the peek to peek phase voltage (V_{abc}) in the grid and convert it to V_d & V_q as shown in the Figure 4-5 below [37].

The RMS value of phase voltage is given by:

$$V_{\phi-RMS} = \frac{V_{peek-peek}}{\sqrt{2}}; \quad (4-1)$$

The line voltage is given by:

$$V_L = \frac{V_{\phi}}{\sqrt{3}}; \quad (4-2)$$

The per unit voltage is given by:

$$V_{pu} = \frac{V_L}{400}; \quad (4-3)$$

The V_d & V_q is given by:

$$\begin{bmatrix} V_d \\ V_q \\ V_0 \end{bmatrix} = \begin{bmatrix} \cos(\omega t) & \cos(\omega t - \frac{2\pi}{3}) & \cos(\omega t + \frac{2\pi}{3}) \\ -\sin(\omega t) & -\sin(\omega t - \frac{2\pi}{3}) & -\sin(\omega t + \frac{2\pi}{3}) \\ \frac{1}{2} & \frac{1}{2} & \frac{1}{2} \end{bmatrix} \begin{bmatrix} V_a \\ V_b \\ V_c \end{bmatrix} \quad (4-4)$$

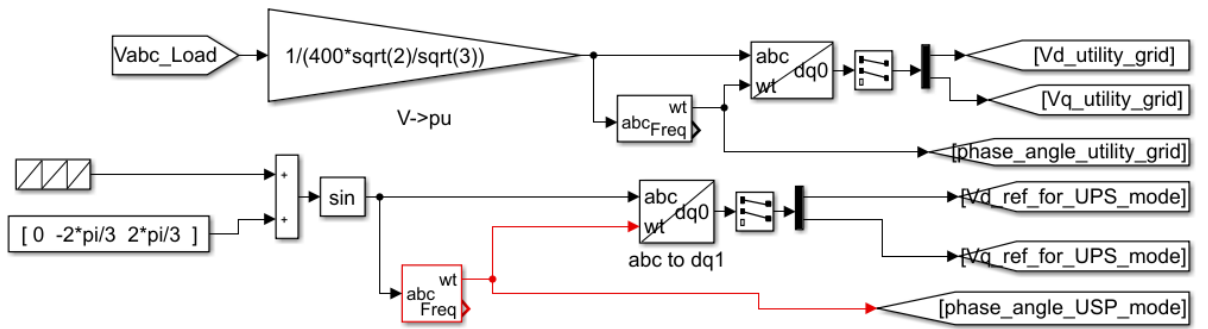


Figure 4-5 V_d & V_q references.

Figure 4-6 illustrates how we set the active and reactive power during the simulation. In one of the sceneries which is discussed in this thesis, the reference value of the real power changes during the simulation using the signal builder block. The reference value of reactive power changes with time by monitoring the reactive power in the grid so that the power factor is close to unity.

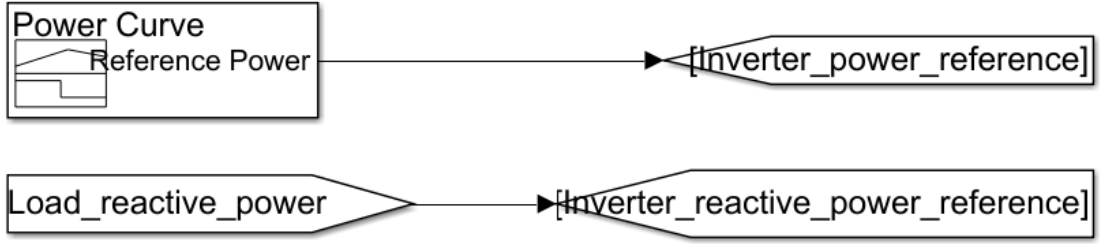


Figure 4-6 Reference value of the real power and reactive power extracted from the inverter.

At on-grid mode (synchronized mode), the inverter regulates the power flow using the controller. The power flow depends on the current flow from the inverter (due to the difference voltage between the inverter and the grid) and the angle between the inverter voltage and the grid voltage. Changing the modulation index of the inverter will change the inverter current. So, the controller controls the reference values of voltage to change the current. To simplify the controller topology, the three-phase system is transferred to d-q system as explained before.

The benefit of using d-q system is that from equation (4-6) $V_{d-inverter}$ reference which generates $I_{d-inverter}$ can be used to control the real power. And from equation (4-8) $V_{q-inverter}$ reference which generates $I_{q-inverter}$ can be used to control the reactive power. The magnitude of V_d & V_q is controlled by the close loop control of real and reactive power as shown in the Figure 4-7 below. It divided the power by 1000 to be per unit.

The power injected from the inverter is given by:

$$P = V_{d-grid} * I_{d-inverter} + V_{q-grid} * I_{q-inverter}; \quad (4-5)$$

But $V_{q-grid} = 0$;

$$\text{So } P = V_{d-grid} * I_{d-inverter}; \quad (4-6)$$

And

$$Q = V_{d-grid} * I_{q-inverter} - V_{q-grid} * I_{d-inverter}; \quad (4-7)$$

But $V_{q-grid} = 0$;

$$\text{So, } Q = V_{d-grid} * I_{q-inverter}; \quad (4-8)$$

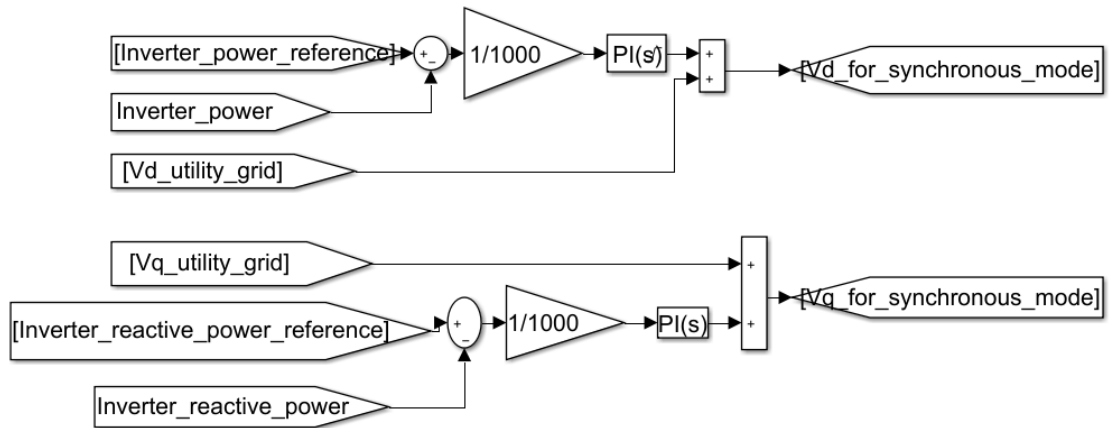


Figure 4-7 d-q reference currents for on grid mode.

The controller is designed such it can changes to UPS mode very fast when it is need, i.e., when there is an interruption or disconnection from the main grid., The controller measures the difference between the load and inverter power and then it generates the d-q values of the voltage. The controller estimates the new reference values of direct voltage (V_d) and quadrature Voltage (V_d) when an interruption happens at any moment. A screenshot of d-q vectors is shown in the Figure 4-8 below.

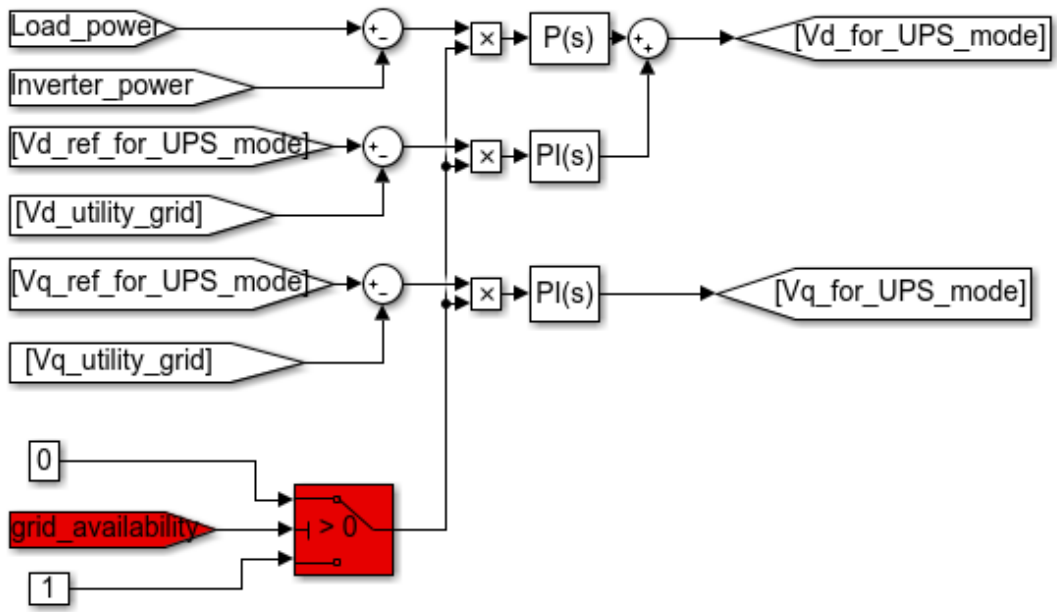


Figure 4-8 d-q vectors generated from the controller for UPS mode

The modulation index of the inverter changes by I_d & I_q as well as by the changes in the DC bus voltage. The controller changes the reference value and mode by using a switch. So, the gate driver signals of the inverter are generated as shown in the Figure 4-9 below.

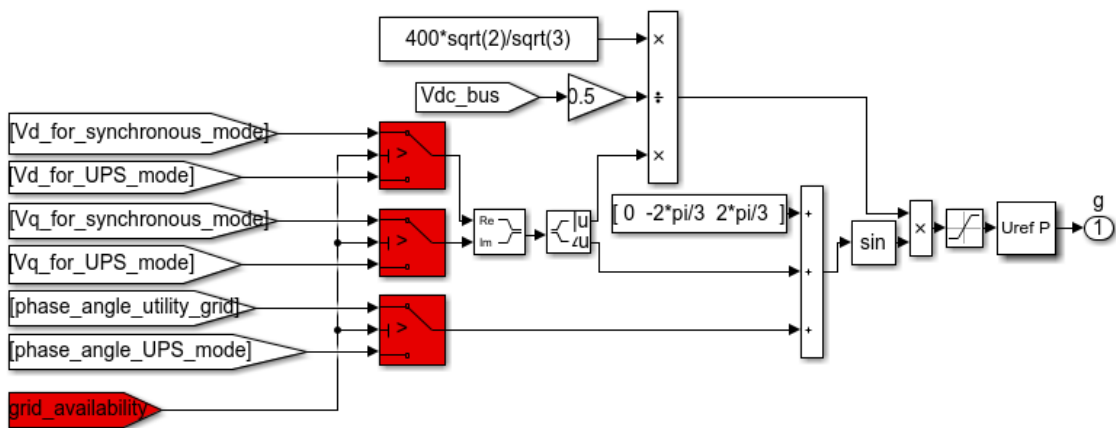


Figure 4-9 Control diagram of the inverter.

Since the voltage stress applied to the power devices of three-level configuration is

half that of the two-level version, this topology was traditionally used for medium voltage drives. Basic behavior of the NPC topology brings significant advantages to the low voltage applications as well [38].

The specification of the Neutral-point clamped three-level inverter used in the simulation is shown in Table 4-2 below.

Table 4-2 The specification of the three level inverter from ABB library.

The components of three level inverter	The specification
Capacitor bank of the inverter	4 mF each one, 8 mF total capacitance
IGBT resistance	1 mΩ
Snubber resistance	1 MΩ
Diode resistance	0.1 mΩ

4.4 Control System of FESS

The simulation model of the whole system is developed in MATLAB/Simulink. it consists mainly from an inner current-loop and an outer speed-loop [39]. The FESS has two main parts: inverters with space vector control components and a flywheel machine. Using the Three-level inverters is good choice especially, the lower voltage steps associated with the switching help in the mitigation of problems related to surge voltages at the motor terminals, leakage current, shaft voltage and bearing current, and so on. The Flywheel is a permanent magnet machine as shown in Figure 4-11.

The equations of digital control of the FESS by using PMSM [17]

$$i_d(k+1) = \frac{T_s}{L_d} \left(v_d(k) - R_s i_d(k) + \omega_e(k) L_q i_q(k) \right) + i_d(k) \quad (4-9)$$

$$i_q(k+1) = \frac{T_s}{L_d} \left(v_q(k) - R_s i_q(k) - \omega_e(k) L_d i_d(k) - \omega_e(k) \lambda_f \right) + i_q(k) \quad (4-10)$$

Where k+1 is the next term.

From (4-9) we get $v_d(k)$

$$v_d(k) = R_s i_d(k) - \omega_e(k) L_q i_q(k) - (i_d(k) - i_d(k+1)) \frac{L_d}{T_s} \quad (4-11)$$

From (4-11) we get $v_q(k)$

$$v_q(k) = R_s i_q(k) + \omega_e(k) L_d i_d(k) + \omega_e(k) \lambda_f (i_q(k+1) - i_q(k)) \frac{L_d}{T_s} \quad (4-12)$$

So, Figure 4-10 below represents Equation (4-11)&(4-12) in the Simulink model.

$$\omega_e(k+1) = \frac{T_s p}{j} \left(T_e(k) - \frac{B_v}{p} \omega_e(k) - T_l(k) \right) + \omega_e(k) \quad (4-13)$$

But, in flywheel $\frac{B_v}{p} \omega_e(k)$ & $T_l(k)$ is around zero;

$$\text{so, } \omega_e(k+1) = \frac{T_s p}{j} (T_e(k)) + \omega_e(k) \quad (4-14)$$

$$\omega_m(k+1) = \frac{T_s}{J} (T_e(k)) + \omega_m(k) \quad (4-15)$$

From (2-15) $T_e = \frac{3}{2} p (\lambda_f i_q - (L_d - L_q) i_q i_d)$

But $L_d = L_q$; applied torque became $T_e = \frac{3}{2} p (\lambda_f i_q)$

$$\omega_e(k+1) = \frac{T_s p}{J} \left(\frac{3}{2} p \lambda_f i_q(k) \right) + \omega_e(k) \quad (4-16)$$

$$\frac{\omega_e(k+1)}{p} - \frac{\omega_e(k)}{p} = \frac{T_s}{J} \left(\frac{3}{2} p \lambda_f i_q(k) \right)$$

$$\omega_m(k+1) - \omega_m(k) = \frac{T_s}{J} \left(\frac{3}{2} p \lambda_f i_q(k) \right)$$

$$i_q(k) = \frac{2}{3} \frac{J}{p \lambda_f T_s} [\omega_m(k+1) - \omega_m(k)] \quad (4-17)$$

So, the torque current command i_q reference as follows:

$$i_{qref}(z) = \left(k_p + \frac{k_i T_s}{z-1} \right) [\omega_m - \omega_{ref}] \quad (4-18)$$

This equation represents in the Simulink as shown in Figure 4-10

below.

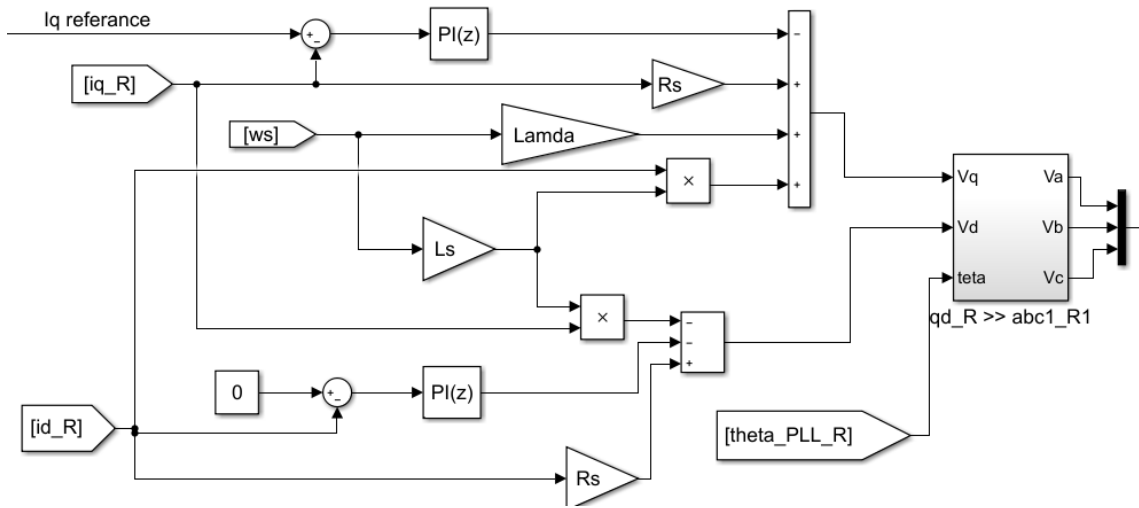


Figure 4-10 Converter Control Model of PMSM

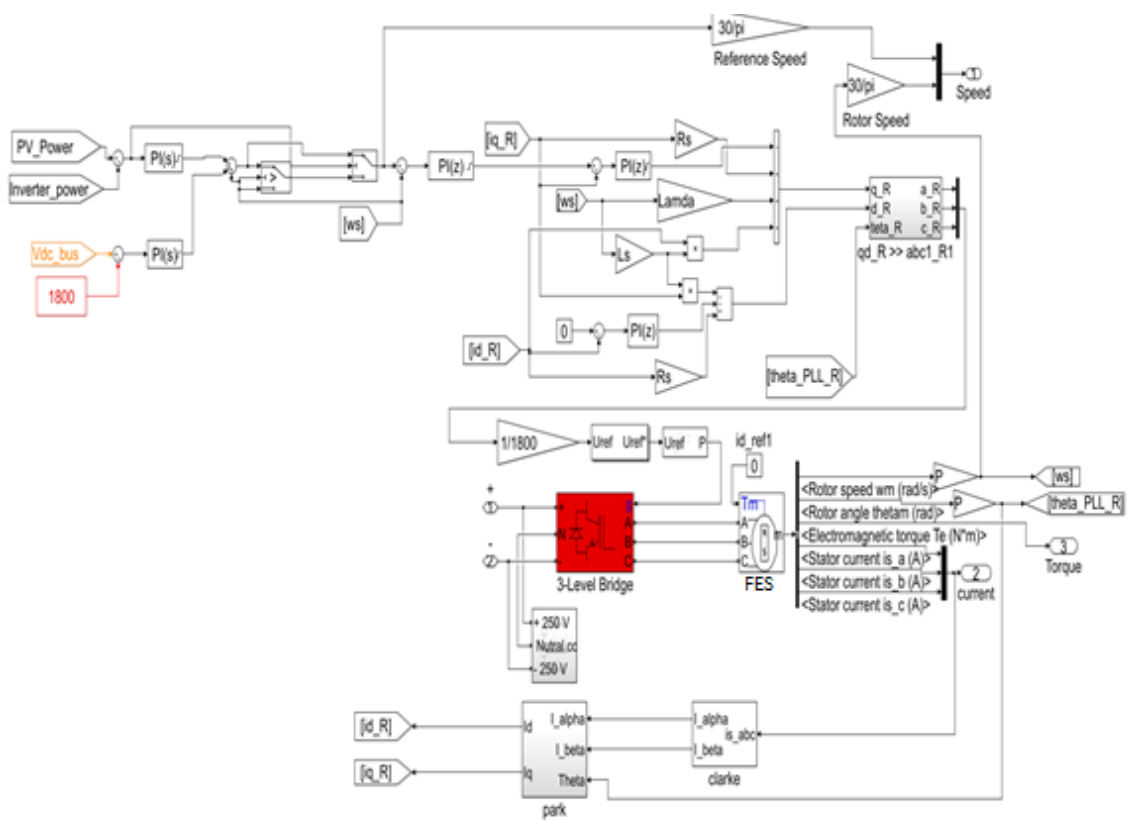


Figure 4-11 Flywheel and its driver.

Flywheel unit is the machine and its inverter, so the flywheel bank is a group of

flywheel units connected in parallel in the same DC bus as shown in Figure 4-12.

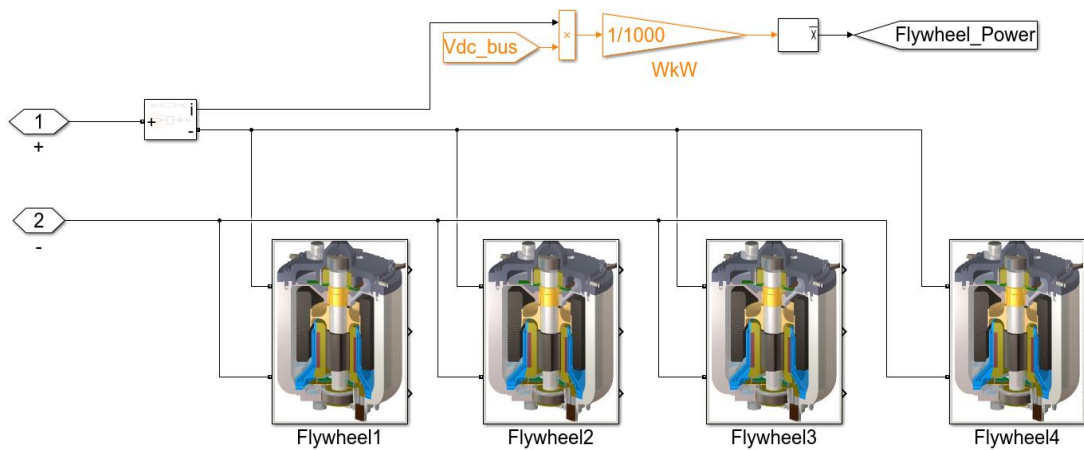


Figure 4-12 Flywheel units connected in parallel.

The following points summarize the FESS control:

The specification of the FESS used in the simulation is shown in Table 4-3 below.

Table 4-3 The specification of the FESS

<i>The components of the FESS</i>	<i>The specification</i>
<i>Flywheel Power</i>	<i>500KVA</i>
<i>Capacitor bank</i>	<i>4 mF each one, 8 mF total capacitance to smooth the DC voltage.</i>
<i>IGBT resistance</i>	<i>0.2 mΩ</i>
<i>Snubber resistance</i>	<i>1 MΩ</i>
<i>Stator phase resistance of PMSM</i>	<i>15 mΩ</i>
<i>Inductances Ld, Lq of PMSM</i>	<i>314.62 μH</i>
<i>Flux linkage of PMSM</i>	<i>167.6348 kV.s</i>
<i>Inertia</i>	<i>50 kg.m²</i>
<i>viscous damping & static friction</i>	<i>Around zero due to magnetic Bering and vacuum box</i>
<i>pole pairs</i>	<i>2</i>
<i>Back EMF waveform</i>	<i>Sinusoidal</i>
<i>Rotor type</i>	<i>Salient pole</i>

Chapter 5. Simulation & Results

Contents

5.1	Fluctuating Solar Irradiation _____	47
5.2	Constant power flow with fluctuating solar irradiation and variable inductance load with power factor correction mode. _____	54
5.3	Charging FESS from the Utility Grid and PVs. _____	63
5.4	The PV and FESS cover the load (100% penetration level of PVs continuously) _____	69
5.5	UPS Mode with variable load. _____	75
5.6	Efficiency Calculation and Measurement: _____	83

A set of simulation experiments have been performed in this chapter to show typical FESS applications in microgrid. The microgrid consists of FESS, PV, and Load. Moreover, we build the system such that it is possible to explore scenarios when the microgrid is connected or disconnected from the main grid. Several metrics such as voltage profile, frequency, and power factor have been studied during this chapter. We defined a set of scenarios as follows:

Scenario 1: Microgrid with fluctuating solar irradiation.

Scenario 2: Microgrid with variable load and fluctuating solar irradiation.

Scenario 3: Charging FESS from the Utility Grid and PVs.

Scenario 4: The PV and FESS cover the load.

Scenario 5: FESS as UPS when disconnecting the utility grid.

5.1 Fluctuating Solar Irradiation

The goal of this scenario is to show the capability of the proposed system to regulate the amount of produced power when the solar irradiance is fluctuating.

In this scenario the load is constant in the microgrid which is 1MW with 0.9 Power Factor. The load is covered from the main grid and FESS. Figure 5-1 presents the

simulation results of this scenario. The inverter provides the network with 800 kW ,484.32KVAR to improve to power factor. The utility grid provides the load with only real power 200 kW, i.e, the inverter compensates the reactive power to have a unity power factor. The fluctuating power from the PV is regulated by the system. The load power in Microgrid is constant but the flywheel stores energy at time of high generation from the PV and feed the power back when there is low energy generation from the PV. This way, the system grants constant amount of power to be injected in the Microgrid.

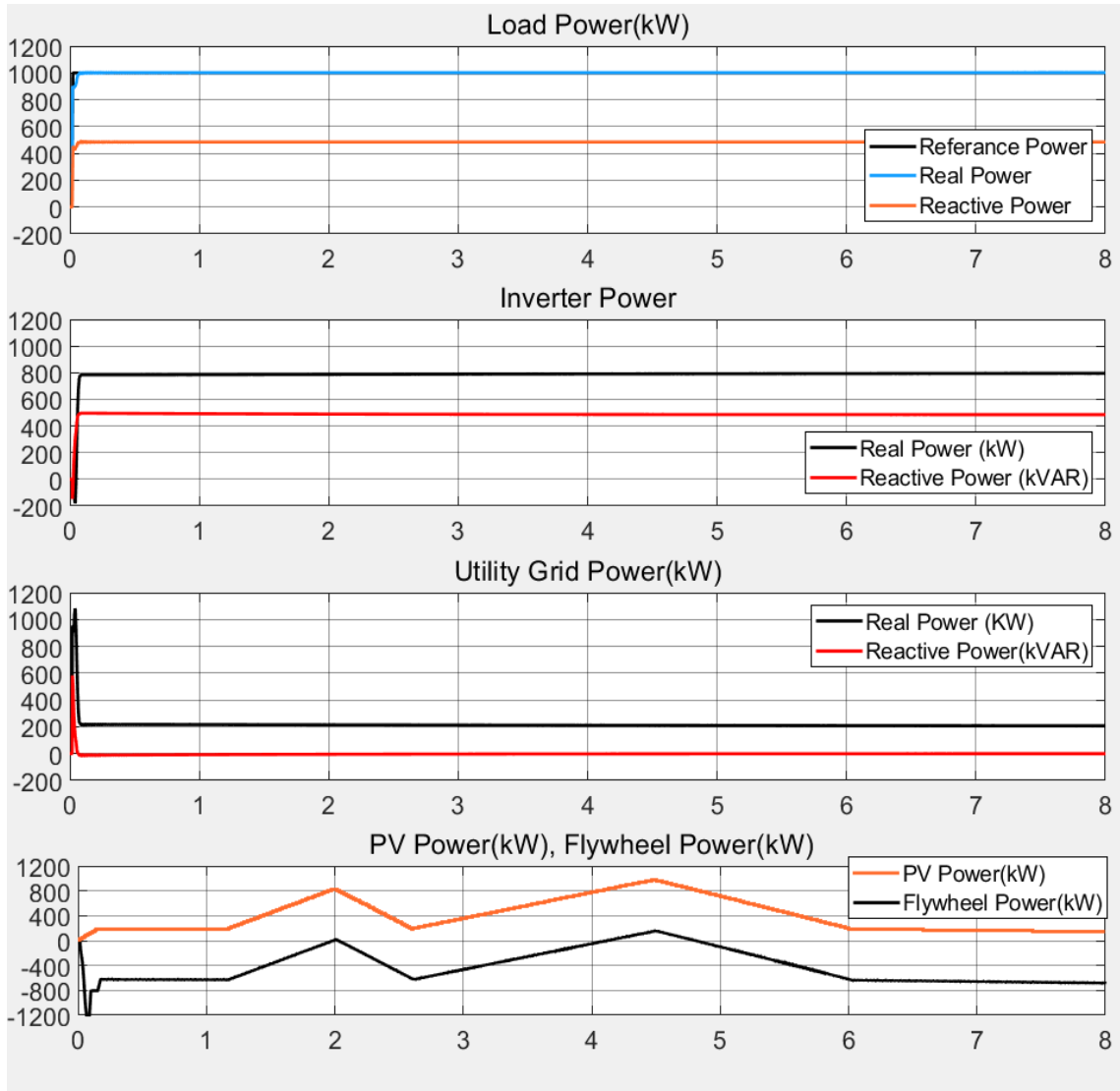


Figure 5-1 Power Flow in the system at variable radiation with compensate the power factor.

Figure 5-2 shows Power Flow in the system without compensate the power factor.

The economic method to compensate the reactive power is by using an automatic power factor correction banks, but in this these we take the technical side of the system.

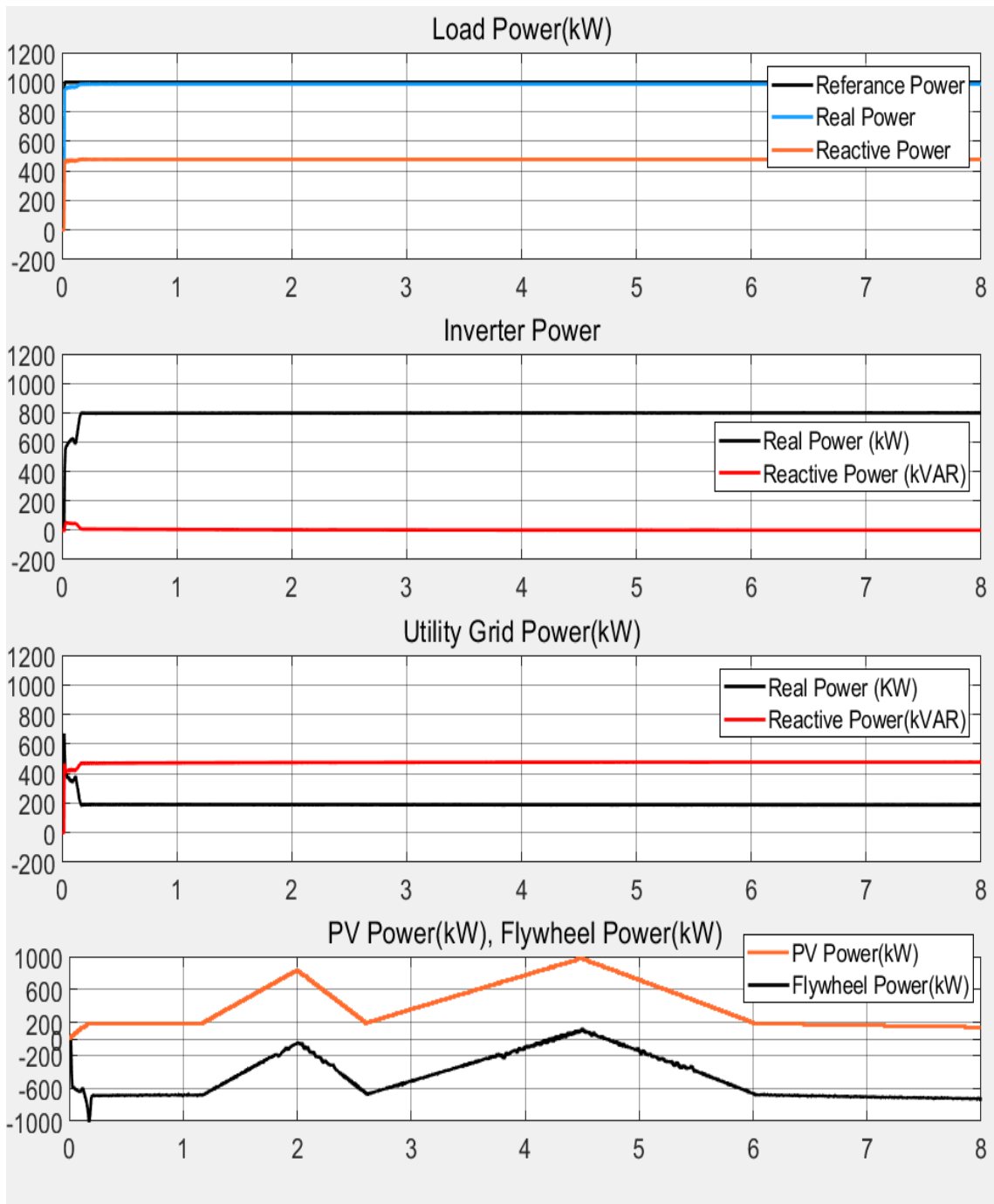


Figure 5-2 Power Flow in the system at variable radiation without compensate the power factor.

Figure 5-3 gives insights how the system was able to maintain a constant power

during the fluctuating in the PV generation. The system regulates the dc voltage in the DC Bus by flywheels driver as shown in Figure 5-3 below. This is done by using the appropriate modulation index. As can be seen in the figure, the changes in the irradiation is reflected on the speed of the flywheel. This way the DC voltage is maintained around 1800 V.

When the external grid availability value is one that means the bypass switch is closed, and when the value is zero the bypass switch is open.

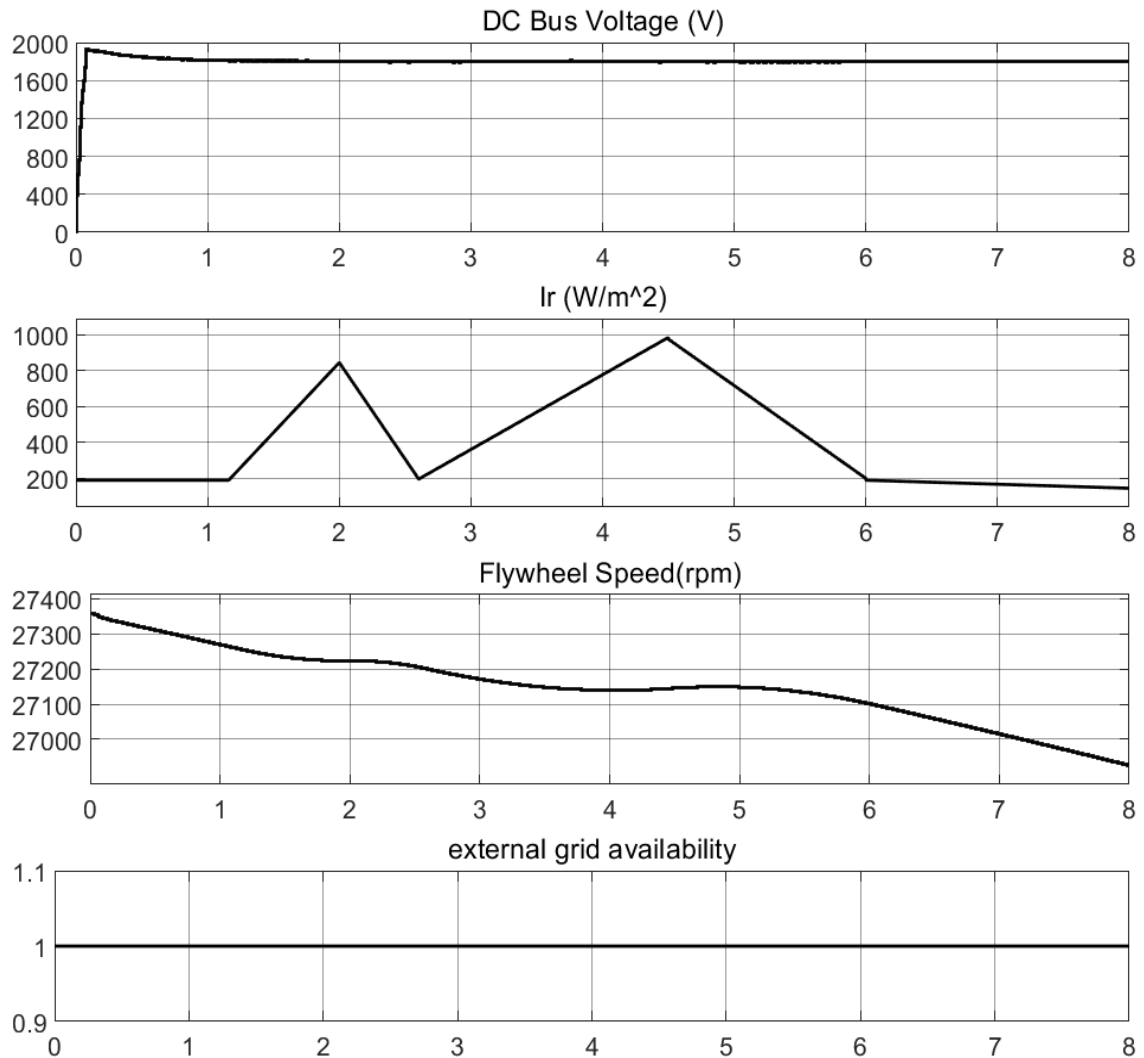


Figure 5-3 Constant DC voltage even when there is fluctuation irradiance.

Although, there is fluctuation on the generated power from the PV, the load voltage is kept constant as can be identified from Figure 5-4 below. Because the load is constant, we have a constant load current, i.e, the loads consumes constant power. Moreover, the current comes from the utility is constant because the load is constant and the fluctuation in PV generation is compensated from the flywheel.

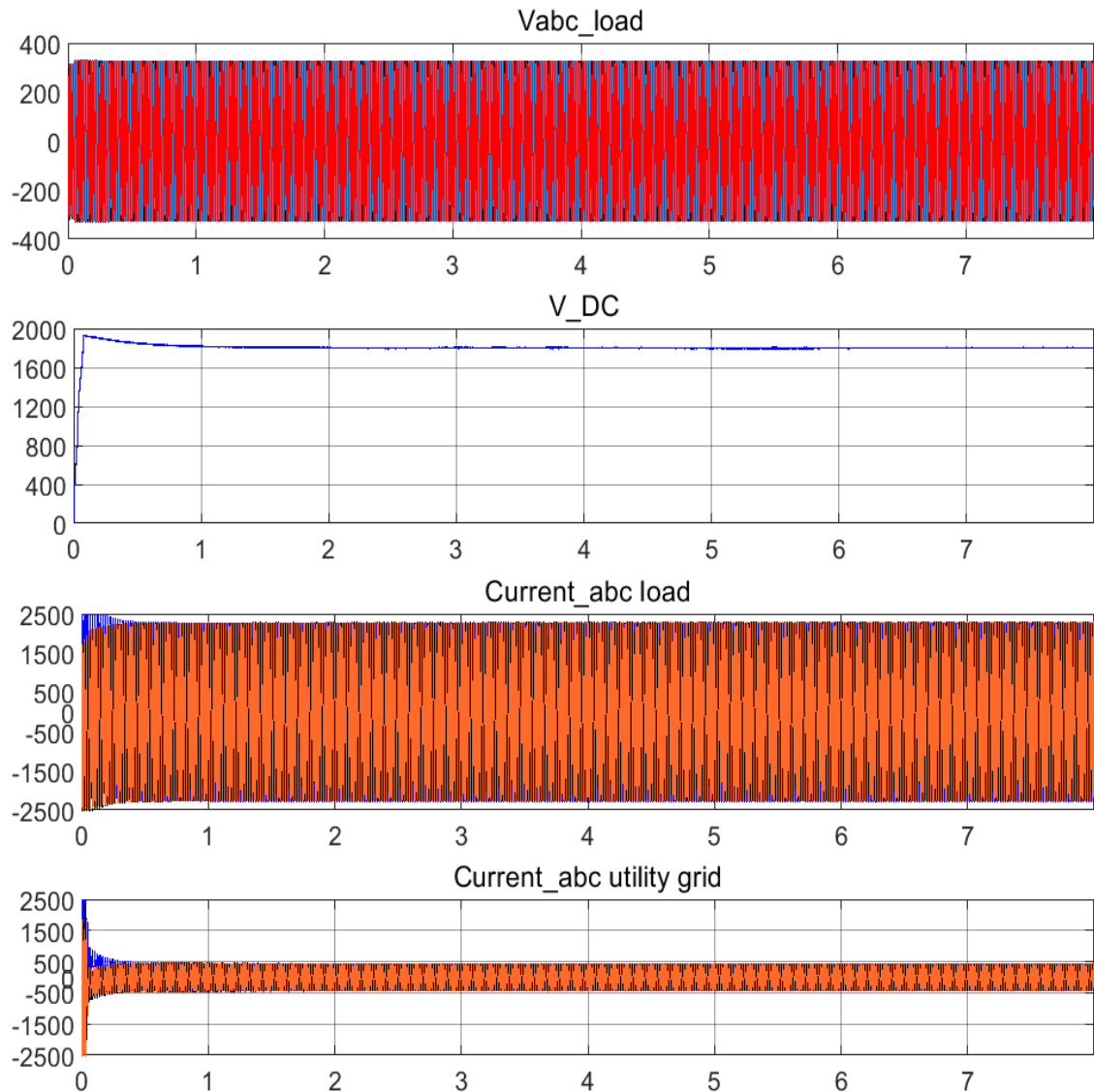


Figure 5-4 Load voltage and current.

The following Figure 5-6 depicts the system frequency (Hz). As can be seen, the frequency remains almost constant.

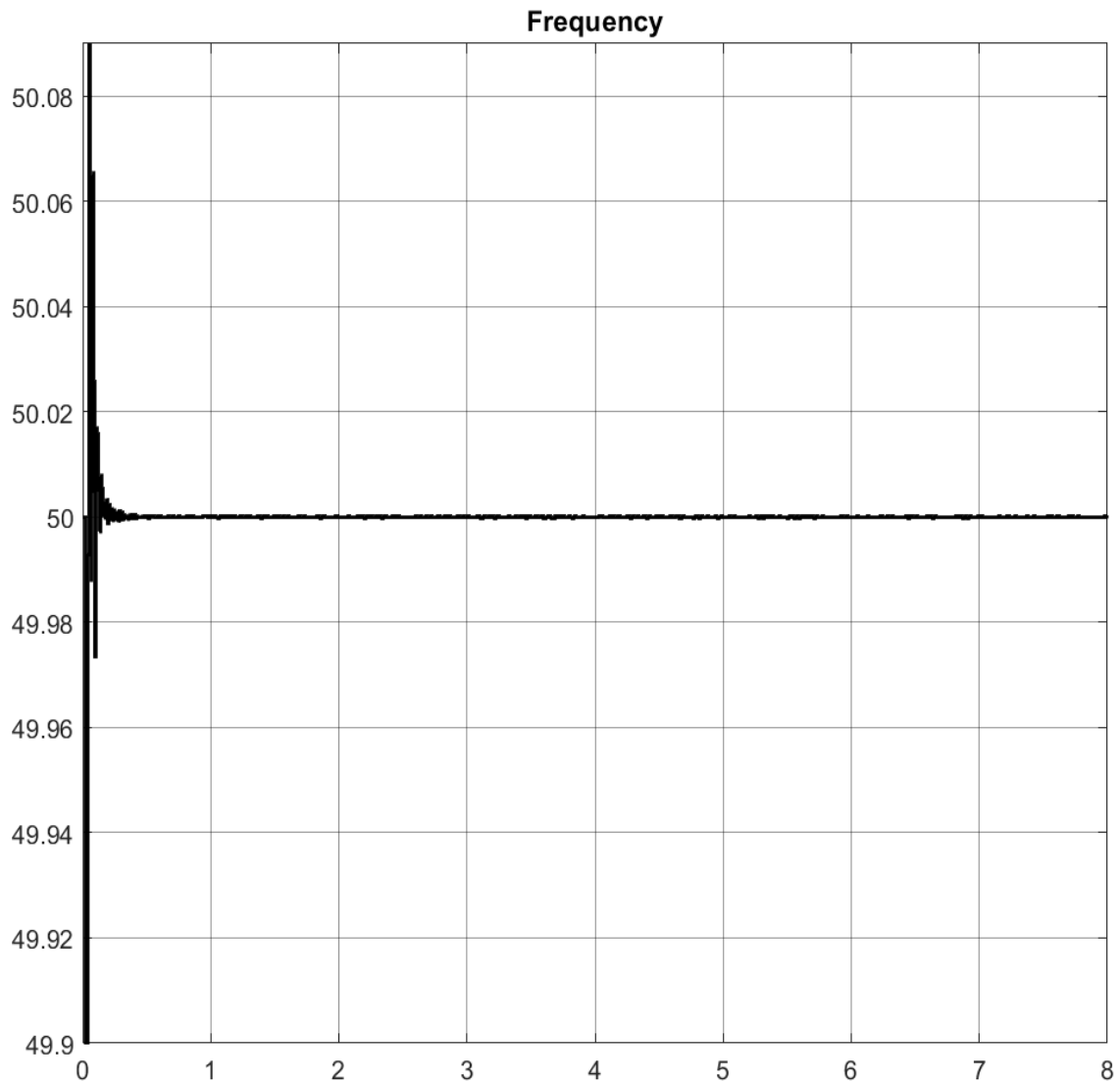


Figure 5-5 Grid Frequency on the Load Bus.

FESS stores the energy as speed in the flywheel. Changing the speed in the flywheel reflects the changes in the DC bus voltage. The FESS is PMSM which has a speed controller and hence to change the flywheel power, we have to change the reference I_q of flywheel. A small variation in the speed of flywheel, from 27400 rpm to 26900 rpm in average, can be seen in Figure 5-6. The mechanical torque in the machine is the mechanical power transferred from electrical to mechanical and vis verse.

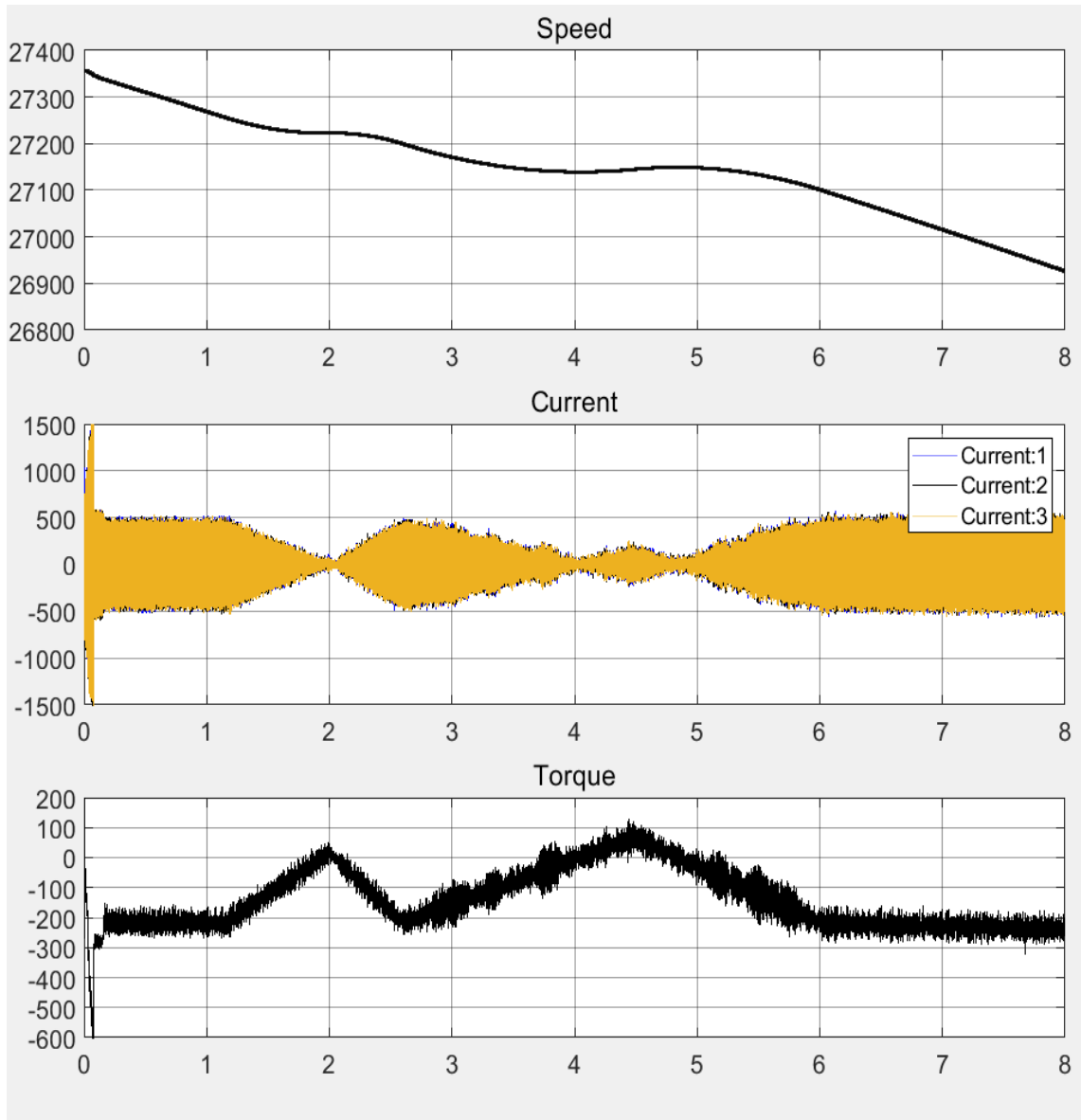


Figure 5-6 Flywheel speed (rpm), currents (Amps) and torque (N.m) at constant power flow to the network.

The I_q and I_d components of PMSM are illustrated in Figure 5-7 below. I_q represents the mechanical torque of the PMSM, i.e., it represents the mechanical power of the machine. I_d represents the difference angle between the perpendicular component of the rotor and stator flux.

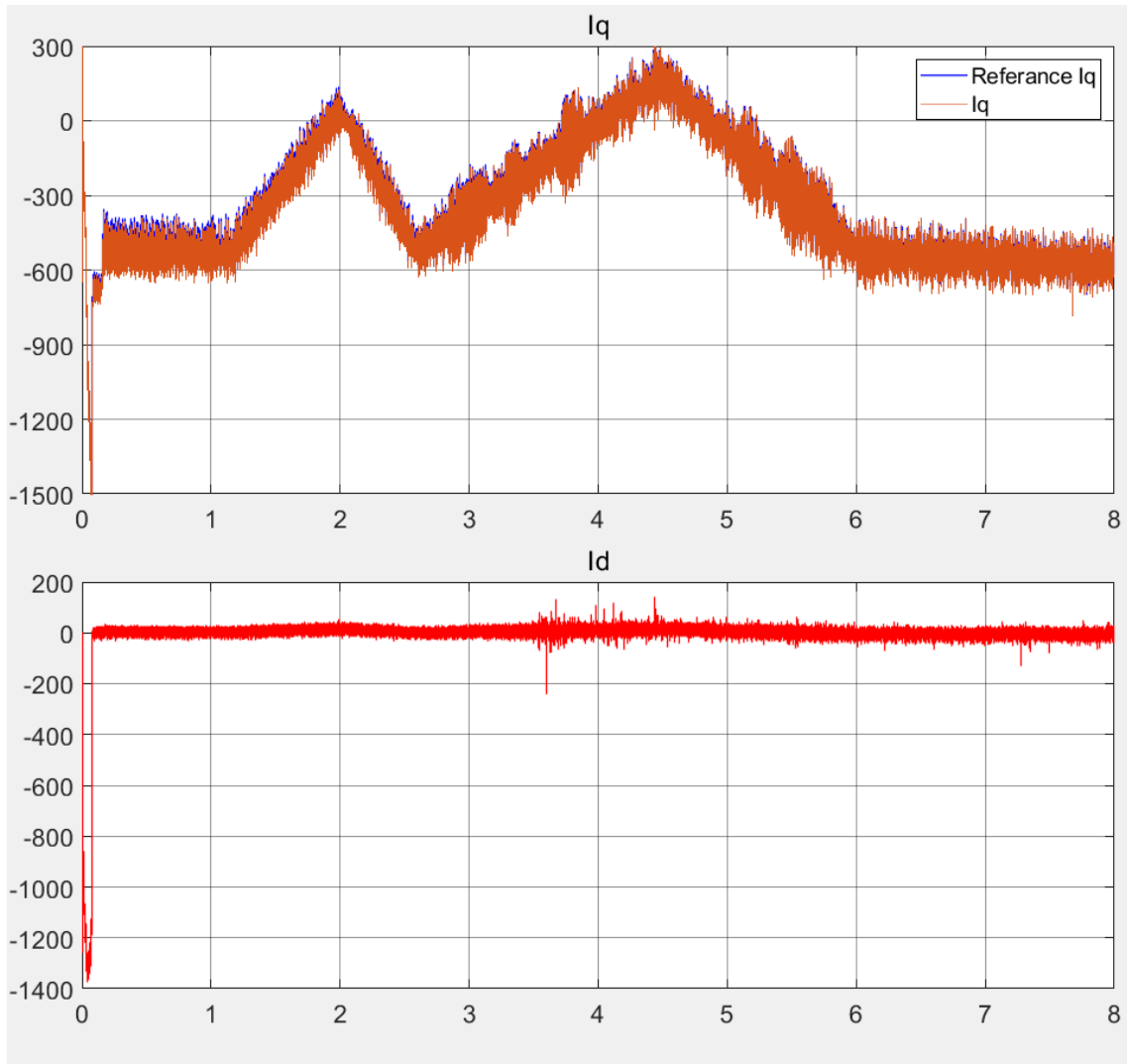


Figure 5-7 Direct and quadrature currents of flywheel and its referace value.

5.2 Constant power flow with fluctuating solar irradiation and variable inductance load with power factor correction mode.

In PVs, the changing in radiation affects in the voltage of dc bus. The inverter extracts the maximum power by changing the modulation index and DC reference voltage. This can have negative impact on the network performance. For instance, it has bad impact on the voltage profile and harmonic distortion. FESS represents a good opportunity to solve these problems because it has a very fast response time to any change in the grid.

The aim of this scenario is to show that the system can withstand the variation not

only in the solar irradiation, but also any changes in the load. This scenario is similar to the previous scenario, but with step changing in the load.

The load has a 0.9 power factor. As can be seen in Figure 5-8 below, the load starts with 300 kW then increases to 600 kW at 2 sec and then increases again to 1000 kW at 3 sec then decreasing to 400 kW at 4 sec and then goes to zero at 5 sec. All these steps occur in 6 seconds with very high variation in solar radiation. Finally, the simulation ends at 8 sec. As can be identified from Figure 5-8 below, the inverter provides the network with a continuous and constant power to the load (500 kW) during the simulation. At the beginning, the inverter covers the load and hence there is no power comes from the utility grid. When the load starts to increase, the difference between the demand and inverter power is imported from the utility grid. Afterwards, when the load becomes zero, the generated power from the inverter is exported to the utility grid. This can be seen from the negative value of the utility grid power. Finally, the inverter was able to compensate the demand reactive power and hence there is no reactive power import from the utility grid.

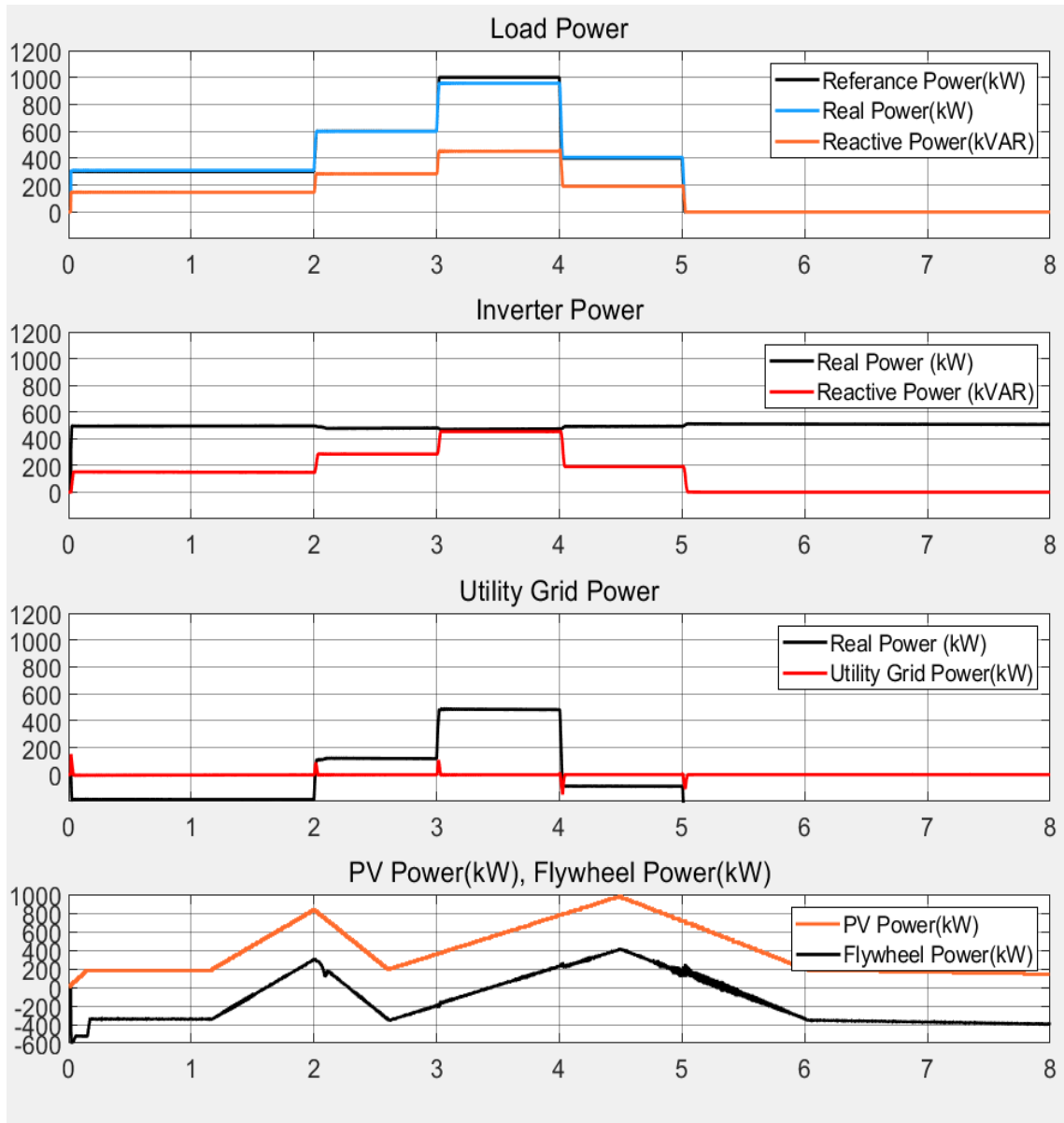


Figure 5-8 Power flow through all components at variable load and constant power flow from the inverter with power factor correction mode.

As indicated in Figure 5-9 below, the voltage profile is stable and the current changes directly with changing in load.

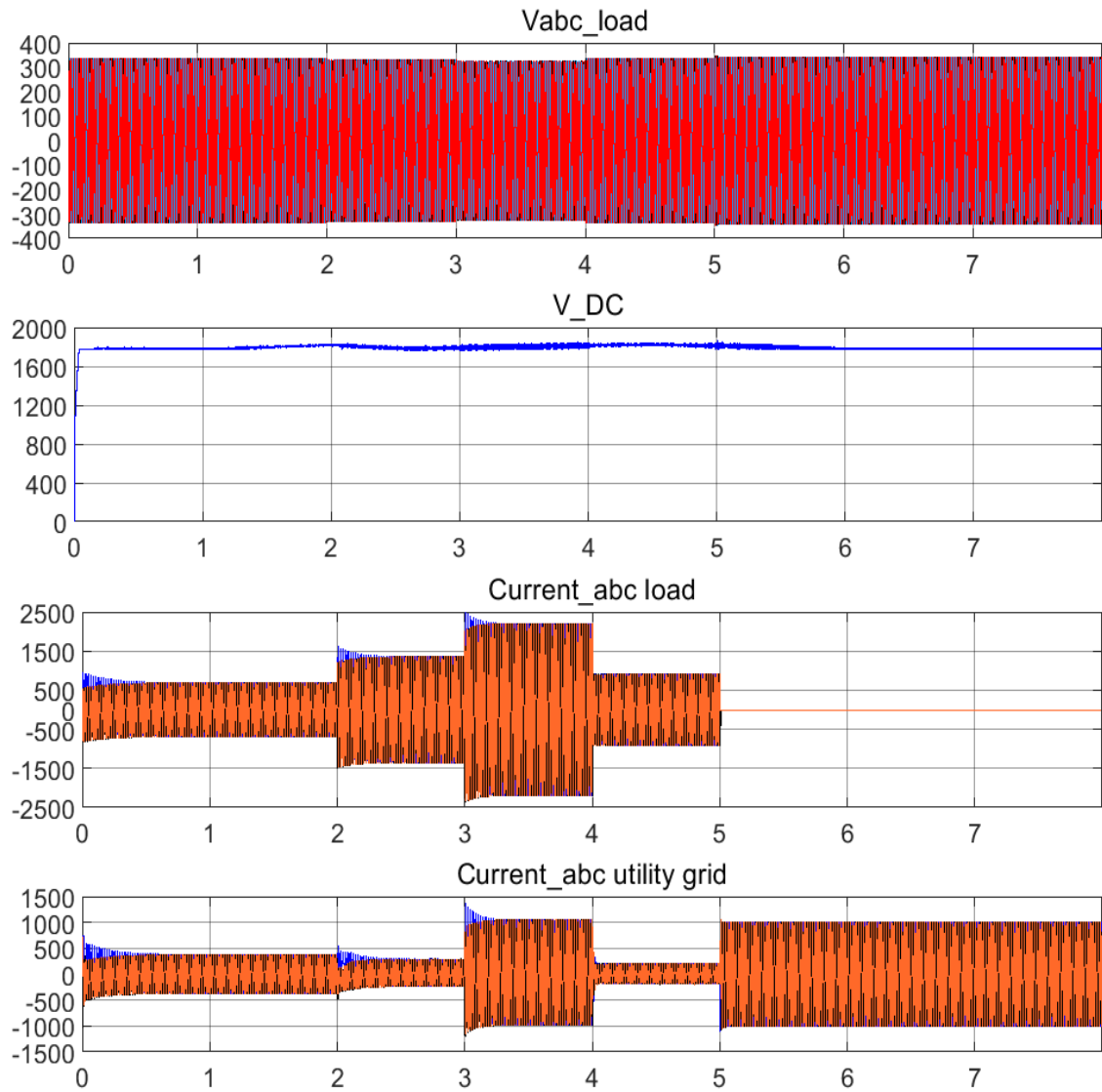


Figure 5-9 Voltage and Currents When Load And Radiation Is Variable.

The following Figure 5-10 depicts the system frequency. As can be seen, the frequency remains almost constant. The increase and decrease in the frequency is due decrease and increase in the load. The response time of the system was very short and was able to maintain almost constant frequency.

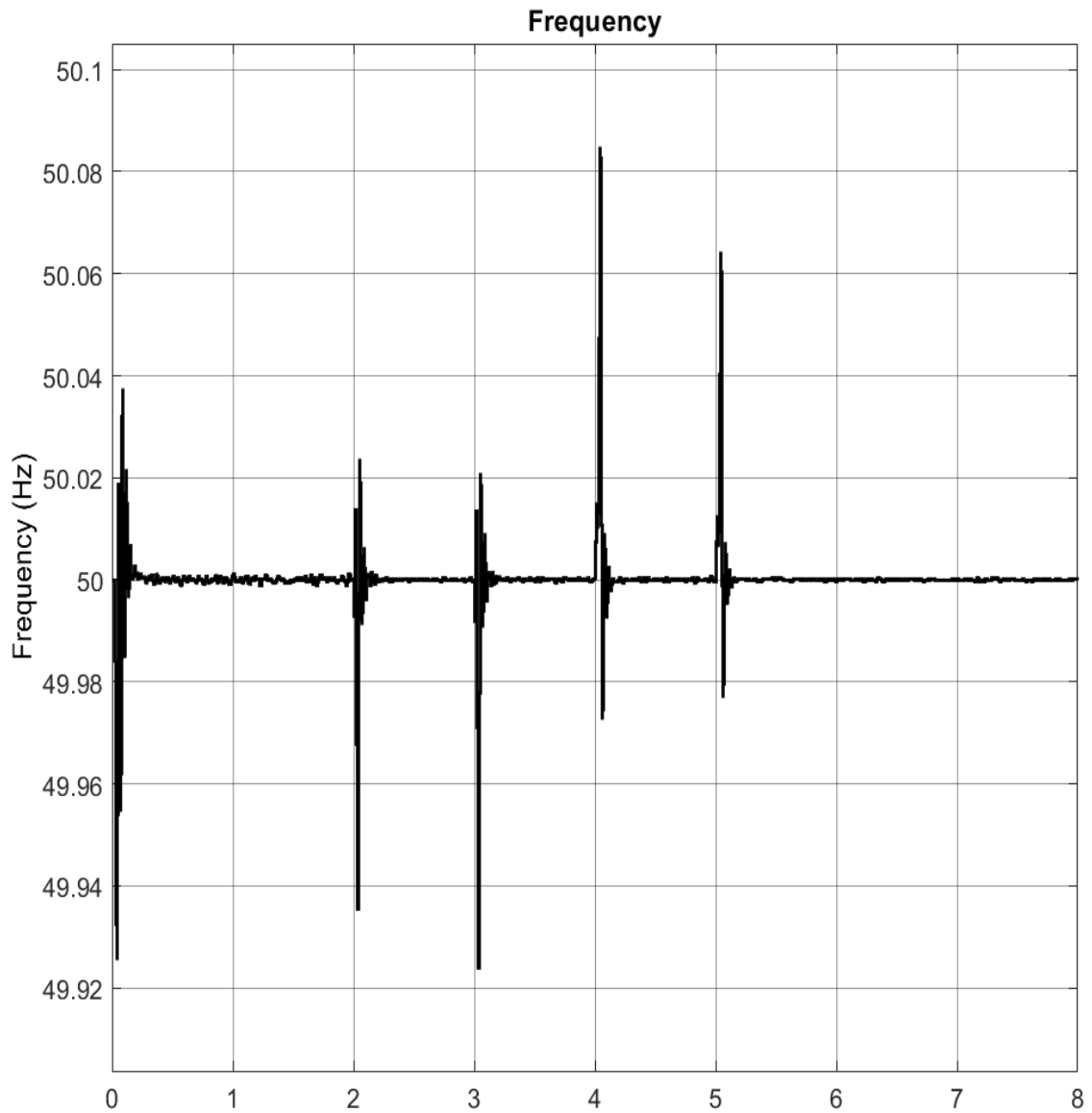


Figure 5-10 Grid Frequency with fluctuating solar irradiation and variable load.

In spite of the fluctuation in the solar irradiance and changes in the load, the proposed system was able to keep constant DC bus voltage throughout the simulation. Regulating the DC bus happened by changing the FESS electrical power flow through changing its speed as shown in Figure 5-11.

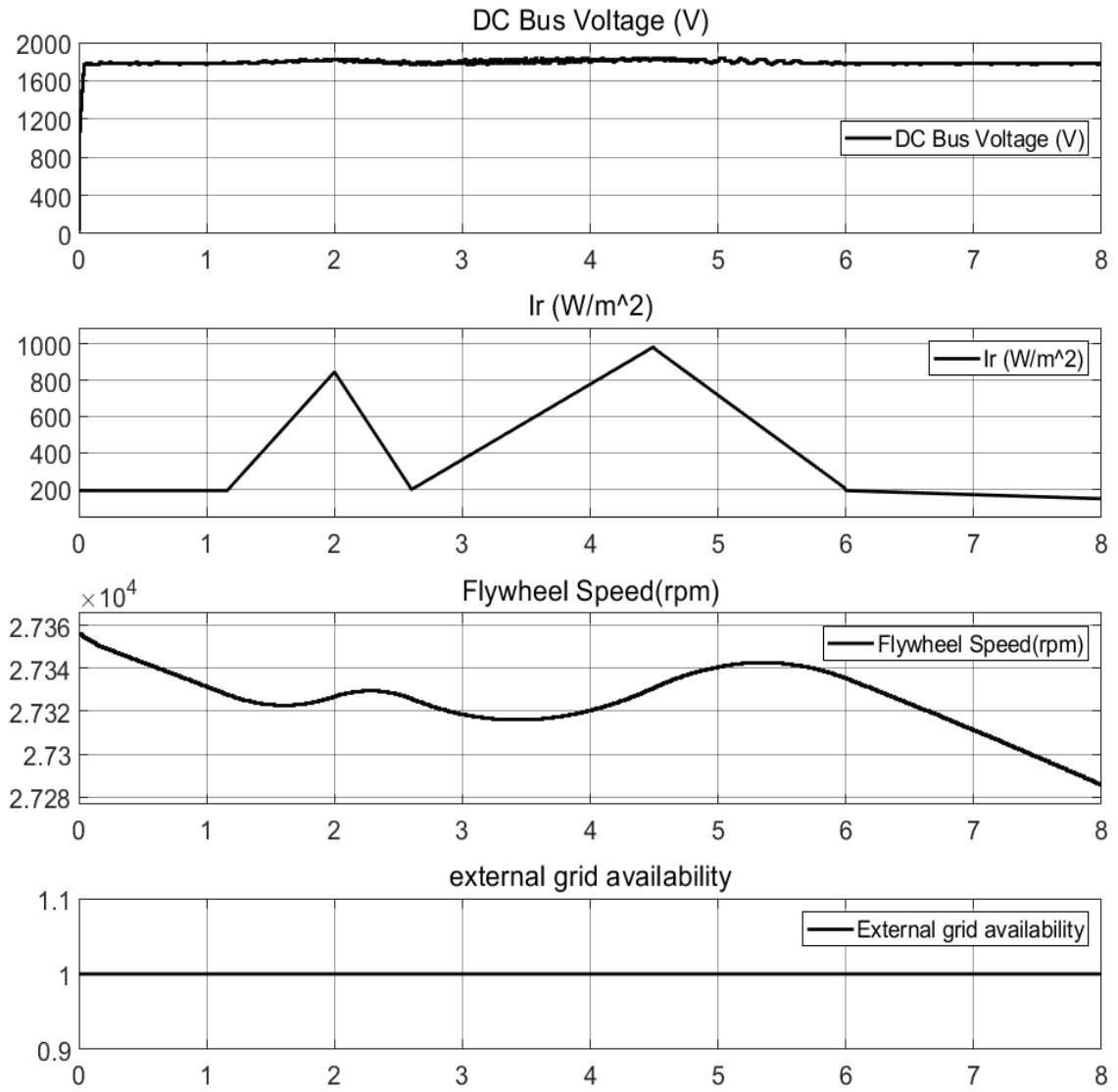


Figure 5-11 Status of system elements with fluctuating solar irradiation and variable load.

FESS Torque shows how the mechanical power changes in the flywheel due to changes in the electrical power in this scenario as shown in Figure 5-12 , Figure 5-13 and Figure 5-14 below.

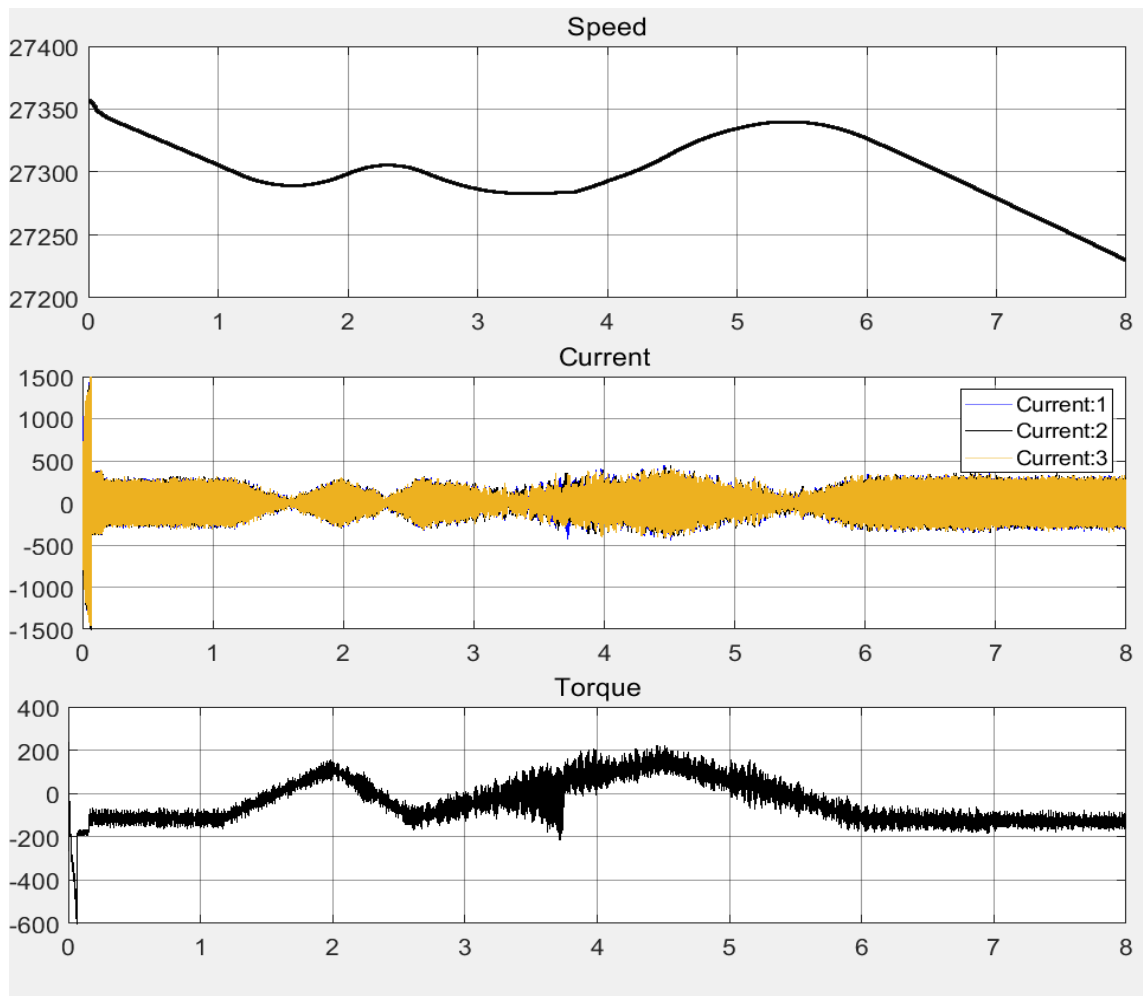


Figure 5-12 Flywheel speed (rpm), currents (Amp) and torque (N.m) at variable load and variable radiation.

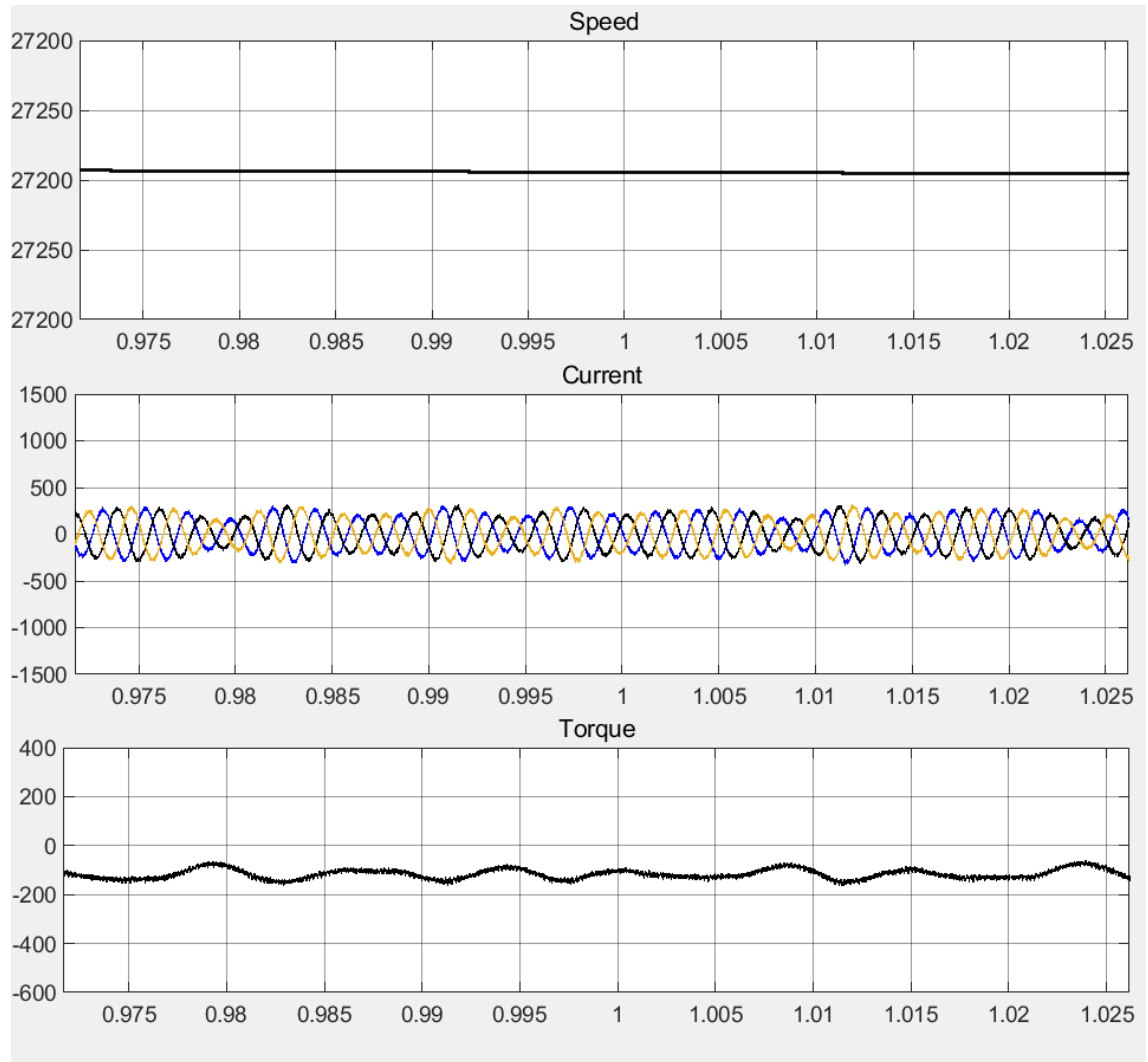


Figure 5-13 Zoom in at second 1 of Flywheel speed (rpm), currents (Amp) and torque (N.m) at variable load and variable radiation.

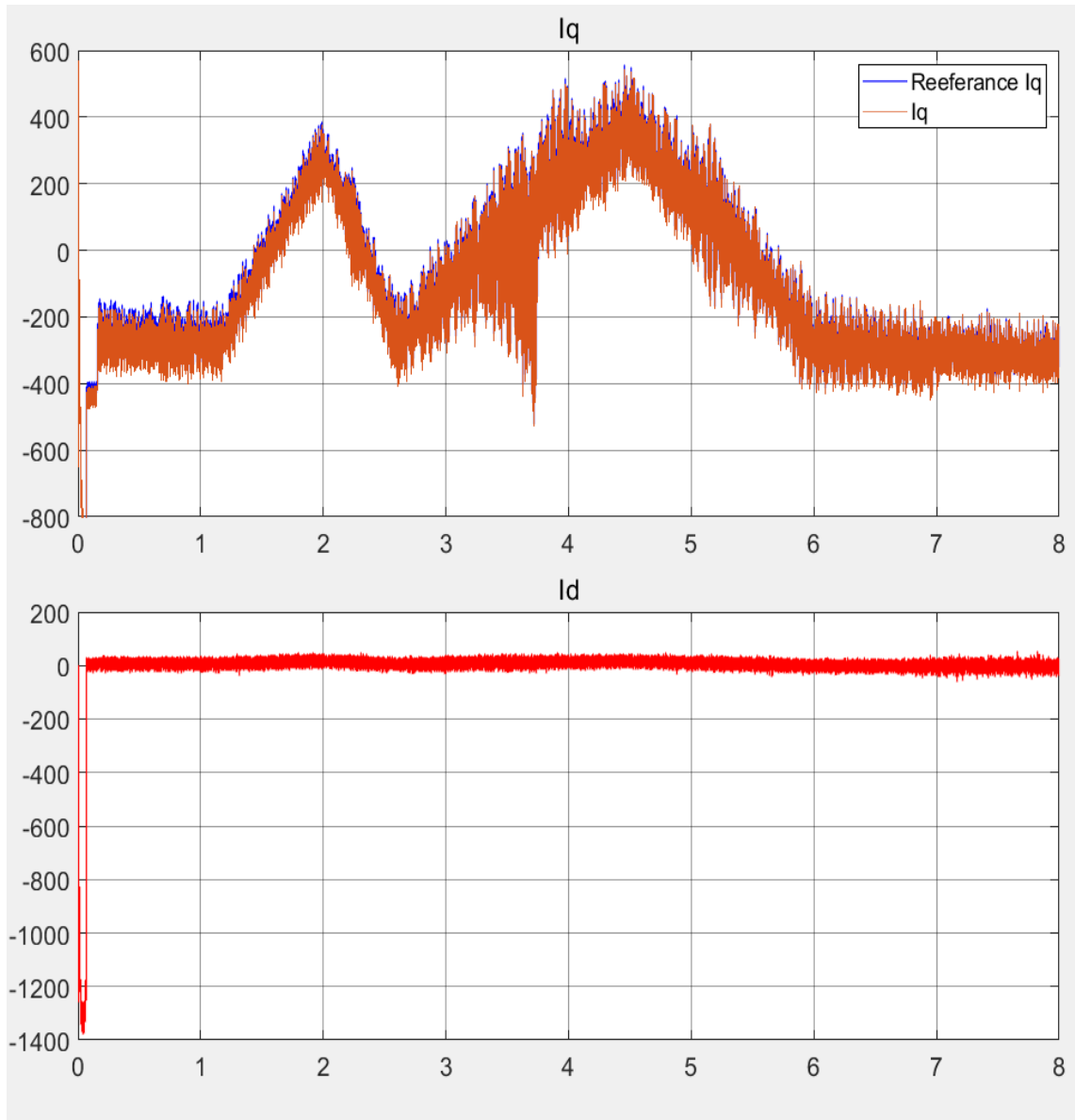


Figure 5-14 Direct and quadrature currents of flywheel with fluctuating solar irradiation and variable load.

5.3 Charging FESS from the Utility Grid and PVs.

In all previous scenarios the FESS was charged from the PVs. In this scenario the FESS will be charged from the utility grid as well as from PVs. The proposed system can control the DC bus reference voltage such that it is able to charge the flywheel from the external grid as can be observed in Figure 5-15 below. In this scenario the on-grid inverter imports a 300 kW from the utility grid. The FESS charging power is 300 kW plus the PVs power.

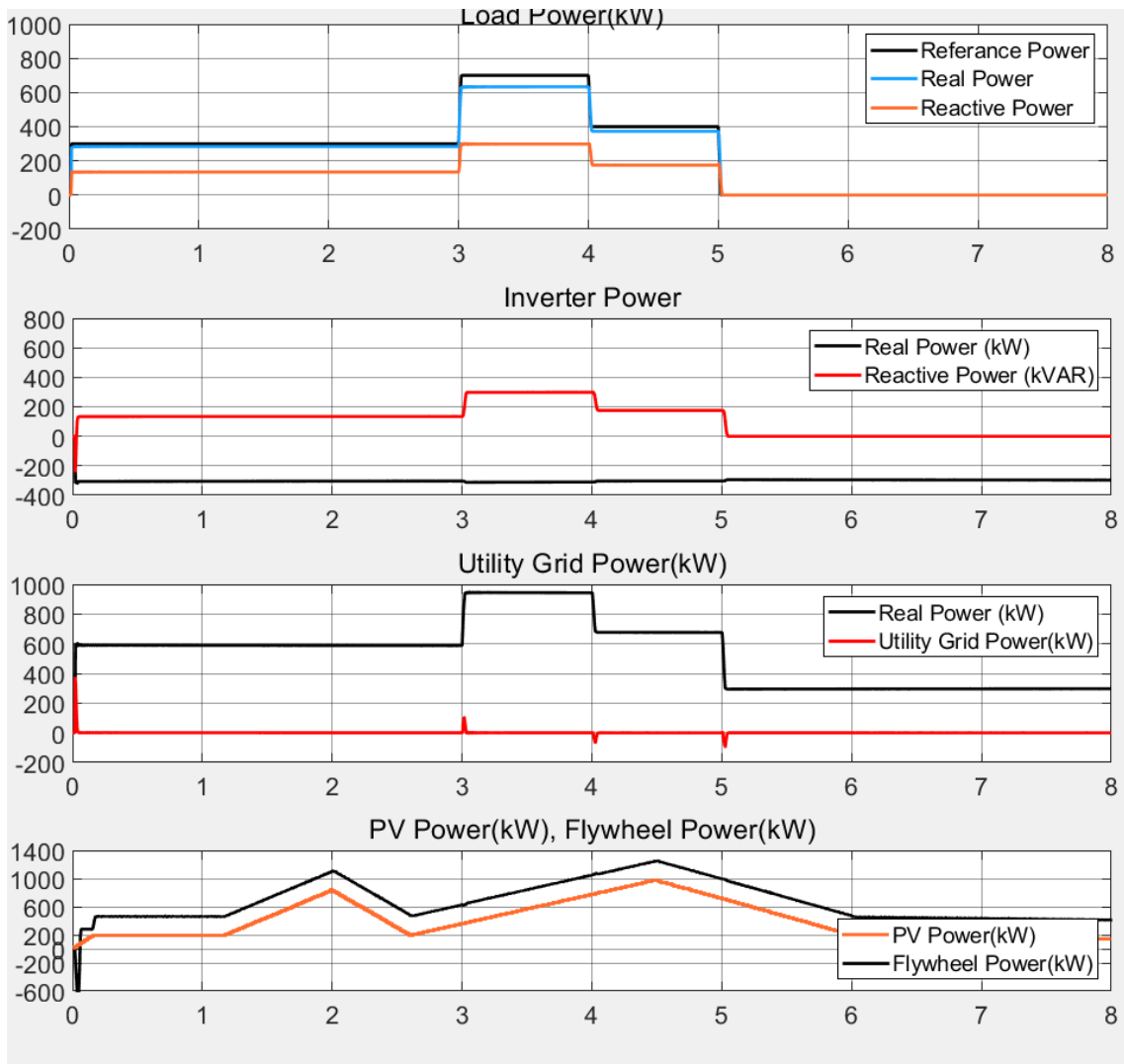


Figure 5-15 Power flow at variable load and radiation when charging from the utility grid with compensating the power factor.

Parameters such as input irradiation, flywheel speed and external grid connectivity are given in Figure 5-16 below. The external availability value "1" means that the Microgrid is connected to the utility grid. The DC bus voltage is regulated to be 1800 V.

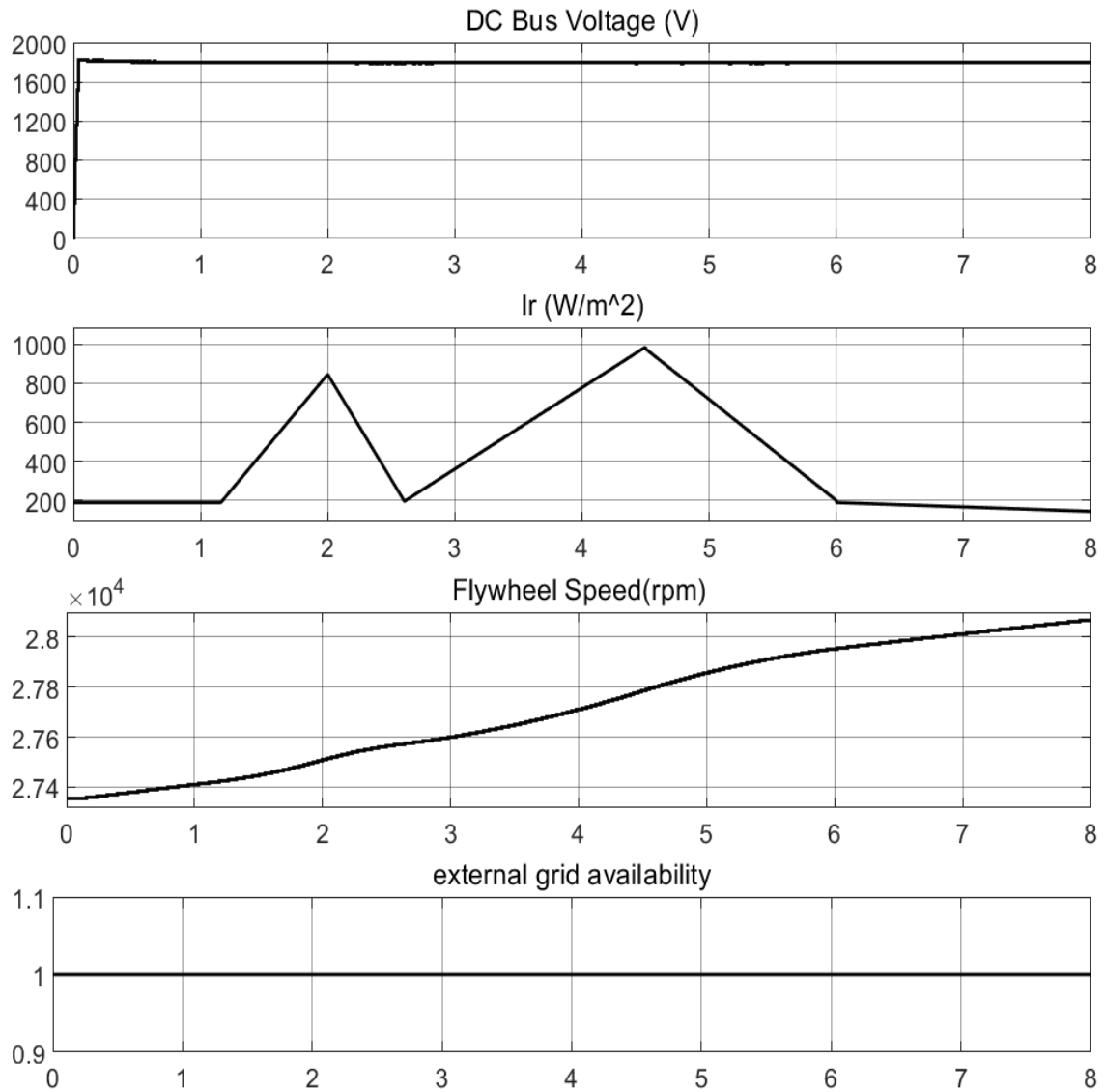


Figure 5-16 The DC bus voltage, irradiance and Flywheel speed when the system imports the power from the utility grid at variable radiation and variable Load.

The frequency of the system is illustrated in Figure 5-17 below. There are some transient periods due to step change in the load. When the load increases steeply the frequency decreases for very short time and then returns to steady state, and visa verse. The variation in the grid frequency is within the accepted range [40].

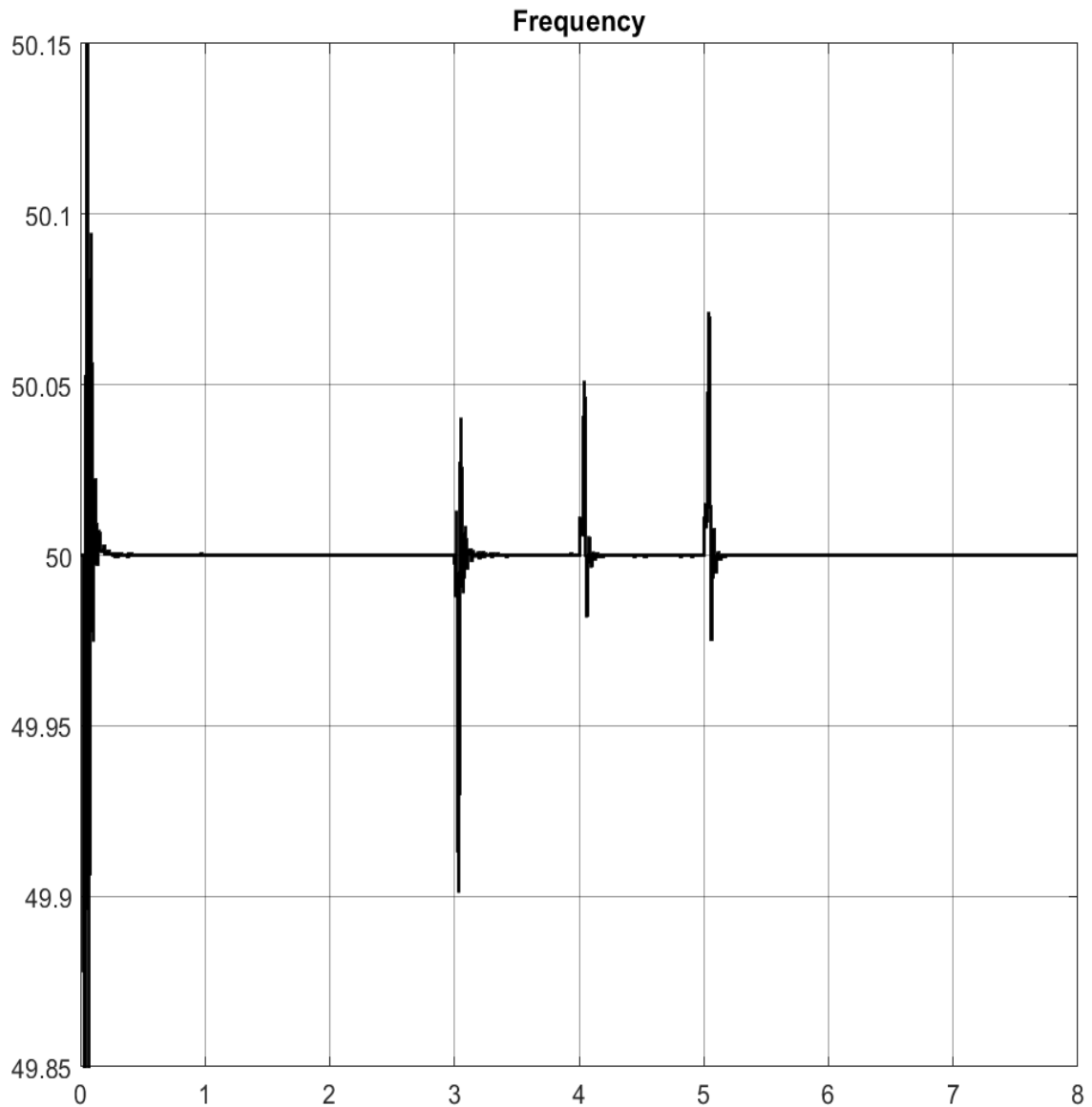


Figure 5-17 The Grid frequency when the system extracts the power from the grid at variable radiation and variable load.

The following Figure 5-18 depicts the system voltage and current when the FESS charges from the microgrid with fluctuations in PV power and step changes in power load.

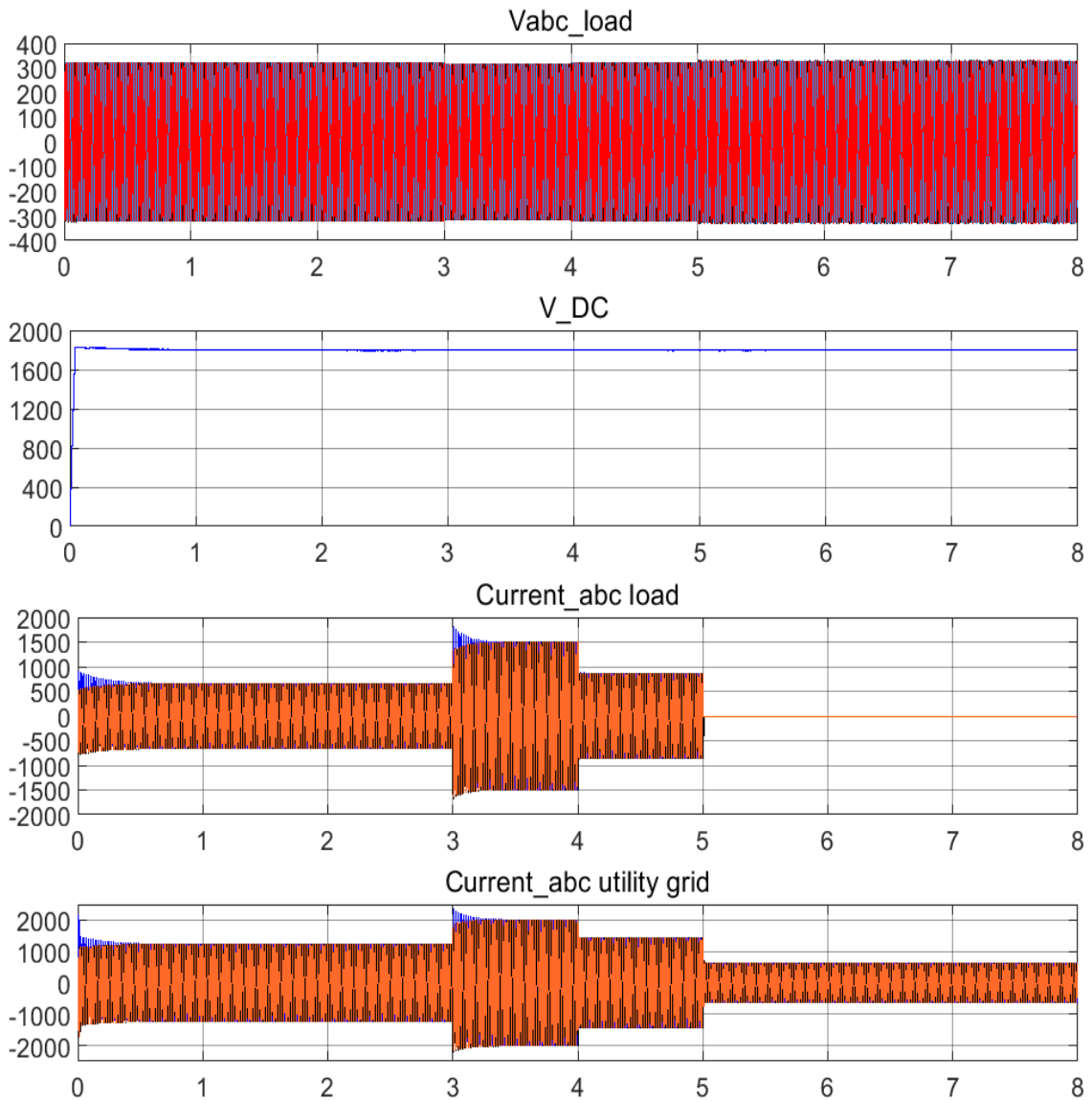


Figure 5-18 The current and voltage when The system extracts the power from the grid at variable radiation and variable load.

Flywheel speed, reference speed, currents and torque of the FESS when charging from the microgrid and from PVs are shown in Figure 5-19 below.

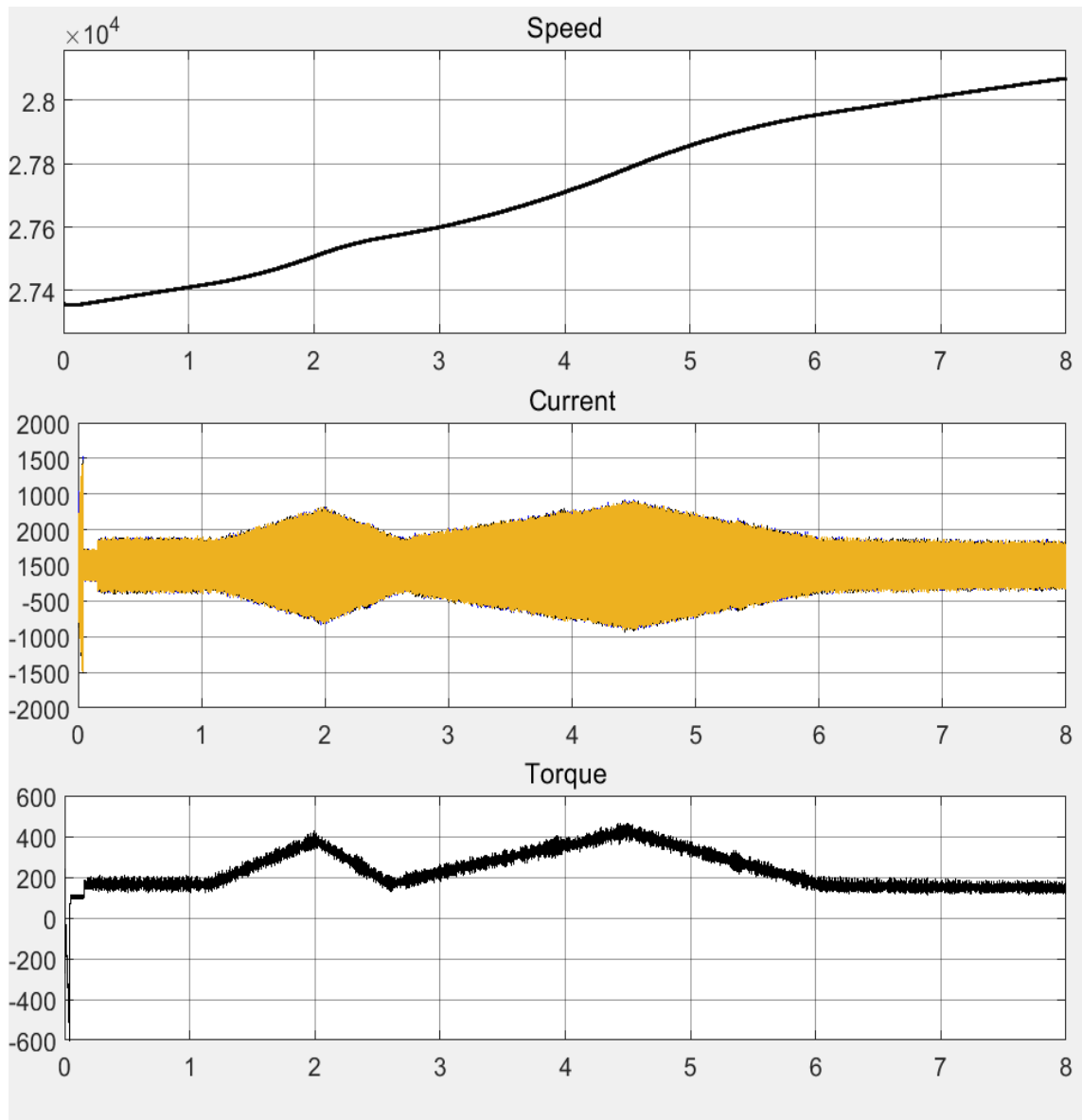


Figure 5-19 Speed, currents and torque of FESS when The system imports the power from the grid at variable radiation and variable load.

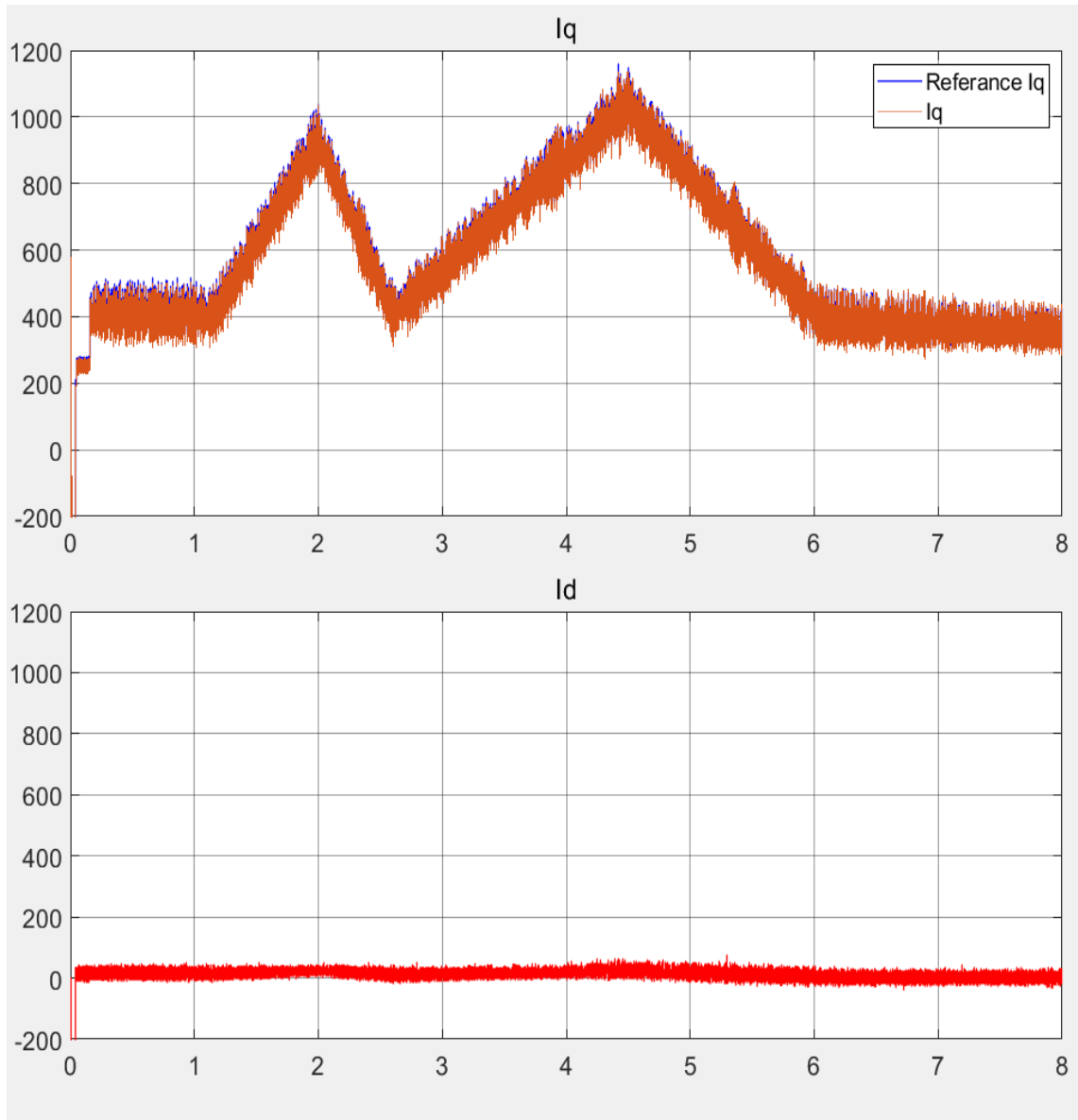


Figure 5-20 I_d , I_q and referace value of I_q when the FESS charges from the grid.

5.4 The PV and FESS cover the load (100% penetration level of PVs continuously)

In this scenario, the system measures the load demand to force the inverter to be able to cover this load, as can be identified from Figure 5-21 below. It is clear that the amount of power produced by inverter from the FESS and PV panels is equal to the load power and hence, the power comes from the utility grid is zero. The inverter was capable to regulate the power flow despite the variations in the radiation and load demand.

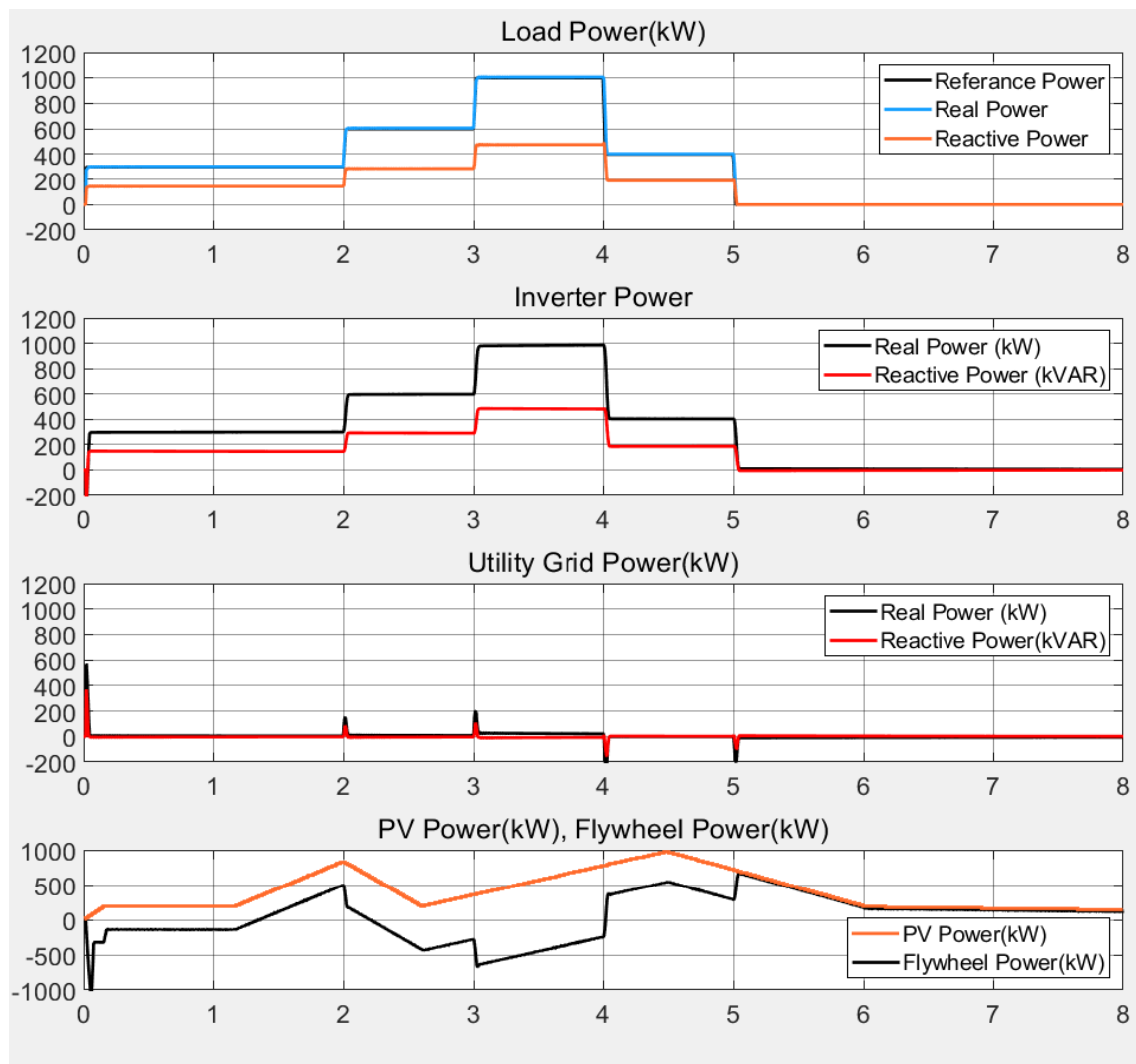


Figure 5-21 Power flow in the system when variable radiation and variable resistive load, inverter produce power equals to demands.

As expected, the current flows from utility grid is around zero as can be seen in Figure 5-22 shows that the. The importance of the utility grid in this case is to have synchronisms between the inverter and utility grid to be ready for any change in power flow.

Figure 5-22 also shows that the voltage profile is stable, the total current from the inverter, and the current from utility grid. The current from utility grid is around zero, the small spikes from utility grid are due to the step changes in the Load.

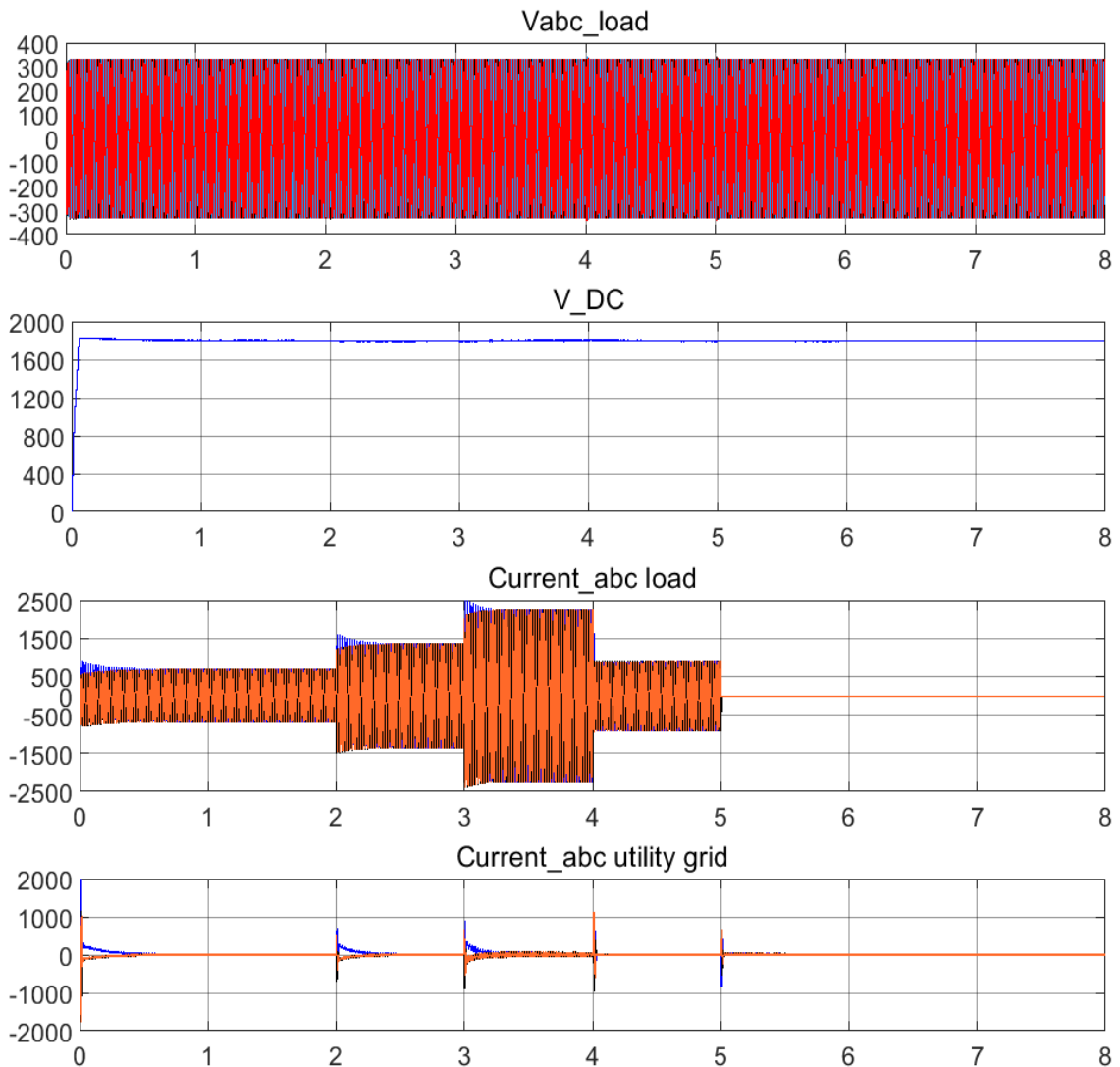


Figure 5-22 Voltage, Current from the utility grid and currents to the load when the inverter covers the total load demand.

Figure 5-23 below shows the regulated DC Voltage, flywheel speed, and the input radiation, In this system flywheels bank contains two flywheels. The speed decreases from 28600 rpm to 28300 rpm when the load was increasing, then the flywheel charges again and the speed increases slightly, when the load decreases.

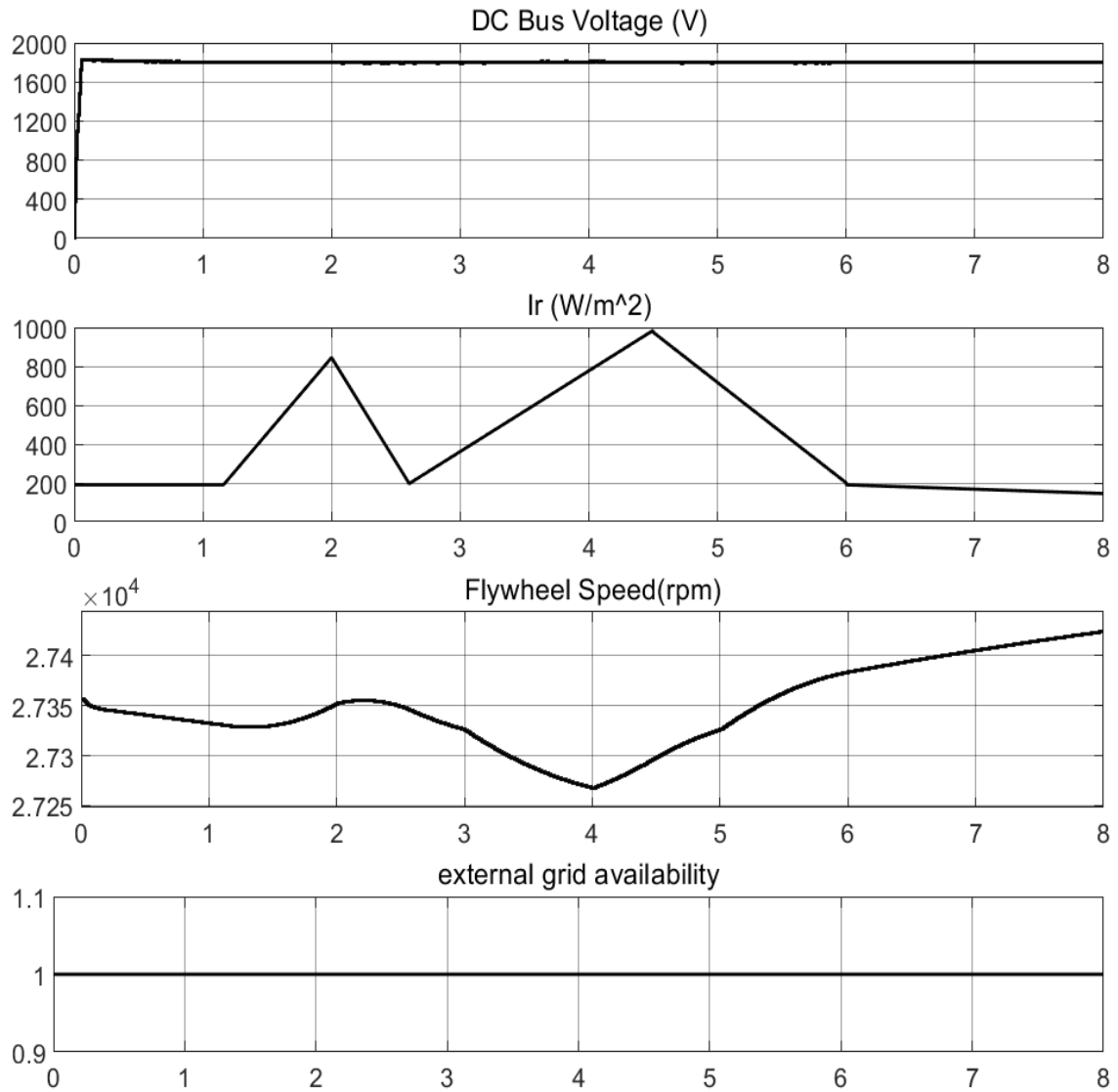


Figure 5-23 The status of DC voltage, radiation and the FESS speed, when the inverter covers the load.

Figure 5-24 depicts the impact of the changes in the system on the system frequency. When the load increases, the frequency goes down slightly and then increases before returning to the normal steady state value.

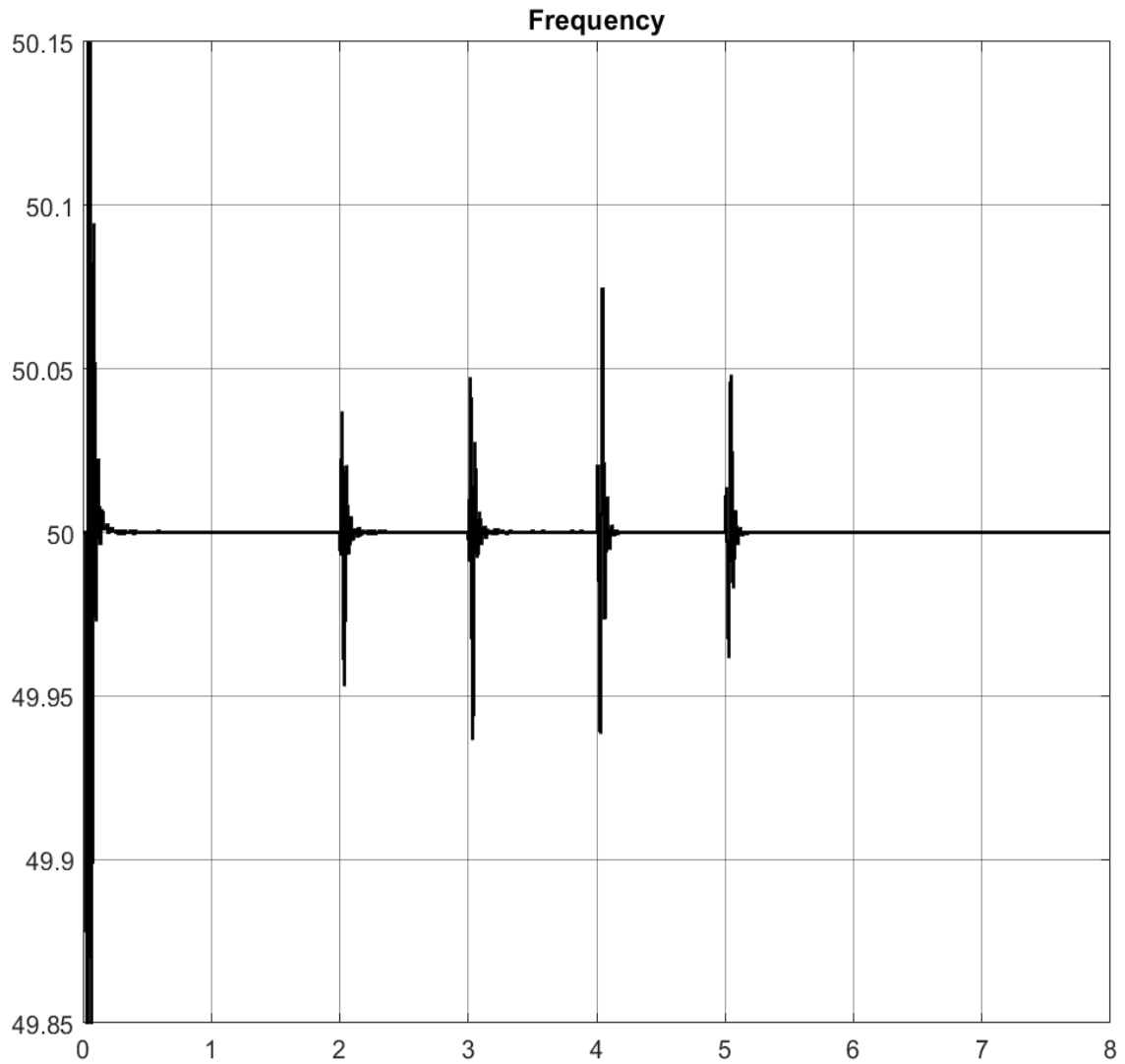


Figure 5-24 Electrical frequency on the grid.

The speed, torque and current of the flywheel are changing according to the availability of the power from the PV as can be observed from Figure 5-25 & Figure 5-26 below. Changing in reference I_q leads to changing is the flywheel speed directly. This means changing in power flow with very fast response.

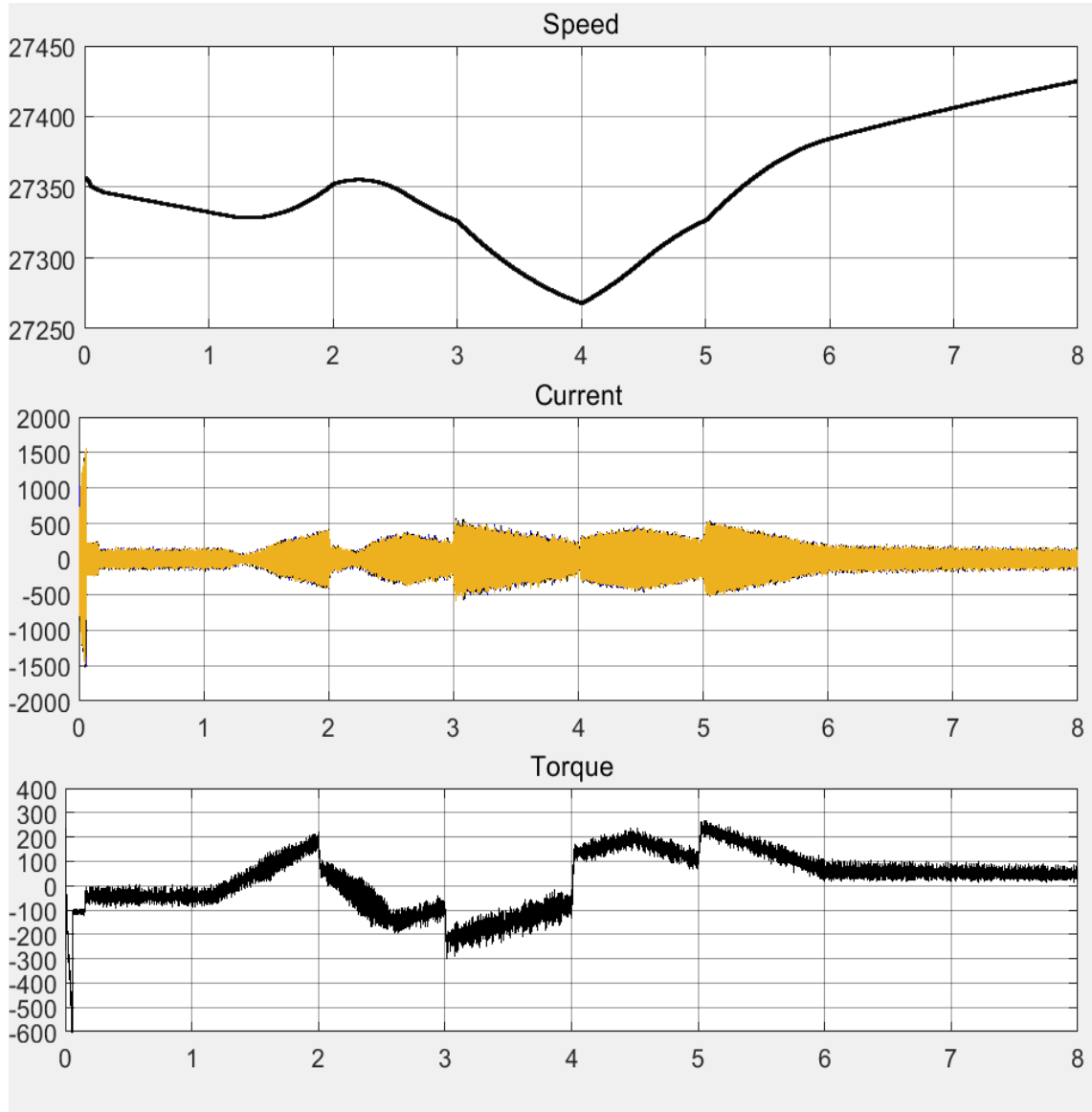


Figure 5-25 Actual speed, reference speed, current and Torque of FESS.

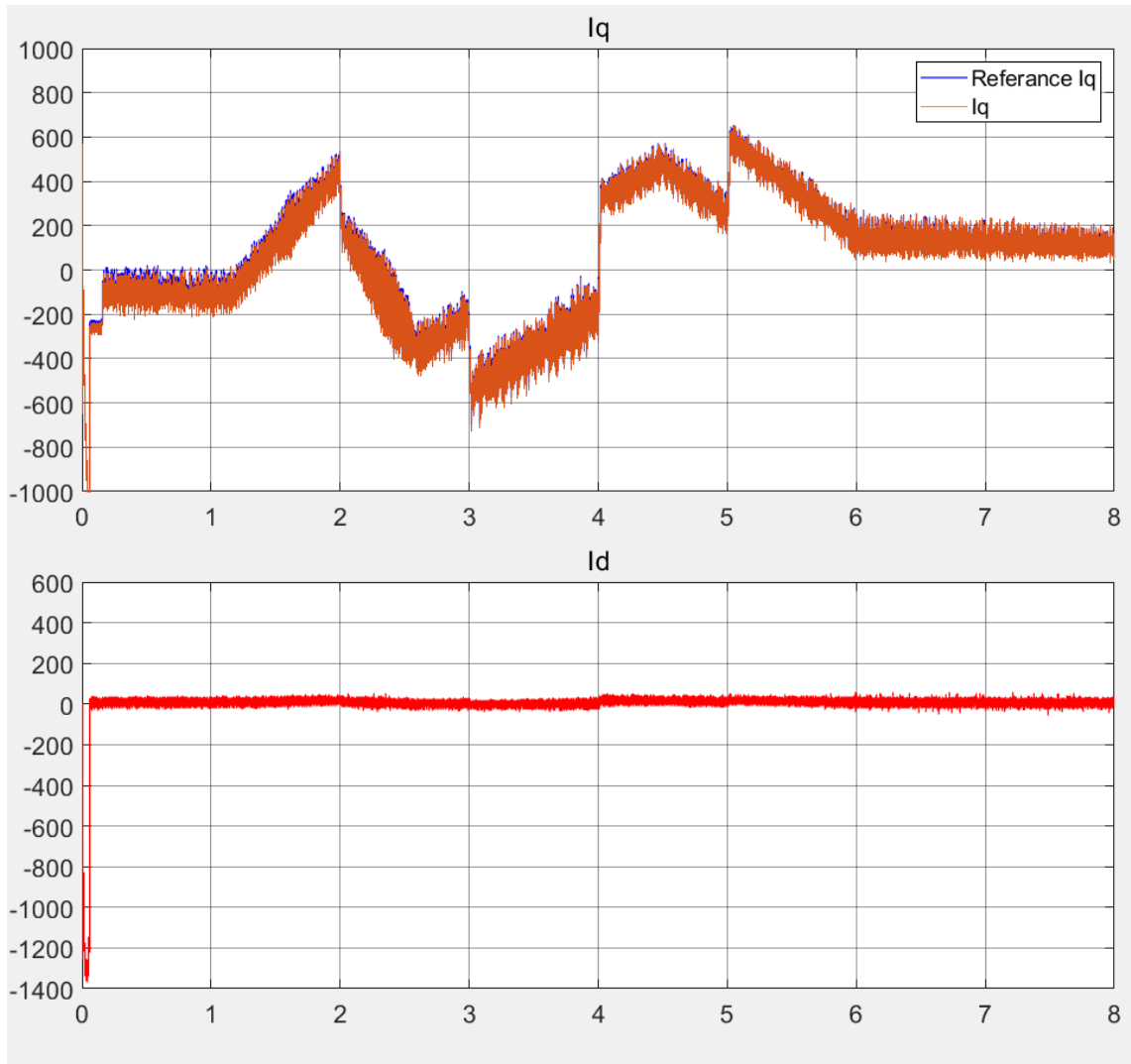


Figure 5-26 I_q , I_d and the reference I_q when the PV and the FESS cover the load.

5.5 UPS Mode with variable load.

In this scenario we explore the behavior of the FESS when there is an interruption from the utility grid. When the utility grid is disconnected, the inverter works as off-grid inverter. Then when the power quality of utility grid returns, the bypass switch connects the microgrid with utility grid, but after synchronizing them.

After connecting the utility grid with the system, FESS inverter extracts a suitable amount of energy such that the power quality in the grid remains at steady state rate of power flow.

To explore the behavior of the proposed system in UPS mode, the simulation takes the worst scenario. Similar to the pervious scenarios, we have four step changes in the load, very fast change in solar power and an interruption happed in the utility grid, then returns after 2 second. All these changes occur in the system component within eight second.

Regulating the solar power by flywheel is explained in the previous section. FESS was secondary source of power: it imports/exports power from/to the utility grid with constant rate or variable rate as needed. In the UPS mode, the system works similarly but with very fast response.

In the input inverter side, the FESS regulates the solar power, so usually, there is no unpredicted changes that can happen suddenly in the inverter side. But in output side of inverter the unpredicted changes may be happen suddenly due to the changes in the load. If a step changes in load happed suddenly, the inverter feeds the load side by side with the utility grid.

The step change in inverter power must be done when an interruption happens. At this state, the inverter is the sole power source. It is clear that the summation in power flow in the microgrid is zero.

Figure 5-27 illustrates the behavior of the different components of the system when an interruption occurs. At time= 2.5 sec, a disconnection from the utility grid occurs and lasts for 2 sec.

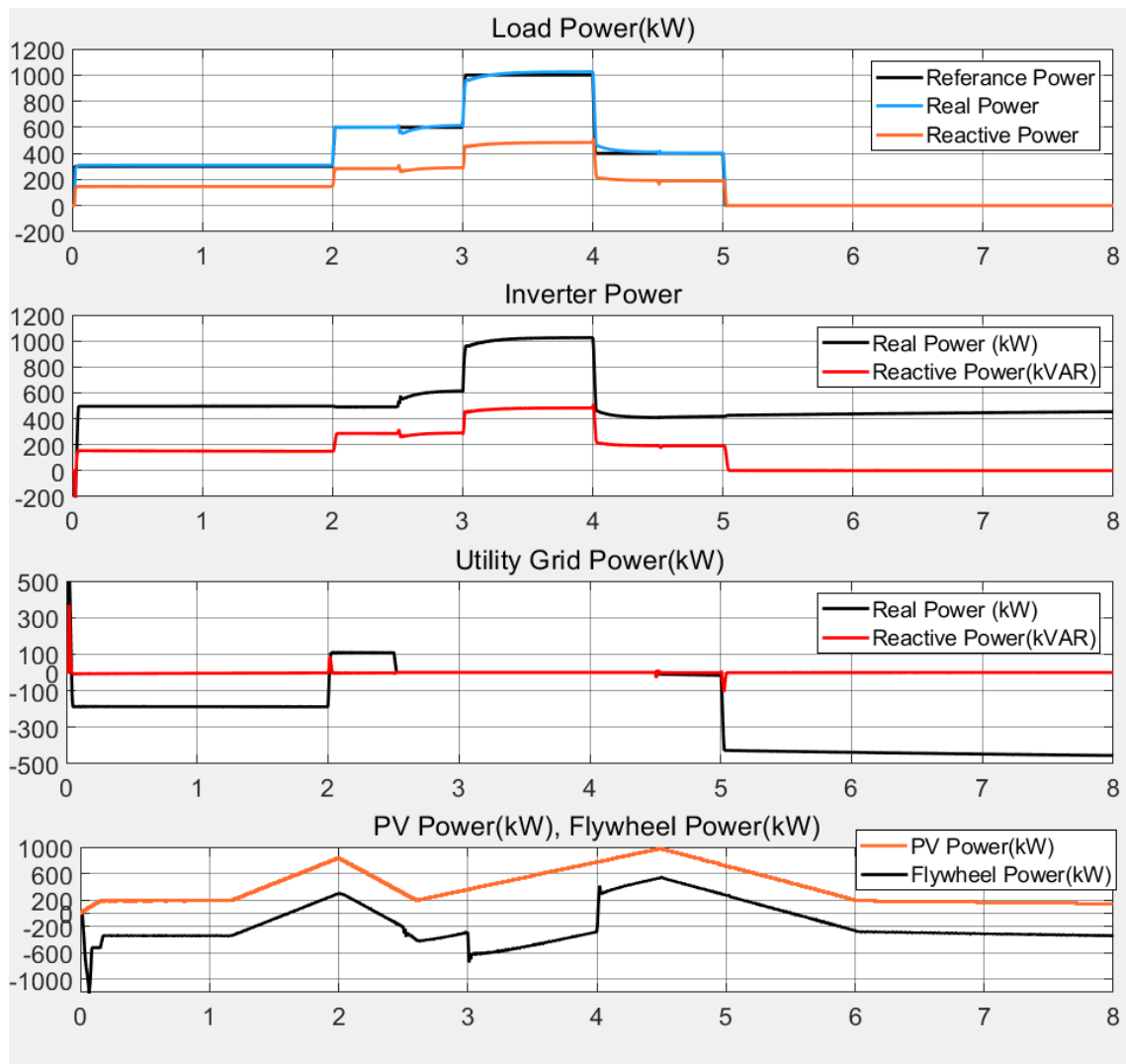


Figure 5-27 system behavior through UPS mode with variable load and variable radiation.

Initially the load was covered from the inverter and as the load increases at sec 2, the utility grid covers the shortage. But now at time=2.5 sec, the disconnection from the utility grid forces the inverter to cover the whole load and so, the power comes from the utility grid becomes zero. In fact, the inverter was able to cover the variable load. At 4.5 second the utility grid returns back, so the inverter returns to inject power synchronized with the grid. In this scenario the inverter returns to inject the power with the same rate as before interruption happened. Note that when the utility grid is online, the inverter can extract the power as you want.

From second 5 to 8, the load becomes zero and therefore the inverter starts to export

power through the transformer to utility grid. This makes it possible to have a Microgrid that works in the connected and isolated modes.

Figure 5-28 shows FESS speed, irradiance, DC voltage, and the utility grid availability. The voltage in DC bus remains constant, the variation in the power flow has impact on the flywheel speed.

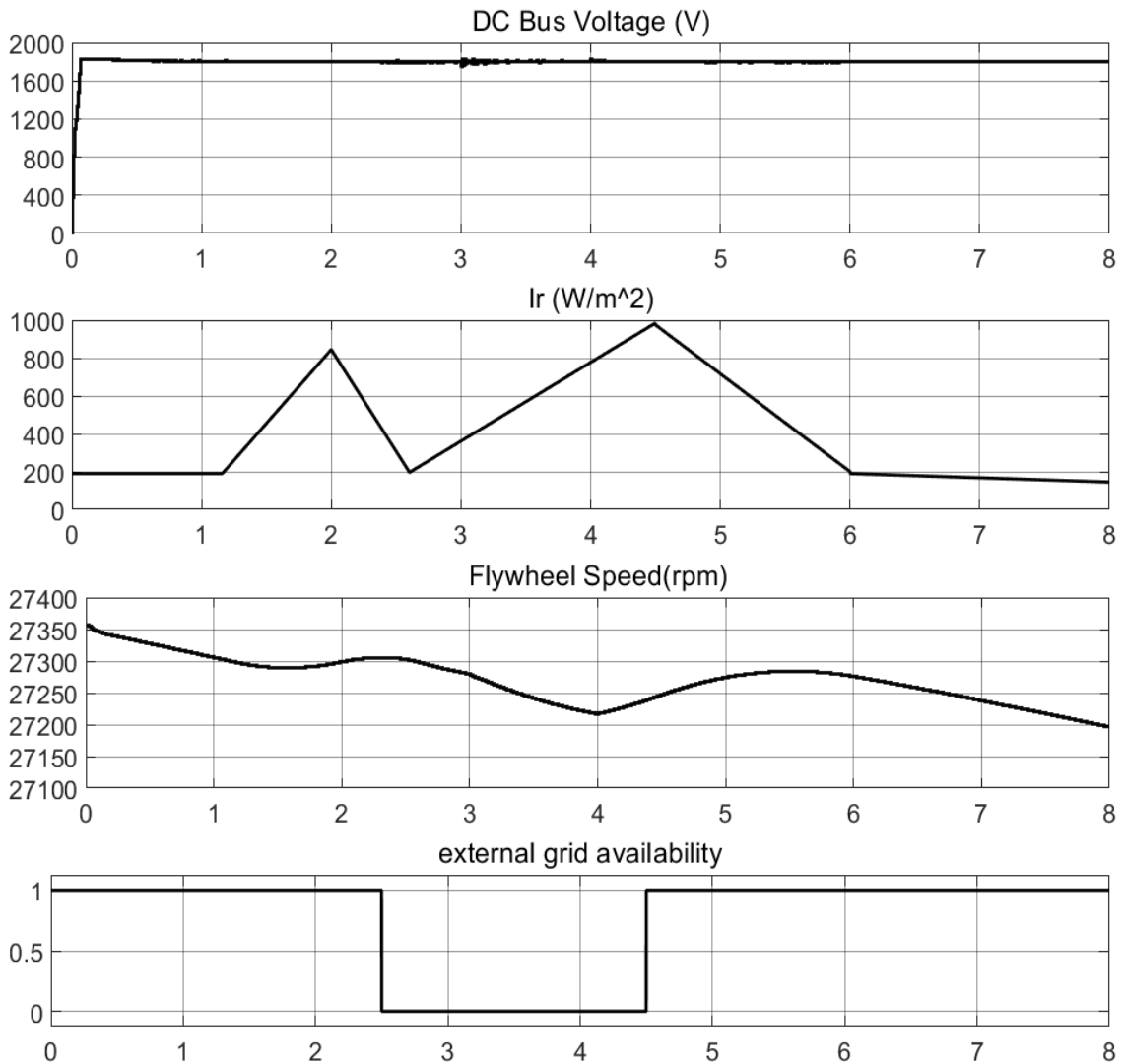


Figure 5-28 Status of FESS element at UPS mode.

Figure 5-29 shows the frequency of the system. There are changes in the frequency due to the changes in the load, i.e., increasing the load leads to decreasing in frequency and vice versa.

In addition of load effect, the inverter power flow affects the frequency, e.g., when the inverter injects the power, the frequency will increase. Although we have relatively high changes in the frequency, we are still within the accepted limits. The main reason behind these changes in the frequency is the disconnection from the utility grid.

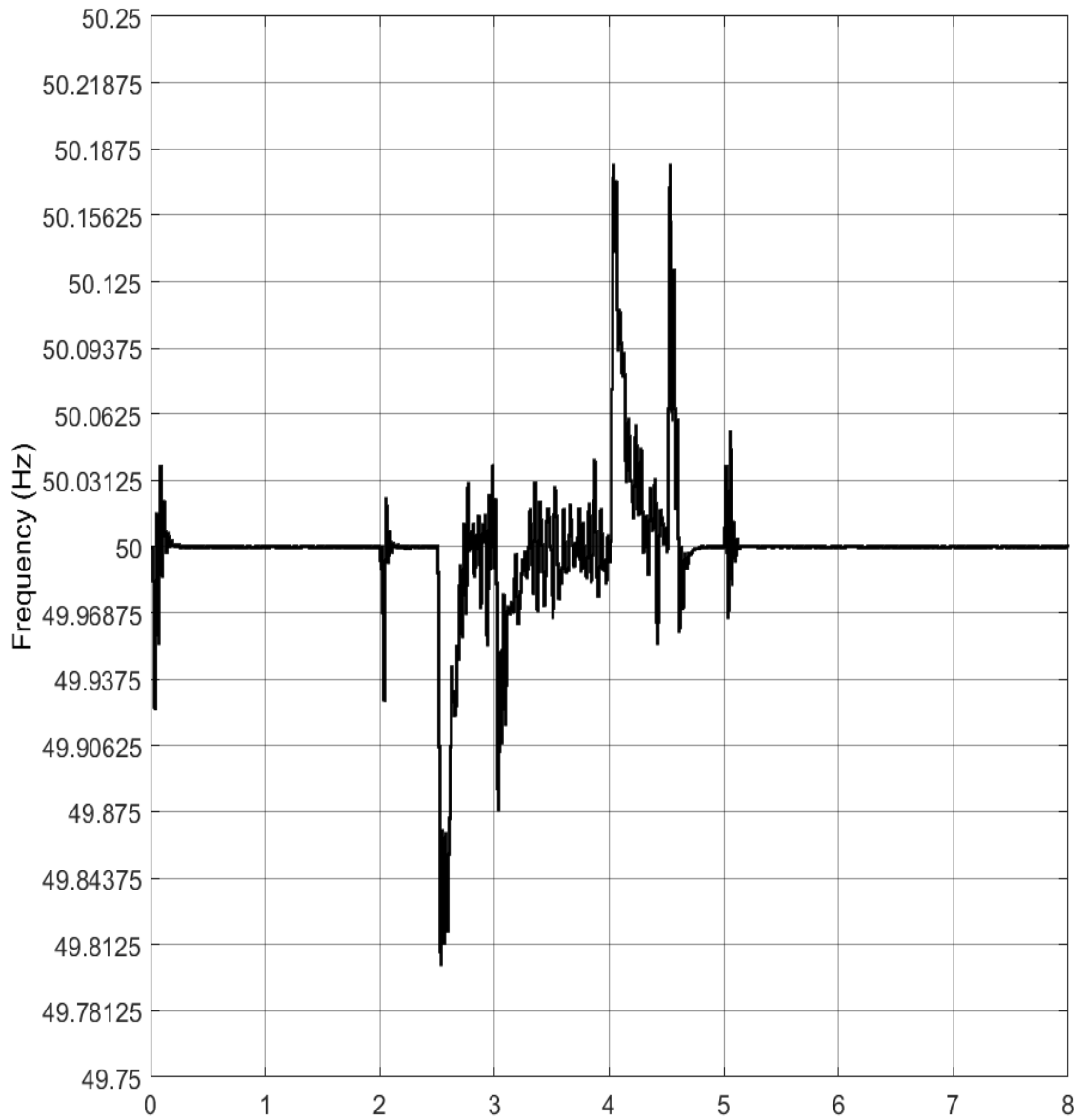


Figure 5-29 Frequency of the system at UPS mode.

In UPS mode when the bypass disconnects the utility grid, the inverter regulates the output voltage easily because the input dc voltage is controlled, i.e., the output current regulated by changing the modulation index as can be seen in Figure 5-30.

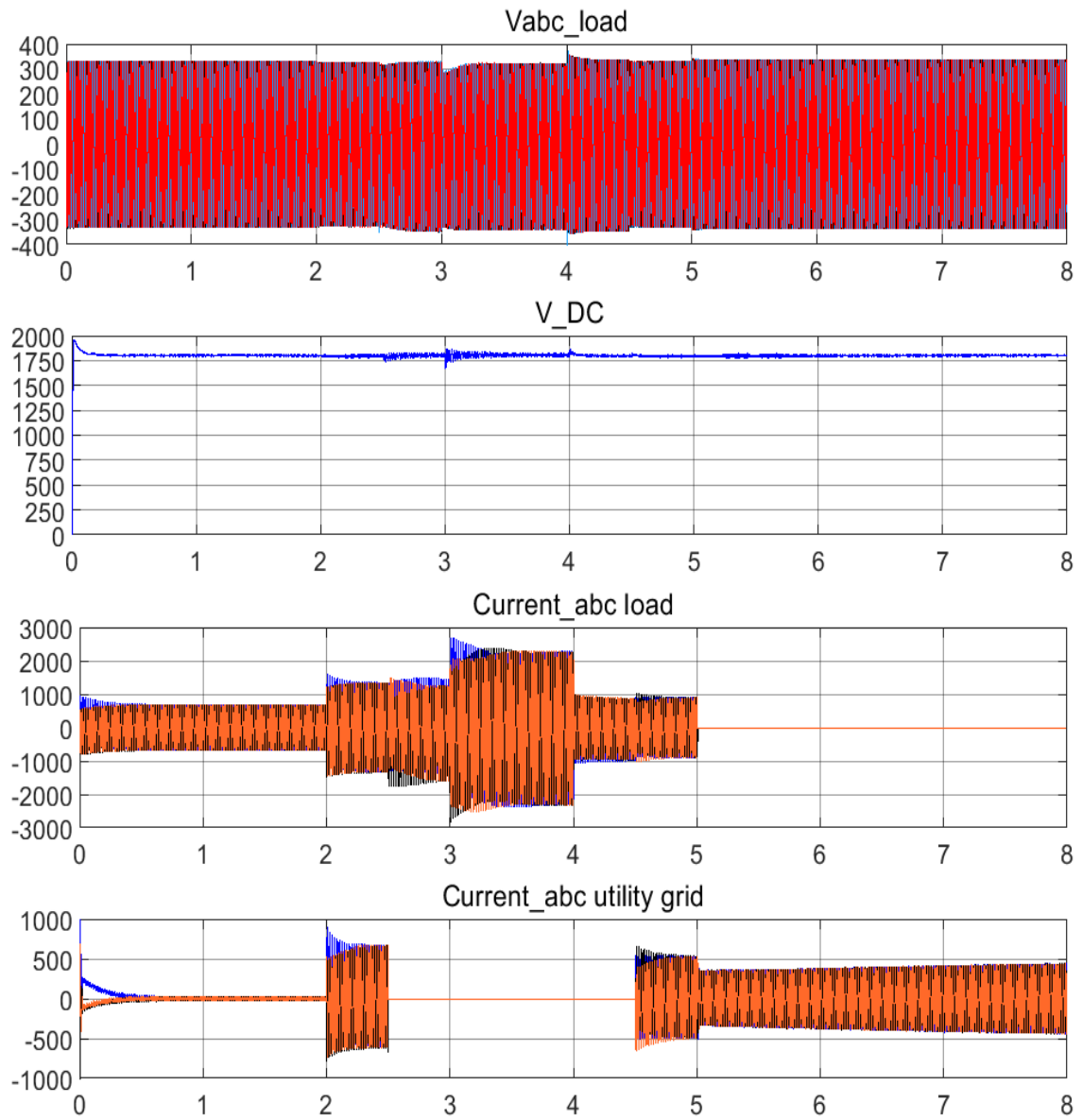


Figure 5-30 Voltage and current profile of the system at UPS mode.

The following Figures (Figure 5-31 & Figure 5-32) shows the speed, current Id, Iq, Iq reference and Torque of the Flywheel in the UPS mode.

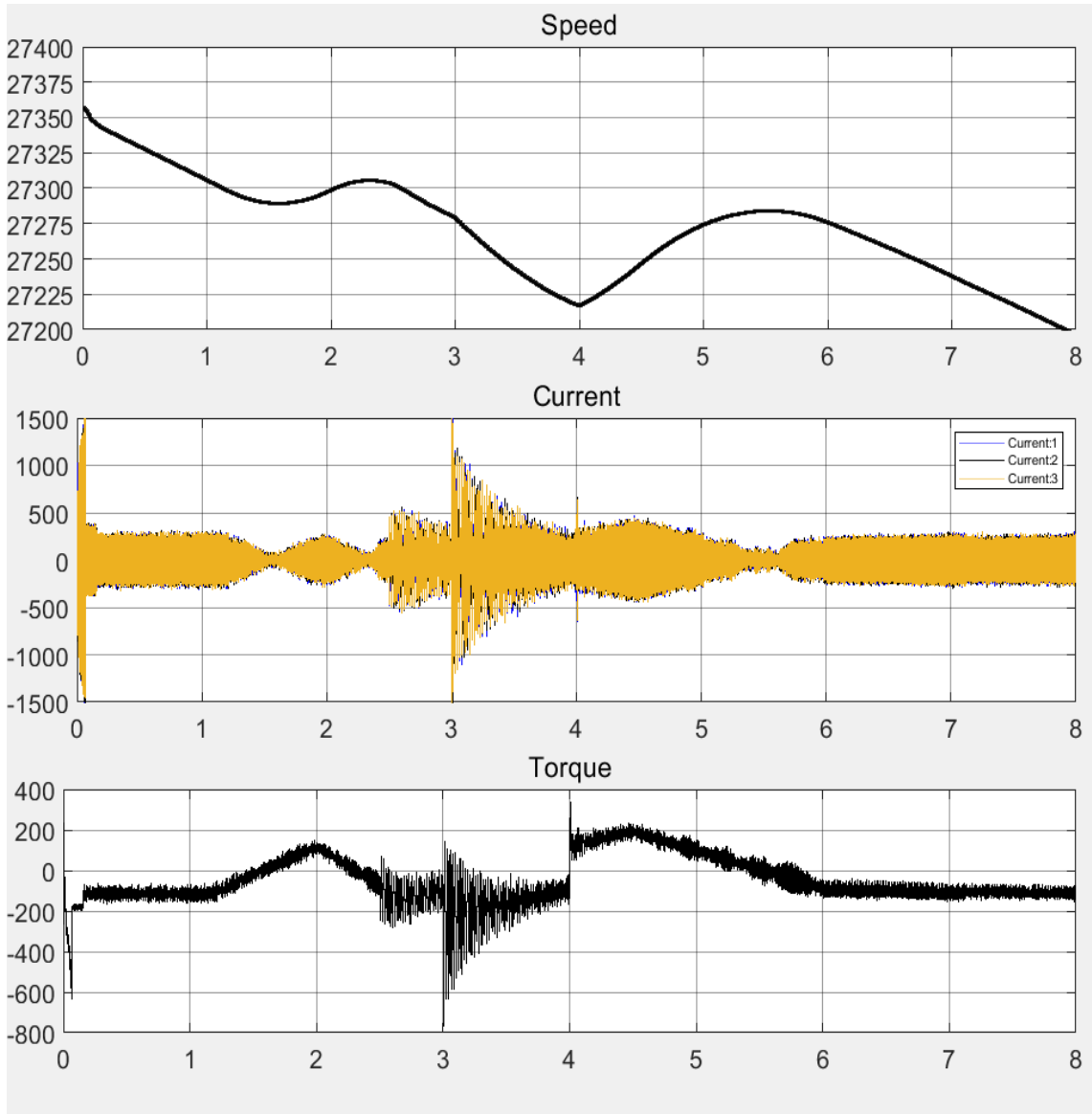


Figure 5-31 FESS speed, current and torque at UPS mode.

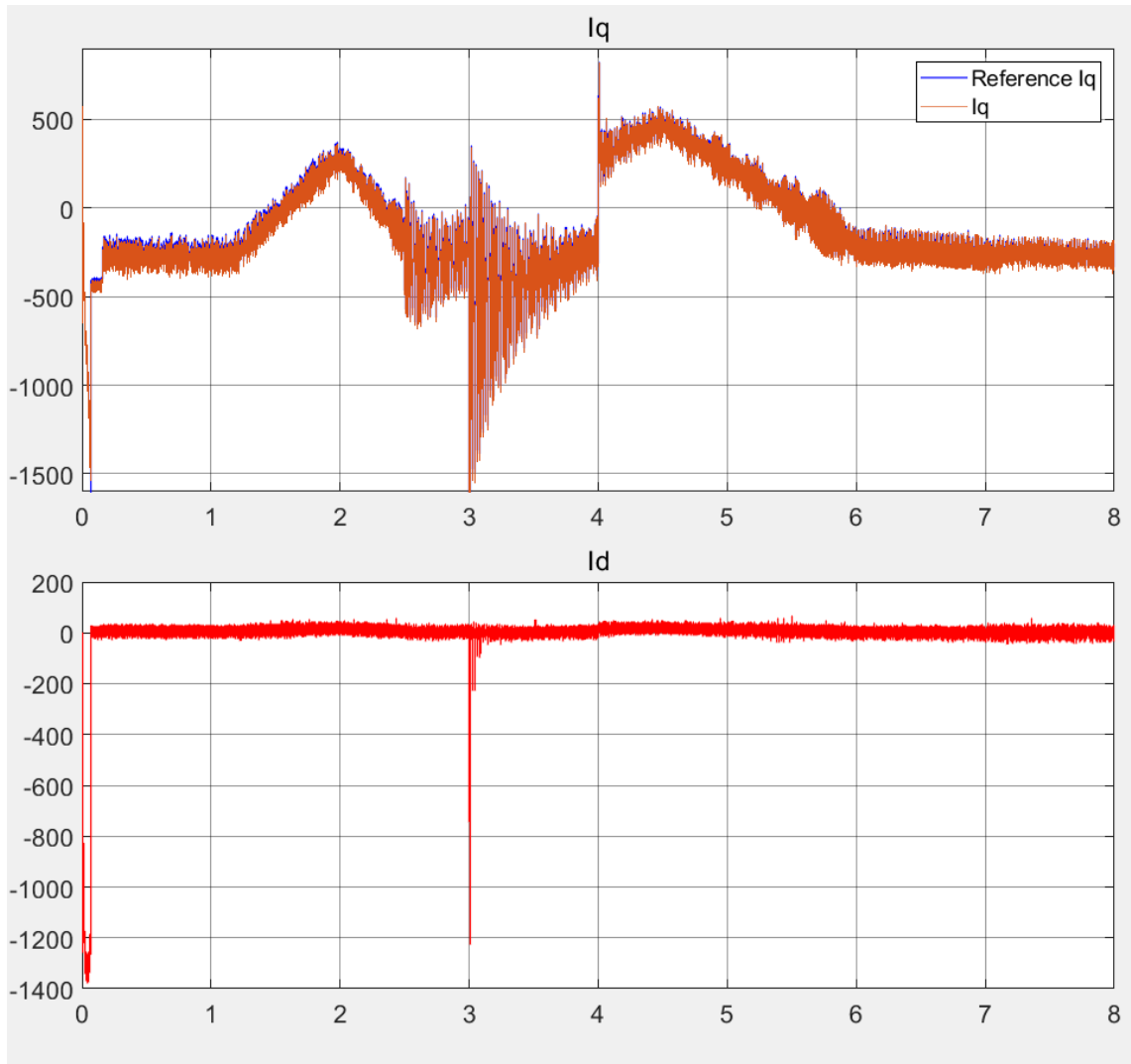


Figure 5-32 Flywheel I_d , I_q and I_q reference at UPS mode.

5.6 Efficiency Calculation and Measurement:

In this section the simulation estimates the efficiency of the FESS, flywheel machine converts the electrical energy to mechanical energy, the value of angular velocity in the flywheel is the amount of mechanical energy stored in the wheel.

To do the efficiency calculations of FESS we remove the PV from the Microgrid as shown in Figure 5-33 below.

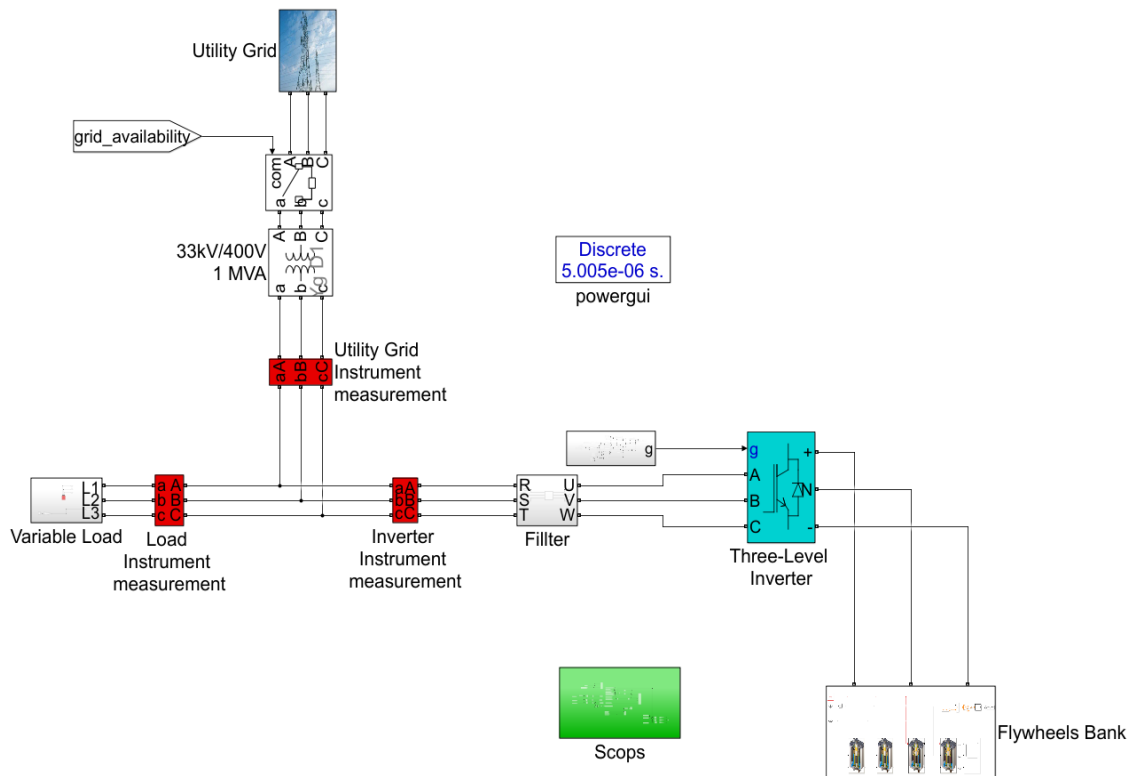


Figure 5-33 System topology of FESS without PVs.

The strategy of efficiency test is to command the on-grid inverter to absorb 400 kW from the network in the time between 2 to 5 second of simulation time, then extract 400 kW to the grid from 5 to 8 second of simulation time.

In the DC bus of FESS there are current and voltage sensors that measure the power and then integrated to measure the energy. One of these integrators measure the charged energy during the first 3 seconds and another one measure the discharged energy during the last 3 seconds.

As can be identified from Figure 5-34, at the period from 2 second to 5 second there was an increase in the speed is from 28050 rpm to 28186 rpm. During this period, the integrator measures 332.6 Wh from the grid as can be seen in Figure 5-35. This is equivalent to converting the electrical energy to mechanical rotational energy by 136 rpm increasing in each flywheel. So, at the charging period, the system converts 2.4456 Wh from on-grid inverter to 1rpm rotational speed.

At the period from 5 second to 8 second there was a decrease in the speed from 28186 rpm to 28050. During this period, the integrator measures 331 Wh from the FESS. This is equivalent to converting the 136 rpm of mechanical rotational energy to 331 Wh. So, at the discharging period, the system converts 1rpm rotational speed to 2.4338 Wh into the grid. In Figure 5-34 shows how flywheel speed (rpm) returns to the same before it is charged at second two.

The Table below summarizes the efficiency calculations.

Table 5-1 Energy flow and efficiency table.

	Charging period (Input Energy)	Discharging period (Output Energy)	Efficiency of FESS
Inverter energy	332.6 WH	331 WH	99.52 % Grid side
Inverter energy per 1 rpm	2.446 WH	2.4338 WH	

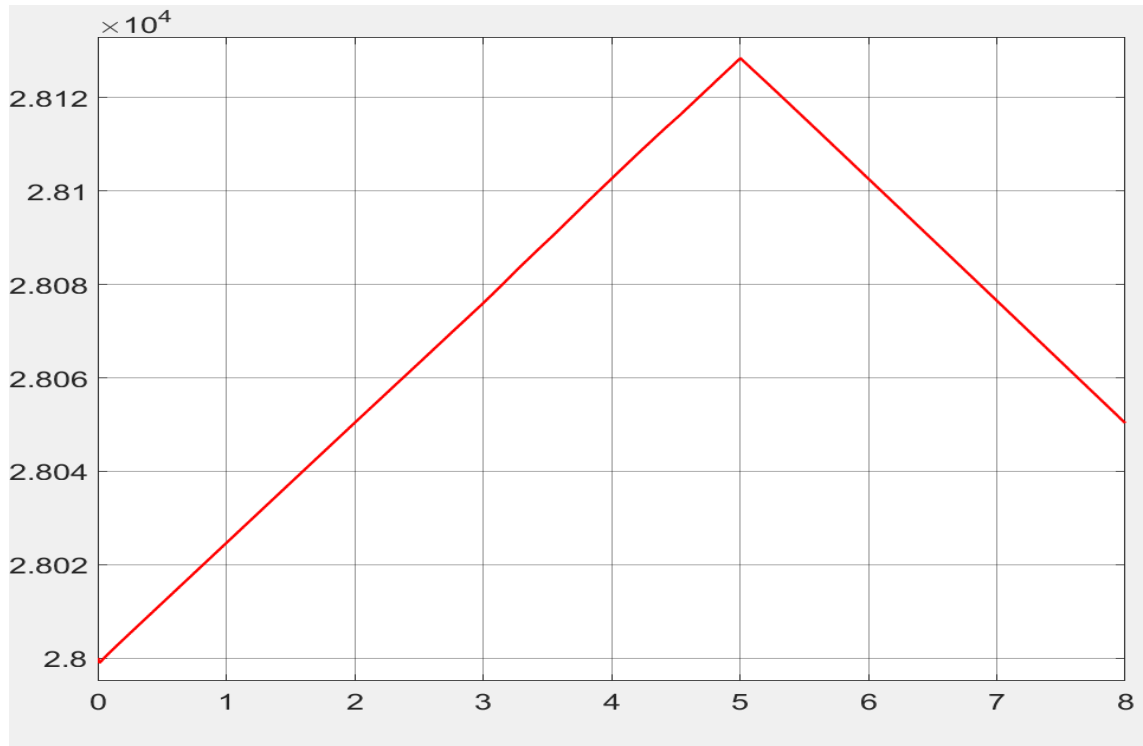


Figure 5-34 Flywheel speed through charging and discharging period.

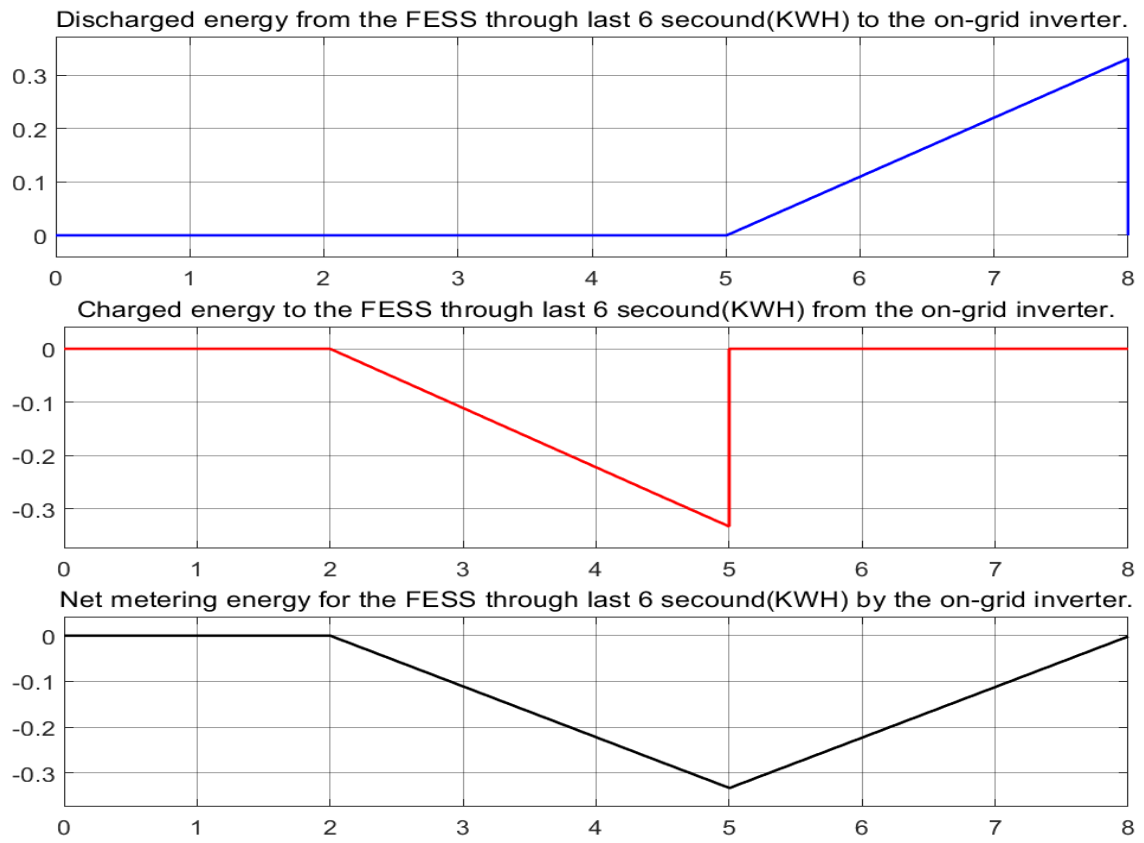


Figure 5-35 Energy meter through charging and discharging period.

Conclusion & Future work

In this thesis, we built a detailed model for FESS with different scenarios using MATLAB Simulink with the diverse components of the microgrid. The results showed that FESS is an attractive choice to solve different problems inside microgrids such as short-term power interruption and compensating the fluctuations from PV systems. We showed also the capability of Flywheel to stabilize the power quality inside the microgrid.

In general, the stability in high penetration levels of distributed generations (DGs) must be high to ensure the power quality issues in the microgrid. In this study, adding the FESS to the DC bus of the inverter increased the stability with no limitation for penetration level. Moreover, this new proposed system manages to change the mode smoothly between off-grid inverter in UPS mode and on-grid inverter with high penetration levels.

As future work, the evaluating the efficiency in detailed with a smart controller considering the forecasting in the microgrid could be applied with PVs in traditional design, then adding the FESS in the system using the traditional topology and with the proposed topology. Power flow should be monitored for long period to compare between them to estimate the feasibility. A smart algorithm could be also developed to manage the power flow in the optimum cases taking into consideration the load and the PV forecast production.

References

- [1] Owusu, P.A. and Asumadu-Sarkodie, " A review of renewable energy sources, sustainability issues and climate change mitigation," *Cogent Engineering*, vol. 3, no. 1, p. 1167990, 2016.
- [2] Molina, Marcelo Gustavo., "Dynamic modelling and control design of advanced energy storage for power system applications," *Dynamic Modelling.*, no. IntechOpen, 2010.
- [3] J. A. Peças Lopes, Senior Member, IEEE, C. L. Moreira, and A. G. Madureira., "Defining Control Strategies for MicroGrids Islanded Operation.," *IEEE TRANSACTIONS*, vol. 21, no. IEEE TRANSACTIONS ON POWER SYSTEMS, 2006.
- [4] Mustafa E. Amiryar and Keith R. Pullen, "A Review of Flywheel Energy Storage System Technologies and Their Applications," *Applied Sciences*, vol. 7.3, p. 286, 2017.
- [5] Raijmakers, L. H. J., D. L. Danilov, R-A. Eichel, and P. H. L. Notten. , "A review on various temperature-indication methods for Li-ion batteries.," *Applied energy* , vol. 240, pp. 918-945, 2019.
- [6] A.R. Dehghani-Sanija,b,*, E. Tharumalingama, M.B. Dusseaulta,b, R. Fraserb,c, "Study of energy storage systems and environmental challenges of batteries," *Elsevier*, vol. 104, no. Renewable and Sustainable Energy Reviews, p. 192–208, 2019 .
- [7] Bernardes, A. M., D. Croce Romano Espinosa, and JA Soares Tenório, "Recycling of batteries: a review of current processes and technologies," *Journal of Power Sources* , vol. 130, pp. 291-298, 2004.
- [8] Linden D, Reddy TB., Handbook of batteries. 3rd ed., New York: McGraw-Hill, 2002.
- [9] C. A. Vincent, "Lithium batteries: a 50-year perspective, 1959–2009,"

Elsevier, vol. 134, no. Solid State Ionics, p. 159–167, 2000.

- [10] Yuning Zhang a, *, Xianghao Zheng a, Jinwei Li b, Xiaoze Du a, "Experimental study on the vibrational performance and its physical," *elsevier*, vol. 130, no. Renewable Energy, pp. 667-676, 2019.
- [11] Farihan Mohamad, Jiashen Teh, Ching-Ming and Liang-Rui Chen, "Development of Energy Storage Systems for Power," *energies*, no. Review, 2018.
- [12] Jansen, Ralph, and Timothy Dever, "G2 flywheel module design.," in *2nd international energy conversion engineering conference*, 2004.
- [13] Carrillo, C., A. Feijóo, and J. Cidrás, "Comparative study of flywheel systems in an isolated wind plant," *Renewable Energy*, vol. 34, no. 3, pp. 890-898, 2009.
- [14] R. Arghandeh, StudentMember, IEEE, M. Pipattanasomporn, Senior Member, IEEE, and S. Rahman, "Flywheel Energy Storage Systems for Ride-through Applications in a Facility Microgrid," *TRANSACTIONS ON SMART GRID*, vol. 3, 2012.
- [15] Xiaojun Li, Student Member, IEEE, Bahareh Anvari, Student Member, IEEE, Alan Palazzolo, Zhiyang Wang and Hamid Toliyat, Fellow, IEEE, "A Utility Scale Flywheel Energy Storage System with a Shaft-less, Hub-less, High Strength Steel Rotor," *IEEE TRANSACTIONS*, vol. 65.8 , no. INDUSTRIAL ELECTRONICS, pp. 6667-6675, 2018.
- [16] Xiaodong Sun, Senior Member, IEEE, Zhijia Jin, Shaohua Wang, Zebin Yang, Ke Li, Yeman Fan and Long Chen, "Performance Improvement of Torque and Suspension Force for a Novel Five-Phase BFSPM Machine for Flywheel Energy Storage Systems.," *Transactions*, no. Transactions on Applied Superconductivity, 2019.
- [17] Mohammad Ghanaatian and Saeed Lotfifard, "Control of Flywheel Energy Storage," *Transactions on Sustainable Energy*, 2019.
- [18] Boldea, Ion, and Syed A. Nasar., *Electric drives.*, CRC press., 2016.

- [19] N. a. R. M. Niveditha, "Modeling of permanent magnet synchronous machine using Matlab's Simscape language.," *International Journal for Trends in Engineering & Technology*, no. 14., pp. 56-59., 2016.
- [20] LIU Ting-ting, TAN Yu, WU Gang, WANG Shu-mao, "Simulation of PMSM vector control system based on Matlab/Simulink," in *international conference on measuring technology and mechatronics automation*, 2009.
- [21] Ton, D.T. and Smith, M.A., "The US department of energy's microgrid initiative.," *The Electricity Journal*, vol. 25, no. 8, pp. 84-94, 2012.
- [22] R.H.Lasseter, Fellow, IEEE, "Microgrid," in *2002 IEEE Power Engineering Society Winter Meeting.*, 2002.
- [23] Chowdhury and Badrul H, "Power quality," *IEEE potentials*, vol. 20, no. 2, pp. 5-11, 2001.
- [24] Martzloff, Francois D., and Thomas M. Gruz., "Power quality site surveys: Facts, fiction, and fallacies," *IEEE Transactions on Industry Applications* , vol. 24, no. 6 , pp. 1005-1018., 1988.
- [25] Chattopadhyay, Surajit, Madhuchhanda Mitra, and Samarjit Sengupta, "Sag, swell, interruption, undervoltage and overvoltage," in *Electric Power Quality*, Dordrecht, Springer, 2011, pp. 39-42.
- [26] Acha, Enrique, Vassilios Agelidis, Olimpo Anaya, and Timothy John Eastham Miller, *Power electronic control in electrical systems*, 2001: Elsevier.
- [27] N. Hamsic', A. Schmelter ', A. Mohd', E. Ortjohann', E. Schultze, A. Tuckey, J. Zimmermann, "Increasing Renewable Energy Penetration in Isolated Grids Using a Flywheel Energy Storage System," *POWERENG*, 2007.
- [28] Abdalkarim Awad, Iyad Tumar, Mohammed Hussein, Wasel Ghanem, and Jaser A. Sa'ed, "PV output power smoothing using flywheel storage system," in *2017 IEEE International Conference on Environment and Electrical Engineering and 2017 IEEE Industrial and Commercial Power*

Systems , Europe, 2017.

- [29] Sebastián, R. and Alzola, R.P., " Flywheel energy storage systems: Review and simulation for an isolated wind power system.," *Renewable and Sustainable Energy Reviews*, vol. 16, no. 9, pp. 6803-6813, 2012.
- [30] Arani, AA Khodadoos, "Review of Flywheel Energy Storage Systems structures and applications in power systems and microgrids," *Renewable and Sustainable Energy Reviews* , vol. 69, pp. 9-18, 2017.
- [31] H. Toodeji, "A developed flywheel energy storage with built-in rotating supercapacitors.," *Turkish Journal of Electrical Engineering & Computer Sciences* , vol. 27.1 , pp. 213-229, 2019.
- [32] L. G. B. F. B. L. C. A. F. F. G. a. A. Z. Barelli, "Flywheel hybridization to improve battery life in energy storage systems coupled to RES plants.," *Energy*, vol. 173, pp. 937-950, 2019.
- [33] Lawrence, R. G., Craven, K. L. and Nichols, G. D., " Flywheel ups," *IEEE Industry Applications Magazine*, vol. 9, no. 3, pp. 44-50, 2003.
- [34] Patel, Hiren, and Vivek Agarwal., " MATLAB-based modeling to study the effects of partial shading on PV array characteristics," *IEEE transactions on energy conversion*, vol. 23, no. 1, pp. 302-310, 2008.
- [35] Bianconi, Enrico, Javier Calvente, Roberto Giral, Emilio Mamarelis, Giovanni Petrone, Carlos Andrés Ramos-Paja, Giovanni Spagnuolo, and Massimo Vitelli., "A fast current-based MPPT technique employing sliding mode control," *IEEE Transactions on Industrial* , vol. 60 , no. 3, pp. 1168-1178., 2012.
- [36] Shang, L., Jiabing, H. U., Xiaoming, Y. U. A. N. and Huang, Y., "Improved virtual synchronous control for grid-connected VSCs under grid voltage unbalanced conditions," *journal of Modern Power Systems and Clean Energy* , vol. 7, no. 1, pp. 174-185, 2019.
- [37] L. S. Czarnecki, "Instantaneous Reactive Power p-q Theory and Power Properties of Three-Phase Systems," *IEEE TRANSACTIONS ON POWER*

DELIVERY, vol. 21, no. 1, pp. 362-367, 2003.

- [38] H. -. Krug, T. Kume and M. Swamy, ""Neutral-point clamped three-level general purpose inverter - features, benefits and applications,"" in *IEEE 35th Annual Power Electronics Specialists Conference*, Aachen, Germany,, 2004.
- [39] Liu, Ting-ting, Yu Tan, Gang Wu, and Shu-mao Wang, "Simulation of PMSM vector control system based on Matlab/Simulink," *In 2009 international conference on measuring technology and mechatronics automation*, vol. 2, pp. 343-346. *IEEE*, 2009., vol. 2, pp. 343-346., 2009.
- [40] Verma, R. and Sahu, P., "Frequency fluctuation in power system: Sources, control and minimizing techniques.," *International Journal of Advanced Research in Electrical*, vol. 3, 2014.
- [41] Zhou, Long, and ZhiPing Qi, ""Modeling and simulation of flywheel energy storage system with IPMSM for voltage sags in distributed power network,"" in *Mechatronics and Automation*, 2009.
- [42] Anvari, Bahareh, et al, "A coreless permanent-magnet machine for a magnetically levitated shaft-less flywheel," *IEEE Transactions on Industry Applications*, 2018.
- [43] Hans J. Bomemann, Michael Sander., "Conceptual System Design of a 5 MWh/100 MW Superconducting Flywheel.," *IEEE TRANSACTIONS ON APPLIED SUPERCONDUCTIVITY.*, vol. VOL. 7, 1997.
- [44] John W. Finch and Damian Giaouris, "Controlled AC electrical drives," *IEEE Transactions on Industrial Electronics*, vol. 55, no. 2, pp. 481-491, 2008.
- [45] Lappalainen, Kari, and Seppo Valkealahti, "Effects of PV array layout, electrical configuration and geographic orientation on mismatch losses caused by moving clouds.," *Solar Energy*, vol. 144 , pp. 548-555, 2017.
- [46] RICHARD REDL, SENIOR MEMBER, "Electromagnetic environmental impact of power electronics equipment," *Proceedings of the*

IEEE , vol. 89, no. 6, pp. 926-938, 2001.

- [47] Zhou, Long, and Zhi ping Q, "Modeling and control of a flywheel energy storage system for uninterruptible power supply," in *Sustainable Power Generation and Supply*, 2009.
- [48] Woyte, Achim, Vu Van Thong, Ronnie Belmans, and Johan Nijs, "Voltage fluctuations on distribution level introduced by photovoltaic systems," *IEEE Transactions on energy conversion*, vol. 21, no. 1, pp. 202-209, 2006.

Appendix:

```

function D = PandO(Param, Enabled, V, I)
% MPPT controller based on the Perturb & Observe algorithm.
% D output = Duty cycle of the boost converter (value between 0 and 1)
% Enabled input = 1 to enable the MPPT controller
% V input = PV array terminal voltage (V)
% I input = PV array current (A)
% Param input:
Dinit = Param(1); %Initial value for D output
Dmax = Param(2); %Maximum value for D
Dmin = Param(3); %Minimum value for D
deltaD = Param(4); %Increment value used to increase/decrease the duty cycle D
% ( increasing D = decreasing Vref )
persistent Vold Pold Dold;
dataType = 'double';
if isempty(Vold)
    Vold=0;
    Pold=0;
    Dold=Dinit;
end
P= V*I;
dV= V - Vold;
dP= P - Pold;
if dP ~= 0 & Enabled ~=0
    if dP < 0
        if dV < 0
            D = Dold - deltaD;
        else
            D = Dold + deltaD;
        end
    end
end

```

```
else
  if  $dV < 0$ 
     $D = D_{old} + \text{delta}D;$ 
  else
     $D = D_{old} - \text{delta}D;$ 
  end
end
else  $D = D_{old};$ 
end
if  $D \geq D_{max} \mid D \leq D_{min}$ 
   $D = D_{old};$ 
end
 $D_{old} = D;$ 
 $V_{old} = V;$ 
 $P_{old} = P;$ 
```